

**UCSF**

**UC San Francisco Electronic Theses and Dissertations**

**Title**

Nociceptor structure and function during vincristine-induced neuropathy in rat

**Permalink**

<https://escholarship.org/uc/item/6mx0527w>

**Author**

Tanner, Kimberly D.

**Publication Date**

1997

Peer reviewed|Thesis/dissertation

Nociceptor Structure and Function during  
Vincristine-induced Neuropathy in Rat

by

Kimberly D. Tanner

**DISSERTATION**

**Submitted in partial satisfaction of the requirements for the degree of**

**DOCTOR OF PHILOSOPHY**

**in**

Neuroscience

**in the**

**GRADUATE DIVISION**

**of the**

**UNIVERSITY OF CALIFORNIA**

**San Francisco**



copyright ©1997

by

Kimberly D. Tanner

for  
Mom  
and  
Dad

...of course!



## Acknowledgments

I feel extraordinarily privileged to have been a graduate student in neuroscience at the University of California at San Francisco. The members of this neuroscience community create a very special atmosphere of collegiality and learning. In particular, I thank the neuroscience program directors Lou Reichardt and Michael Stryker for their thoughtfulness and effort in creating this community. I also thank all of the graduate students, postdocs, research associates, and faculty that have contributed to my scientific development over the years. Whether learning about the neurobiology of *Manduca sexta* in student journal club, arguing about synaptic plasticity in a seminar class, or examining the data in recent papers in Friday afternoon journal club, I was consistently impressed and inspired by the creativity and dedication of my colleagues.

As most people know by now, I have always aspired to share my enthusiasm for science with others, especially young people. Throughout graduate school, I have found my work with the UCSF Science and Health Education Partnership (SEP) to be both sustaining and rewarding. It has renewed my own fervor for science and has allowed me the opportunity to develop the skills to express my enthusiasm to students, teachers, and the general public. I look forward to an academic career in neuroscience that will include a strong commitment to science education outreach in the public schools. For these experiences, I thank my colleagues at SEP: Liesl Chatman, Helen Doyle, Katherine Nielsen, and Tracy Stevens, as well as my teacher partner Patricia Kudritzki and my scientist buddy Erin Peckol. I am a better teacher and a better scientist for having known each of them.

In the course of my thesis work, I have had the good fortune to work with two exceptional young faculty members at UCSF. Peter Ohara has been unstintingly generous with his time, expertise, and opinions. His philately, hucksterism, and sarcasm are always appreciated. Kim Topp was and continues to be the ideal collaborator. Her cellular perspective complements my own systems neuroscience approach, producing rich scientific discussion and experimentation.

In the end, though, graduate school is about being in a laboratory. Graduate school is long journey that is only completed with the support and encouragement of friends and colleagues. Every member of the Jon Levine's Peripheral Pain Army over the past six years has contributed profoundly to my development as a scientist and a person. The camaraderie of my fellow Levine lab graduate students made everything easier. Thank you, Sara Ahlgren, Michael Gold, Robert Gear, and Holly Strausbaugh. Five individuals been with

me for my entire journey through graduate school. Michael Gold was my closest scientific colleague in the lab and is an invaluable friend. His keen acumen and critical eye are an inspiration to me, and I look forward to his scientific collaboration and friendship throughout my lifetime. Beneath his gruff exterior, Dave Reichling is one of the most gentle people I know. He taught me that as a scientist, one can never be too rigorous and to be highly suspicious of anyone who thinks otherwise. Through weekly excursions with Dave, I also came to understand that Gordo's makes the best burrito in the Inner Sunset. Sachia Khasar's broad smile and ever-growing beard greeted me each morning and encouraged me along the way. Paul Green unfailingly provided a role model of a scientist who was able to successfully balance life in and out of the laboratory. Despite being twice my age, Bobalong Gear has been a peer in the true sense of the word. Through the forest of electronic equipment between our physiology rigs, he has been an enduring source of wit, wisdom, and worldliness.

Most importantly, I thank my mentor, Jon Levine. Jon has been extremely tolerant of my constant scientific criticism and youthful energy. Our intellectual discussions and struggles over the years have broadened my perspective on neuroscience, taught me to think in new ways, and helped me to focus my own scientific passion. Jon has been a wonderful advisor because he himself is a graduate student at heart, always able to empathize with the trials and tribulations of experimental science. Jon teaches everyone that the key to achieving your goals, both scientifically and personally, lies within yourself. I thank him for teaching me that lesson and appreciate the times he believed in me even when I doubted myself.

Lastly, there are people that it would be trivial to thank. Mom and Dad. And Henry.

# **Nociceptor Structure and Function in Vincristine-Induced Neuropathy in Rat**

Kimberly D. Tanner

University of California, San Francisco

Doctoral Program in Neuroscience

July 11, 1997

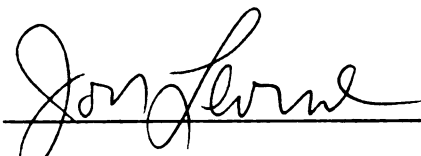
Chemotherapy-induced pain is a form of neuropathic pain caused by drugs such as vincristine and taxol that is characterized by painful paresthesias and dysesthesias. Vincristine-induced painful neuropathy has been hypothesized to result from the effects of vincristine on neuronal microtubules, causing peripheral nerve injury and secondary alteration of nociceptor function. However, no studies have examined nociceptor structure or function during vincristine-induced neuropathy and hyperalgesia. To test the hypothesis that vincristine increases the sensitivity of nociceptors, I performed electrophysiological studies on nociceptive neurons in vincristine-treated rats. 45% of vincristine-treated nociceptors were markedly hyperresponsiveness to sustained mechanical stimulation. A subset of these hyperresponsive vincristine-treated nociceptors were also hyperresponsive to heat stimulation. Mean conduction velocities of A- and C-fibers in vincristine-treated rats were significantly slowed. All other aspects of nociceptor function assayed were unaffected, suggesting that vincristine does not cause a generalized enhancement of nociceptor function, but rather specifically interferes with neural mechanisms underlying evoked responses. In addition, hyperresponsive vincristine-treated nociceptors fired in two distinct temporal modes, a variable frequency mode correlated with ISIs <100 msec or a constant frequency mode correlated with ISIs between 100-300 msec. These data suggest that multiple cellular mechanisms may contribute to nociceptor hyperresponsiveness and that the time scale of these mechanisms may be different. Although vincristine-induced neuropathy has been hypothesized to occur due to disruption of the axonal cytoskeleton, no studies have examined the cytoskeleton during vincristine-induced neuropathy and

hyperalgesia. I performed morphometric analysis on unmyelinated sensory axons in vincristine-treated rats. Although there was no loss of axonal microtubules, vincristine-treated axons had significantly more disoriented microtubules as compared to controls, suggesting disruption of the cytoskeleton. Unmyelinated axons in vincristine-treated rats had significantly larger cross-sectional areas, suggesting swelling of axons. These studies of vincristine-induced neuropathy provide the first evidence that changes in cytoskeleton may be linked with nociceptor responsiveness in the production of neuropathic pain and may provide insight into mechanisms of neuropathic pain of different etiologies. The abnormalities in nociceptor structure and function could underlie hyperalgesia observed in vincristine-treated rats, as well as the paresthesias and dysesthesias experienced by patients receiving vincristine as a chemotherapeutic agent.



Kimberly D. Tanner

Ph.D. Candidate in Neuroscience



Jon D. Levine, MD, PhD

Thesis Advisor



Allan I. Basbaum, PhD

Thesis Committee Chairperson

## Table of Contents

Title Page.....	i
Copyright Page.....	ii
Dedication.....	iii
Acknowledgments/Preface.....	iv
Abstract.....	vi
Table of Contents.....	viii
List of Figures and Tables.....	x
Chapter I: Introduction.....	1
References.....	13
Chapter II: Mechanical hyperresponsiveness of nociceptors in vincristine-induced painful neuropathy in rat.....	19
Abstract.....	20
Introduction.....	21
Methods.....	23
Results.....	30
Discussion.....	35
References.....	41
Chapter III: Nociceptors in vincristine-induced painful neuropathy in rat are hyperresponsive to multiple stimulus modalities.....	68
Abstract.....	69
Introduction.....	70
Methods.....	72
Results.....	79
Discussion.....	83
References.....	89

Chapter IV:	Temporal analysis of nociceptor hyperresponsiveness during vincristine-induced painful neuropathy in rat.....	107
	Abstract.....	108
	Introduction.....	109
	Methods.....	111
	Results.....	118
	Discussion.....	122
	References.....	128
Chapter V:	Microtubule disorientation and axonal swelling in unmyelinated sensory axons during vincristine-induced painful neuropathy in rat.....	148
	Abstract.....	149
	Introduction.....	150
	Methods.....	152
	Results.....	156
	Discussion.....	161
	References.....	166
Chapter VI:	Summary and future directions.....	191

## List of Figures and Tables

### Chapter II:

Figure 1:	Experimental paradigm and electrophysiological recording period.....	47
Figure 2:	Vincristine causes a slowing of the conduction velocity of both A-fibers and C-fibers.....	49
Figure 3:	Vincristine does not decrease the heat activation threshold of C-fibers.....	51
Figure 4:	Vincristine does not decrease the mechanical activation threshold of C-fibers.....	53
Figure 5:	C-fiber responses to sustained mechanical stimulation are reproducible...	55
Figure 6:	Vincristine causes increased responsiveness to sustained mechanical stimulation in a subset of C-fibers.....	57
Figure 7:	The responses to sustained mechanical stimulation in vincristine-treated rats are bimodal.....	59
Figure 8:	Time course of responses to sustained mechanical stimulation in control and vincristine-treated C-fibers.....	61
Figure 9:	Hyperresponsiveness in C-fibers is not correlated with receptive field location, conduction velocity, or mechanical threshold.....	63
Table 1:	Spontaneous activity in the saphenous nerve of control and vincristine- treated rats.....	65
Table 2:	Distribution of C-fiber classes in the saphenous nerve of control and vincristine-treated rats.....	66
Table 3:	Responses of C-fibers in the saphenous nerve of control and vincristine- treated rats to sustained mechanical stimulation.....	67

### **Chapter III:**

Figure 1:	Schematic of experimental timeline.....	95
Figure 2:	Vincristine does not decrease the heat activation threshold of nociceptors.....	97
Figure 3:	Vincristine causes heat hyperresponsiveness in high-firing vincristine- treated nociceptors.....	99
Figure 4:	Heat hyperresponsiveness occurs in high-firing but not low-firing vincristine-treated nociceptors.....	101
Figure 5:	Heat hyperresponsiveness occurs in some, but not all, high-firing vincristine-treated nociceptors.....	103
Figure 6:	Hyperresponsiveness in nociceptors is not correlated with receptive field location, conduction velocity, mechanical threshold, or heat threshold.....	105



## **Chapter IV:**

Figure 1:	Examples of control, low-firing vincristine, and high-firing vincristine nociceptor response patterns to sustained mechanical stimulation.....	132
Figure 2:	Temporal characteristics of the responses of control and low-firing vincristine-treated nociceptors.....	134
Figure 3:	Hyperresponsive vincristine-treated nociceptors respond to mechanical stimulation in a constant frequency firing mode or a variable frequency firing mode .....	136
Figure 4:	Distribution of interspike intervals for entire nociceptor response to mechanical stimulation.....	138
Figure 5:	Distribution of interspike intervals for the burst period of the nociceptor response to mechanical stimulation.....	140
Figure 6:	Distribution of interspike intervals for the plateau period of the nociceptor response to mechanical stimulation.....	142
Figure 7:	Temporal firing mode in hyperresponsive nociceptors is not correlated with receptive field location.....	144
Table 1:	Characteristics of control, low-firing, and high-firing vincristine-treated nociceptors.....	146
Table 2:	Characteristics of variable frequency mode and constant frequency mode high-firing vincristine-treated nociceptors.....	147

## **Chapter V:**

Figure 1:	Schematic of experimental timeline.....	173
Figure 2:	Peripheral nerve appears normal at the light level during vincristine-induced neuropathy.....	175
Figure 3:	Unmyelinated sensory axons appear normal in high magnification electron micrographs during vincristine-induced neuropathy.....	177
Figure 4:	Vincristine treatment alters the cytoskeleton in unmyelinated sensory axons.....	179
Figure 5:	Vincristine treatment decreases the density of microtubules in unmyelinated sensory axons.....	181
Figure 6:	Vincristine treatment does not decrease the total number of microtubules in unmyelinated sensory axons.....	183
Figure 7:	Vincristine treatment increases the axonal cross-sectional area of unmyelinated sensory axons.....	185
Figure 8:	Vincristine treatment decreases the number of cross-sectional microtubules and concomitantly increases the number of tangential microtubules per unmyelinated axon.....	187
Table 1:	Density of unmyelinated axons in the saphenous nerve of control and vincristine-treated rats.....	189
Table 2:	Axonal diameter and form factor for unmyelinated axons in control and vincristine-treated rats.....	190

## **Chapter I:**

### **Introduction**

Nociception and pain perception alert organisms to potentially tissue-damaging and life-threatening stimuli. Noxious stimuli are detected by a specialized class of sensory neurons called nociceptors. In addition to acutely signaling the presence of an intense stimulus, the nociceptive sensory system is also remarkably plastic, increasing its sensitivity following both tissue and nerve injury. Although plasticity in nociceptive circuits in the central nervous system undoubtedly occurs, there is ample evidence that nociceptors alter their response properties following tissue injury and inflammation. Little is known, however, about the response properties of nociceptors during neuropathic pain following nerve injury. In this thesis, I have investigated nociceptor response properties during vincristine-induced painful neuropathy. I present the first evidence that 1) vincristine-induced neuropathy and hyperalgesia are associated with nociceptor hyperresponsiveness, 2) nociceptor hyperresponsiveness may involve alterations in both mechanotransduction and cellular mechanisms of adaptation, 3) impairment of multiple adaptation mechanisms on different time scales may contribute to hyperresponsiveness in different nociceptors, and 4) vincristine causes disorganization of microtubule structure during nociceptor hyperresponsiveness. These studies of vincristine-induced neuropathy provide the first evidence that changes in cytoskeleton may be linked with nociceptor responsiveness in the production of neuropathic pain.

### Primary afferent nociceptors

Nociception and pain, in most instances, are initiated at the peripheral terminals of primary afferent nociceptors. The term “primary afferent nociceptor” was first suggested in 1906 by Sherrington to describe hypothetical afferents in the peripheral nerve that would respond only to noxious stimuli that were potentially tissue damaging (Sherrington, 1906). In the late 1960's Perl and colleagues physiologically described afferents in the peripheral nerve of the cat that were candidate biological correlates of Sherrington's hypothetical nociceptors (Burgess and Perl, 1967; Bessou and Perl, 1969). These nociceptors respond

preferentially to noxious stimulation, allowing them to encode unambiguously noxious information without contamination by non-noxious signals. Afferents that respond preferentially to noxious stimulation are small-diameter fibers with correspondingly slow conduction velocities, including the smallest myelinated A $\delta$ -fibers and unmyelinated C-fibers. Nociceptors in both classes transduce noxious stimuli of multiple modalities, including mechanical, thermal, and chemical energies and generate action potentials that are propagated to the central nervous system (Bessou and Perl, 1969). Thorough knowledge of both the normal and abnormal function of primary afferent nociceptors is key in gaining insight into mechanisms of inflammatory and neuropathic pain and hyperalgesia.

#### Nociceptor sensitization following tissue injury and inflammation

Following tissue injury associated with inflammation, animals exhibit increased sensitivity to sensory stimulation termed hyperalgesia. Hyperalgesia is characterized by a decrease in withdrawal threshold from a noxious stimulus and results in protective behaviors such as guarding of the injured area. Alterations in transduction in nociceptive sensory neurons have been extensively studied following tissue injury and inflammation. Early studies by Perl and colleagues in 1969 suggested that nociceptive afferents exhibited sensitization, consisting of a decrease in activation threshold, an increase in response to a suprathreshold stimulus, and/or the development of spontaneous activity. The magnitude of decrease in A $\delta$  nociceptor thresholds to heat in the area of tissue damage following a cutaneous burn injury correlates well with the magnitude of decrease in the human nociceptive withdrawal threshold (Meyer and Campbell, 1981). In addition, sensitization of C-fiber nociceptors occurs in the area of tissue damage following cutaneous burn injury (LaMotte et al., 1982; LaMotte et al., 1983; LaMotte et al., 1984; Torebjork et al., 1984). Thus, nociceptor sensitization is thought to underlie the development of primary hyperalgesia following tissue injury. Nociceptor sensitization occurs to all modalities of external stimulation and can be induced by tissue injury or by administration of single

inflammatory mediators such as histamine, serotonin, bradykinin, or PGE<sub>2</sub> (Treede et al., 1992; Levine and Taiwo, 1994). Behavioral, pharmacological, and electrophysiological studies have shown that the cyclic AMP second messenger system mediates nociceptor sensitization that is produced by the majority of inflammatory mediators (Taiwo and Levine, 1989; Taiwo and Levine, 1991; Levine et al., 1993; Levine and Taiwo, 1994).

#### Nociceptor dysfunction associated with nerve injury and neuropathy

Peripheral neuropathy occurs following toxic, traumatic, or metabolic injury to peripheral nerve and is usually accompanied by neuropathic pain and hyperalgesia. Injury to peripheral nerve produces a variety of phenotypic, structural, and electrophysiological changes in nociceptive sensory neurons. Studies of changes in the electrophysiological properties of nociceptors following nerve injury have been primarily performed in traumatic injury models of neuropathy such as the chronic constriction injury model (Xie and Xiao, 1990; Kajander and Bennett, 1992; Kajander et al., 1992) and axotomy (Devor et al., 1981; Devor, 1983; Devor, 1986; Devor et al., 1990a; Devor et al., 1990b; Devor and Wall, 1991) and have intensively focused on novel electrogenesis, the development of abnormal spontaneous activity, ectopic discharge, and electrical cross-excitation in sensory axons and dorsal root ganglion cell bodies (Xie and Xiao, 1990; Kajander and Bennett, 1992; Kajander et al., 1992; Devor et al., 1994).

In contrast, alterations in the response properties of the peripheral terminals of injured nociceptors have not been as extensively studied during neuropathy, as they have been during inflammation. Only in diabetic neuropathy (Ahlgren et al., 1992; Ahlgren and Levine, 1994), a metabolic form of nerve injury, have the response properties of nociceptors been examined. In diabetic neuropathy C-fiber nociceptors are hyperresponsiveness to sustained mechanical stimulation without a concomitant decrease in mechanical activation threshold and additionally exhibit abnormal discharges after removal of the stimulus (Ahlgren et al., 1992). Pharmacological studies have shown that inhibitors

of protein kinase C (PKC) attenuate both mechanical hyperalgesia and nociceptor hyperresponsiveness mechanical stimulation (Ahlgren and Levine, 1994). The origins of PKC involvement in nociceptor hyperresponsiveness during diabetic neuropathy is unknown. Preliminary studies of nociceptor response properties during neuropathic pain following chronic constriction injury have shown heat hyperresponsiveness and afterdischarges reminiscent of mechanical hyperresponsiveness and afterdischarges seen in diabetic neuropathy (Koltzenburg et al., 1994).

Importantly, where the response properties of nociceptive neurons during neuropathy have been assayed, the characteristics of increased nociceptor responsiveness differ from those seen following tissue injury and inflammation (Treede et al., 1992; Levine et al., 1993; Levine and Taiwo, 1994). Sensitization of nociceptors during inflammation is characterized by a decrease in activation thresholds, as well as increased responsiveness to a suprathreshold stimulus. Both of these alterations in sensory transduction increase the sensitivity of nociceptors. In contrast, following nerve injury, the activation thresholds of nociceptors are not lowered, but are markedly hyperresponsive to suprathreshold stimulation (Ahlgren et al., 1992). Although studies of diabetic neuropathy demonstrated that the response properties of nociceptors can be altered during neuropathy, it is unknown if this is the case for neuropathic pain following other types of nerve injury.

The study of nociceptor dysfunction in both diabetic and trauma-induced neuropathy models have significant drawbacks. Firstly, in trauma-induced neuropathies in which peripheral nerves are crushed or cut, the axons of many nociceptors are disconnected from the peripheral terminal, the site of stimulus transduction, making the study of response properties extremely difficult. Secondly, the mechanisms underlying nociceptor dysfunction in both diabetic and trauma-induced neuropathy are difficult to determine because the nature of insults to peripheral nerve are complex and poorly defined. Diabetic neuropathy is thought to result from a myriad of changes in peripheral nerve secondary to systemic metabolic imbalance. Trauma-induced neuropathy, following crushing or cutting

peripheral nerve, causes a host of changes including but not limited to local inflammation at the site of nerve injury, chemical toxicity due to suture material, compromise of the axonal membrane, formation of a neuroma, and interruption of the axonal cytoskeleton with potential subsequent impairment of axonal transport. Thus, a model that both has physically intact nociceptors and is caused by an insult to peripheral nerve that is limited in time and effect would be ideal for detailed studies of the transduction properties of nociceptors during neuropathic pain.

#### Vincristine-induced neuropathy

Neuropathic pain following systemic administration of the neurotoxic chemotherapeutic drug, vincristine, provides the opportunity to investigate the response properties of nociceptors during neuropathic pain caused by a neurotoxin known to depolymerize microtubules and alter cytoskeletal function. Chemotherapy-induced pain is caused by neurotoxic drugs such as vincristine and taxol and is characterized by painful paresthesias and dysesthesias. The vinca alkaloid vincristine is a widely used antineoplastic agent that is administered alone or in combination with other drugs in the treatment of many tumor types (Weiss et al., 1974; Kaplan and Wiernik, 1982). The clinical antineoplastic efficacy of vincristine is limited by the development of a dose-dependent sensorimotor neuropathy (Sandler et al., 1969; Holland et al., 1973). This sensorimotor neuropathy appears to occur in two major stages (Weiss et al., 1974; Kaplan and Wiernik, 1982; McCarthy and Skillings, 1992). In the early stage, peripheral axons are damaged by vincristine and the principal symptoms are paresthesias and dysesthesias. In the later stage, which occurs more frequently at higher doses, axons are lost and the principal finding is loss of motor function. Vincristine is thought to exert its antineoplastic effects by binding to tubulin in mitotically active cells, disrupting microtubule formation in mitotic spindles, and thus preventing cell division (Olmsted and Borisy, 1973; Himes et al., 1976; Owellen et al., 1976). The neuropathy observed in patients treated with vincristine has been



hypothesized to result from effects of vincristine on neuronal microtubules resulting in impaired axonal transport in peripheral nerves.

An animal model of vincristine-induced painful neuropathy in the rat has recently been established (Aley et al., 1996). Chronic mechanical hyperalgesia, measured 24 hours after vincristine administration, develops when 10 daily vincristine injections (100 µg/kg) are administered intravenously over a 2-week period. This chronic hyperalgesia develops during the second week of vincristine administration and persists for more than a week following the final injection of vincristine. The hyperalgesia is dose-dependent and occurs at doses of vincristine similar to those administered clinically to achieve anti-neoplastic efficacy (McLeod and Penny, 1969; Sandler et al., 1969; Casey et al., 1973; Holland et al., 1973), although vincristine is administered more frequently in the rat model. Higher doses of vincristine cause loss of motor function in rat (Aley et al., 1996), similar to the later stage of neuropathy in humans. In an anatomical study, I have obtained evidence in this rat model that there is damage to unmyelinated sensory axons before there are any signs of axonal loss (Tanner et al., 1997a). I suggest that vincristine-induced hyperalgesia in the rat is a model of the early stage of vincristine-induced chemotherapeutic neuropathy.

Vincristine-induced neuropathy in the rat offers several advantages for the study of the mechanisms underlying neuropathic pain. Since vincristine is a drug-induced neuropathy, the neuropathic insult can be easily controlled in a dose-dependent manner and the extent of hyperalgesia from animal to animal is quite reproducible. Secondly, unlike traumatic nerve injury, vincristine is not thought to disconnect axons from their peripheral terminals, and thus, allows the opportunity to study transduction at the peripheral terminal which is difficult in other models of neuropathic pain. Thirdly, several lines of evidence suggest that alterations in peripheral nerve function underlie the sensory alterations in vincristine-induced painful peripheral neuropathy. Systemically administered vincristine does not cross the blood brain barrier to a significant extent and is thought to exert its actions in the periphery (Castle et al., 1976; Greig et al., 1990; Zhou et al., 1990). It has

been hypothesized that peripheral neurons are highly sensitive to vincristine because nerve terminal function is dependent on intact axonal transport and maintenance of the peripheral terminal via extremely long axons (Shelanski and Wisniewski, 1969). Of note, the paresthesias and dysesthesias reported in humans are most pronounced in the distal extremities (Sandler et al., 1969; Holland et al., 1973), namely those areas innervated by the longest sensory neurons. Lastly, since the primary mechanism of action of vincristine is known to be the depolymerization of microtubules, vincristine offers the opportunity to examine changes in neuronal function that accompany a somewhat circumscribed insult to the nerve. Since vincristine may primarily affect microtubule-dependent processes such as cytoskeletal structure and axonal transport, it might produce only a subset of the changes caused by a more traditional neuropathic insult such as mechanical injury of the nerve which causes a myriad of changes in peripheral nerve.

Vincristine-induced neuropathy provides the opportunity 1) to examine functional transduction properties of nociceptors in a neuropathy model with a circumscribed insult to peripheral nerve, namely microtubule-dependent processes such as cytoskeletal structure and axonal transport, and 2) to determine whether nociceptor hyperresponsiveness seen in diabetic neuropathy is seen following other forms of nerve injury. Investigations of vincristine-induced peripheral neuropathy may provide insight into the mechanisms underlying not only this neuropathy, but the cause of neuropathic pains produced by a variety of injuries.

#### Nociceptor hyperresponsiveness during vincristine-induced neuropathy

The dysesthesias in humans and hyperalgesia in rats that accompany vincristine-induced neuropathy have been hypothesized to occur due to peripheral nerve injury and alteration of nociceptive sensory neuron function. However, no studies in the literature have examined nociceptive C-fiber function in the setting of vincristine-induced neuropathy. This thesis consists of a series of experiments designed to examine

physiological and anatomical alterations of nociceptor function during vincristine-induced neuropathy. To test the hypothesis that changes in the sensitivity and responsiveness of C-fiber nociceptors occur during the chronic phase of vincristine-induced hyperalgesia, I performed *in vivo* extracellular recordings of single neurons from the saphenous nerve of vincristine-treated rats. Chapter 2 documents that 45% of C-fiber nociceptors in vincristine-treated rats showed marked hyperresponsiveness to suprathreshold mechanical stimulation compared to control C-fibers. These hyperresponsive (“high-firing”) vincristine-treated C-fibers were significantly different from both control C-fibers, as well as from non-hyperresponsive (“low-firing”) vincristine-treated C-fibers. Mean conduction velocities of A-fibers and C-fibers in vincristine-treated rats were significantly slowed. The mean heat and mechanical activation thresholds of C-fibers were not decreased. The distribution of C-fibers among subclasses, and the percentage of spontaneously active neurons in vincristine-treated rats were not statistically different from controls. Vincristine, therefore, does not cause a generalized alteration of neuronal function, but rather specifically interferes with neural mechanisms underlying the evoked response to external stimulation.

Chapter 3 addresses potential mechanisms of nociceptor hyperresponsiveness during vincristine-induced neuropathy. C-fiber hyperresponsiveness may stem from an impairment of general adaptation mechanisms following neuronal activation. Alternatively, nociceptor hyperresponsiveness in vincristine-treated rats may be specific to mechanical stimulation. Although the mechanisms of mechanical transduction are unknown, models have postulated a role for cytoskeletal elements and vincristine is known to cause disruption of the microtubular cytoskeleton. To distinguish between these possibilities and gain insight into mechanisms of nociceptor hyperresponsiveness, I used *in vivo* extracellular recordings to examine the responses of vincristine-treated nociceptors to heat stimulation. Based on their responsiveness to mechanical stimulation, nociceptors from vincristine-treated rats could be classified as either hyperresponsive or non-hyperresponsive nociceptors, as described previously (Tanner et al., 1997b). Vincristine can cause heat

hyperresponsiveness in vincristine-treated nociceptors that are also hyperresponsive to mechanical stimulation. As a population, high-firing vincristine-treated C-fibers had significantly greater responses to heat stimulation than low-firing vincristine-treated or control C-fibers. Thus, mechanisms of vincristine-induced nociceptor hyperresponsiveness involve general cellular adaptation mechanisms that contribute to nociceptor responses to multiple stimulus modalities. However, heat hyperresponsiveness was pronounced in only a subset of mechanically hyperresponsive nociceptors and was never detected in the absence of mechanical hyperresponsiveness. These data suggest that vincristine may also specifically alter mechanotransduction.

Chapter 4 provides additional insight into the mechanisms of nociceptor hyperresponsiveness during vincristine-induced neuropathy. In addition to firing more than twice as many action potentials as control nociceptors, hyperresponsive vincristine-treated nociceptors also appeared to fire in distinct temporal patterns that were not seen in the responses of control or low-firing vincristine-treated nociceptors. An investigation of the characteristics of these temporal firing patterns may yield insight into mechanisms of nociceptor hyperresponsiveness. To analyze this change in firing pattern, the distribution of interspike intervals and plots of instantaneous frequency were constructed for the responses to mechanical stimulation of vincristine-treated and control nociceptors. Instantaneous frequency plots reveal that hyperresponsive vincristine-treated nociceptors fired in one of two characteristic firing patterns. One mode was a variable frequency firing pattern with alternating periods of high and low firing frequency, whereas the second mode was a constant frequency firing pattern. The variable frequency mode is correlated with a high percentage of ISIs less than 100 msec, whereas the constant frequency mode is correlated with a high percentage of ISIs in the range of 100-300 msec. In addition, hyperresponsive nociceptors that fire in constant frequency mode have significantly higher mechanical thresholds compared to both those that fire in variable frequency mode and control nociceptors; there was no difference in the conduction velocities of these populations.

These data suggest that multiple cellular mechanisms may contribute to vincristine-induced hyperresponsiveness in nociceptors, that the time scale of these mechanisms may be different, and that the temporal characteristics of hyperresponsiveness are correlated with the mechanical threshold of the nociceptor.

Chapter 5 describes structural changes in unmyelinated axons that might contribute to the functional hyperresponsiveness of nociceptors during vincristine-induced neuropathy. Vincristine-induced neuropathy has been hypothesized to occur due to disruption of the axonal cytoskeleton and secondary impairment of axonal transport. Although there are clear alterations in axonal microtubule structure following application of vincristine to peripheral nerve *in vitro* (Green et al., 1977) or after injection of vincristine into the endoneurial space *in vivo* (Schlaepfer, 1971), there have been no quantitative ultrastructural studies of microtubule structure in peripheral nerve during vincristine-induced neuropathic hyperalgesia. To test the hypothesis that changes in the structure of microtubules in nociceptive sensory neurons accompany vincristine-induced hyperalgesia, I performed morphometrical analysis on unmyelinated axons in the saphenous nerve of vincristine-treated rats. There was a significant decrease in microtubule density in unmyelinated axons from vincristine-treated rats when compared to control axons. This decrease in microtubule density was not due to a difference in the mean number of microtubules per axon in vincristine-treated nerves. Rather, there was a significant increase in the cross-sectional area of unmyelinated axons in vincristine-treated rats, suggesting a swelling of axons. Although there was no loss of axonal microtubules, vincristine-treated axons had significantly fewer microtubules per axon cut in cross-section and significantly more tangentially-oriented microtubules as compared to controls, suggesting disorganization of cytoskeletal structure. Neither light nor electron microscopic level analysis revealed any gross morphological differences between control and vincristine-treated nerves, and there was no evidence of unmyelinated fiber loss. These data constitute

the first quantitative ultrastructural analysis of unmyelinated axons in the peripheral nerve during a neuropathic hyperalgesia.

In conclusion, I present the first evidence that vincristine-induced neuropathy and hyperalgesia are associated with nociceptor hyperresponsiveness. Further analysis revealed that nociceptor hyperresponsiveness may involve alterations in both mechanotransduction and cellular mechanisms of adaptation and that impairment of multiple adaptation mechanisms on different time scales may contribute to hyperresponsiveness in different nociceptors. In addition, I have shown that vincristine causes disorganization of microtubule structure during nociceptor hyperresponsiveness. Thus, vincristine-induced neuropathy appears to be a model of neuropathic pain in which changes in the cytoskeleton may be linked with nociceptor responsiveness. Since the profile of nociceptor dysfunction in vincristine-induced neuropathy is quite similar to that seen in diabetic neuropathy, data from this thesis provides further evidence that alterations in nociceptor function in neuropathic pain is distinct from that seen in inflammatory pain and prompts the hypothesis that there may be common mechanisms of neuropathic pain that occurs following nerve injury of diverse etiologies.

## References

Ahlgren SC, Levine JD (1994). Protein kinase C inhibitors decrease hyperalgesia and C-fiber hyperexcitability in the streptozotocin-diabetic rat. *J Neurophysiol* 72, 684-692.

Ahlgren SC, White DM, Levine JD (1992). Increased responsiveness of sensory neurons in the saphenous nerve of the streptozotocin-diabetic rat. *J Neurophysiol* 68, 2077-2085.

Aley KO, Reichling DB, Levine JD (1996). Vincristine hyperalgesia in the rat: a model of painful vincristine neuropathy in humans. *Neuroscience* 73, 259-265.

Bessou P, Perl ER (1969). Response of cutaneous sensory units with unmyelinated fibers to noxious stimuli. *J Neurophysiol* 32, 1025-43.

Burgess PR, Perl ER (1967). Myelinated afferent fibres responding specifically to noxious stimulation of the skin. *J Physiol (Lond)* 190, 541-62.

Casey EB, Jelliffe AM, Le QP, Millett YL (1973). Vincristine neuropathy. Clinical and electrophysiological observations. *Brain* 96, 69-86.

Castle MC, Margileth DA, Oliverio VT (1976). Distribution and excretion of (3H)vincristine in the rat and the dog. *Cancer Res* 36, 3684-3689.

Devor M (1983). Potassium channels moderate ectopic excitability of nerve-end neuromas in rats. *Pain* 17, 321-39.

Devor M (1986). Neuropathic pain and injured nerve: peripheral mechanisms. *Exp Neurol* 92, 522-32.

Devor M, Janig W, Michaelis M (1981). Ectopic adrenergic sensitivity in damaged peripheral nerve axons in the rat. *Exp Neurol* 72, 63-81.

Devor M, Janig W, Michaelis M (1990a). Modulation of activity in dorsal root ganglion neurons by sympathetic activation in nerve-injured rats. *J Neurophysiol* 64, 1733-46.

Devor M, Jänig W, Michaelis M (1994). Modulation of activity in dorsal root ganglion neurons by sympathetic activation in nerve-injured rats. *J Neurophysiol* 71, 38-47.

Devor M, Keller CH, Ellisman MH (1990b). Spontaneous discharge of afferents in a neuroma reflects original receptor tuning. *J Neurophysiol* 64, 1733-1746.

Devor M, Wall PD (1991). Cross-excitation in dorsal root ganglia of nerve-injured and intact rats. *Br Med Bull* 47, 619-30.

Green LS, Donoso JA, Heller BI, Samson FE (1977). Axonal transport disturbances in vincristine-induced peripheral neuropathy. *Ann Neurol* 1, 255-262.

Greig NH, Soncrant TT, Shetty HU, Momma S, Smith QR, Rapoport SI (1990). Brain uptake and anticancer activities of vincristine and vinblastine are restricted by their low cerebrovascular permeability and binding to plasma constituents in rat. *Cancer Chemother Pharmacol* 26, 263-268.



Himes RH, Kersey RN, Heller BI, Samson FE (1976). Action of the vinca alkaloids vincristine, vinblastine, and desacetyl vinblastine amide on microtubules in vitro. *Cancer Res* 36, 3798-3802.

Holland JF, Scharlau C, Gailani S, Krant MJ, Olson KB, Horton J, Shnider BI, Lynch JJ, Owens A, Carbone PP, Colsky J, Grob D, Miller SP, Hall TC (1973). Vincristine treatment of advanced cancer: a cooperative study of 392 cases. *Cancer Res* 33, 1258-1264.

Kajander KC, Bennett GJ (1992). Onset of a painful peripheral neuropathy in rat: a partial and differential deafferentation and spontaneous discharge in A beta and A delta primary afferent neurons. *J Neurophysiol* 68, 734-744.

Kajander KC, Wakisaka S, Bennett GJ (1992). Spontaneous discharge originates in the dorsal root ganglion at the onset of a painful peripheral neuropathy in the rat. *Neurosci Lett* 138, 225-228.

Kaplan RS, Wiernik PH (1982). Neurotoxicity of antineoplastic drugs. *Semin Oncol* 9, 103-130.

Koltzenburg M, Kees S, Budweiser S, Ochs G, Toyka K (1994). The properties of unmyelinated nociceptive afferents change in a painful chronic constriction neuropathy. In *Proc 7th World Cong Pain*, G Gebhart, D Hammond, T Jensen, ed. (Seattle: IASP Press), pp. 511-522.

LaMotte RH, Thalhammer JG, Robinson CJ (1983). Peripheral neural correlates of magnitude of cutaneous pain and hyperalgesia: a comparison of neural events in monkey with sensory judgments in human. *J Neurophysiol* 50, 1-26.

LaMotte RH, Thalhammer JG, Torebjork HE, Robinson CJ (1982). Peripheral neural mechanisms of cutaneous hyperalgesia following mild injury by heat. *J Neurosci* 2, 765-81.

LaMotte RH, Torebjork HE, Robinson CJ, Thalhammer JG (1984). Time-intensity profiles of cutaneous pain in normal and hyperalgesic skin: a comparison with C-fiber nociceptor activities in monkey and human. *J Neurophysiol* 51, 1434-50.

Levine JD, Fields HL, Basbaum AI (1993). Peptides and the primary afferent nociceptor. *J Neurosci* 13, 2273-2286.

Levine JD, Taiwo Y (1994). Inflammatory Pain. In *Textbook of Pain*, PD Wall, R Melzack, ed. (Edinburgh: Churchill Livingstone), pp. 45-56.

McCarthy GM, Skillings JR (1992). Jaw and other orofacial pain in patients receiving vincristine for the treatment of cancer. *Oral Surg Oral Med Oral Pathol* 74, 299-304.

McLeod JG, Penny R (1969). Vincristine neuropathy: an electrophysiological and histological study. *J Neurol Neurosurg Psychiatry* 32, 297-304.

Meyer RA, Campbell JN (1981). Myelinated nociceptive afferents account for the hyperalgesia that follows a burn to the hand. *Science* 213, 1527-9.

Olmsted JB, Borisy GG (1973). Microtubules. *Annu Rev Biochem* 42, 507-540.

Owellsen RJ, Hartke CA, Dickerson RM, Hains FO (1976). Inhibition of tubulin-microtubule polymerization by drugs of the Vinca alkaloid class. *Cancer Res* 36, 1499-1502.

Sandler SG, Tobin W, Henderson ES (1969). Vincristine-induced neuropathy. A clinical study of fifty leukemic patients. *Neurology* 19, 367-374.

Schlaepfer WW (1971). Vincristine-induced axonal alterations in rat peripheral nerve. *J Neuropathol Exp Neurol* 30, 488-505.

Shelanski ML, Wisniewski H (1969). Neurofibrillary degeneration induced by vincristine therapy. *Arch Neurol* 20, 199-206.

Sherrington CS (1906) *The integrative action of the nervous system*. New Haven: Yale University Press.

Taiwo YO, Levine JD (1989). Contribution of guanine nucleotide regulatory proteins to prostaglandin hyperalgesia in the rat. *Brain Res* 492, 400-3.

Taiwo YO, Levine JD (1991). Further confirmation of the role of adenylyl cyclase and of cAMP-dependent protein kinase in primary afferent hyperalgesia. *Neuroscience* 44, 131-5.

Tanner K, Levine J, Topp K (1997a). Microtubule disorientation and axonal swelling in unmyelinated sensory axons during vincristine-induced painful neuropathy in rat. *J. Neurosci. submitted.*

Tanner KD, Reichling DB, Levine JD (1997b). Mechanical hyperresponsiveness of nociceptors in vincristine-induced neuropathy in rat. *submitted.*

Torebjork HE, LaMotte RH, Robinson CJ (1984). Peripheral neural correlates of magnitude of cutaneous pain and hyperalgesia: simultaneous recordings in humans of sensory judgments of pain and evoked responses in nociceptors with C-fibers. *J Neurophysiol* 51, 325-39.

Treede RD, Meyer RA, Raja SN, Campbell JN (1992). Peripheral and central mechanisms of cutaneous hyperalgesia. *Prog Neurobiol* 38, 397-421.

Weiss HD, Walker MD, Wiernik PH (1974). Neurotoxicity of commonly used antineoplastic agents (second of two parts). *N Engl J Med* 291, 127-133.

Xie YK, Xiao WH (1990). Electrophysiological evidence for hyperalgesia in the peripheral neuropathy. *Sci China [b]* 33, 663-672.

Zhou XJ, Martin M, Placidi M, Cano JP, Rahmani R (1990). In vivo and in vitro pharmacokinetics and metabolism of vincaalkaloids in rat. II. Vinblastine and vincristine. *Eur J Drug Metab Pharmacokinet* 15, 323-332.

## **Chapter II:**

### **Mechanical hyperresponsiveness of nociceptors in vincristine-induced painful neuropathy in rat**

## Abstract

Neuropathic pain accompanies peripheral nerve injury following a wide variety of insults including metabolic disorders, traumatic injury, and neurotoxic drugs. Chemotherapy-induced neuropathic pain, caused by neurotoxic drugs such as vincristine and taxol, occurs in cancer patients who receive these drugs as antineoplastic agents. Although a variety of remediations have been attempted, the absence of knowledge concerning the mechanisms of chemotherapeutic-induced neuropathic pain has hindered the development of treatment strategies. Vincristine, a widely used chemotherapeutic agent, produces a painful peripheral neuropathy in humans (Sandler et al., 1969; Holland et al., 1973) and mechanical hyperalgesia in rats (Aley et al., 1996). To test the hypothesis that alterations in C-fiber nociceptor function occur during vincristine-induced painful peripheral neuropathy, we performed *in vivo* extracellular recordings of single neurons from the saphenous nerve of vincristine-treated rats. C-fiber nociceptor responsiveness to sustained mechanical stimulation was profoundly enhanced in vincristine-treated rats; 45% of C-fiber nociceptors in vincristine-treated rats showed marked hyperresponsiveness ( $124 \pm 5$  action potentials (APs)) as compared to control C-fibers ( $59 \pm 4$  APs). Mean conduction velocities of A-fibers and C-fibers in vincristine-treated rats were significantly slowed. The mean heat and mechanical activation thresholds of C-fibers, the distribution of C-fibers among subclasses, and the percentage of spontaneously active neurons in vincristine-treated rats were not statistically different from controls. Vincristine, therefore, does not cause a generalized alteration of neuronal function, but rather appears to interfere with neural mechanisms underlying the evoked response to external stimulation. Investigation of the mechanisms underlying vincristine-induced C-fiber hyperresponsiveness may lend insight into mechanisms of chemotherapy-induced neuropathic pain, as well as neuropathic pain caused by other insults.

## **Introduction**

Chemotherapy-induced pain is a form of neuropathic pain caused by neurotoxic drugs such as vincristine and taxol and is characterized by painful paresthesias and dysesthesias. The vinca alkaloid vincristine is a widely used antineoplastic agent that is administered alone or in combination with other drugs in the treatment of many tumor types (Weiss et al., 1974; Kaplan and Wiernik, 1982). Vincristine is thought to exert its antineoplastic effects by binding to tubulin in mitotically active cells, disrupting microtubule formation in mitotic spindles, and thus preventing cell division (Olmsted and Borisy, 1973; Himes et al., 1976; Owellen et al., 1976). The clinical antineoplastic efficacy of vincristine is limited by the development of a dose-dependent sensorimotor neuropathy (Sandler et al., 1969; Holland et al., 1973). This sensorimotor neuropathy appears to occur in 2 major stages (Weiss et al., 1974; Kaplan and Wiernik, 1982; McCarthy and Skillings, 1992). In the early stage, peripheral axons are damaged by vincristine and the principal symptoms are paresthesias and dysesthesias. In the later stage, which occurs more frequently at higher doses, axons are lost and the principal finding is loss of motor function.

Recently, we established an animal model of vincristine-induced painful neuropathy in the rat (Aley et al., 1996). Systemic administration of vincristine (100  $\mu\text{g}/\text{kg}$ ), administered intravenously over a 2-week period, produces mechanical hyperalgesia that develops during the second week of vincristine administration and persists for more than a week following the final injection of vincristine. The hyperalgesia is dose-dependent and occurs at doses of vincristine similar to those administered clinically to achieve anti-neoplastic efficacy (McLeod and Penny, 1969; Sandler et al., 1969; Casey et al., 1973; Holland et al., 1973). Higher doses of vincristine also cause loss of motor function in rat (Aley et al., 1996), similar to the later stage of neuropathy in humans. Preliminary anatomical evidence suggests that there is damage to unmyelinated sensory axons before there are any signs of axonal loss in this rat model (Tanner et al., 1997). Therefore, we

propose that vincristine-induced hyperalgesia in the rat is a model of the early stage of vincristine-induced chemotherapeutic neuropathy.

Several lines of evidence suggest that alterations in peripheral nerve function contribute to the sensory alterations in vincristine-induced painful peripheral neuropathy. Systemically administered vincristine does not cross the blood brain barrier to a significant extent (Castle et al., 1976; Greig et al., 1990; Zhou et al., 1990). It has been hypothesized that peripheral neurons are highly sensitive to vincristine because nerve terminal function is dependent on intact axonal transport and maintenance of the peripheral terminal via extremely long axons (Shelanski and Wisniewski, 1969). Interestingly, the paresthesias and dysesthesias reported in humans are most pronounced in the distal extremities (Sandler et al., 1969; Holland et al., 1973), namely those areas innervated by the longest sensory neurons.

To test the hypothesis that changes in the sensitivity and responsiveness of C-fiber nociceptors occur during vincristine-induced hyperalgesia, we used *in vivo* single-unit electrophysiological techniques to examine peripheral sensory neurons in vincristine-treated rats.



## Methods

### *Animals*

Experiments were performed on 200-400 g male Sprague-Dawley rats (Bantin and Kingman, Fremont, CA). Rats were housed in a temperature- and humidity-controlled environment and were maintained on a 12 hour light/dark cycle. Food and water were available *ad libitum*. Experiments were approved by the Committee on Animal Research at UCSF.

### *Vincristine Treatment*

Vincristine sulfate (Sigma, St. Louis, MO) was dissolved in saline to a stock concentration of 1 mg/ml, with pH between 4.5 and 5.2. The drug was then diluted daily in saline to a concentration of 100  $\mu\text{g/ml}$  that was administered intravenously into the tail vein at a dose of 100  $\mu\text{g/kg}$  followed by 0.5 ml saline. Treatments occurred daily (Monday through Friday) for 2 weeks with the dosage calculated on daily body weight. This dosage regimen was chosen because it produced maximal hyperalgesia in the absence of motor impairment in most rats (Aley et al., 1996). Vincristine-treated rats weighed  $309 \pm 7$  g ( $n=35$ ) at the time of electrophysiological recording. Control rats were weight-matched,  $321 \pm 8$  g ( $n=30$ ), and untreated; previous behavioral experiments demonstrated that repeated intravenous saline injections had no effect on behavioral nociceptive threshold (Aley et al., 1996). Experimental rats were used for electrophysiological recordings during the peak phase of chronic vincristine-induced hyperalgesia that occurred in the absence of the drug, that is from 1-5 days following the final injection of vincristine (see Figure 1A). This recording window was chosen based on behavioral data which showed that the mechanical withdrawal threshold of > 90% of vincristine-treated rats was decreased >15% during these 5 days (K.O. Aley and J.D. Levine, unpublished observations). At this dose of vincristine, 18% of rats were euthanized prior to electrophysiological recording because of the development of motor impairment.

*In vivo single unit electrophysiology*

The single-unit electrophysiological recording techniques employed have been described previously (Ahlgren et al., 1992). Briefly, rats were anesthetized with pentobarbital sodium (65 mg/kg i.p.) and additional anesthetic was administered throughout the experiment to maintain areflexia. Recordings were made from the saphenous nerve, the cutaneous nerve that innervates the medial-dorsal hindpaw where mechanical hyperalgesia to vincristine was characterized (Aley et al., 1996). The skin overlying the saphenous nerve was retracted at mid-thigh level. The nerve was exposed and dissected free from surrounding tissue and vessels and maintained in a pool of 37°C mineral oil. Bipolar stimulating electrodes were placed under the nerve at a distal site to enable electrical stimulation (Stimulator S-88, Grass Medical Instruments, Quincy, MA and Stimulus Isolator NL-800, Neurolog, Medical Systems Corp., Greenvale, NY) of peripheral neurons. At a proximal site, a portion of the nerve was desheathed to expose axons. The nerve was crushed proximal to the recording site to prevent the elicitation of flexor reflexes during electrical stimulation of the nerve. Fine fascicles of axons were then dissected from the nerve with sharpened jeweler's forceps and placed on a silver wire recording electrode. Action potentials (APs) from individual fibers were amplified and filtered (Neurolog, Medical Systems Corp., Greenvale, NY) and then stored on tape (Video Cassette Recorder 420K, A. R. Vetter Co., Rebersburg, PA), as well as being discriminated by amplitude (Winston Electronics Co., San Francisco, CA) and displayed on a chart recorder on-line. The animal was sacrificed by pentobarbital overdose at the end of the recording session.

### Characterization of fiber types

#### *Conduction velocity and classification*

Conduction velocity was determined by dividing the distance between the recording and stimulating electrodes, which measured between 20 and 33 mm, by the latency of the AP following an electrical stimulus to the whole nerve. Fibers that conducted at  $<2$  m/s were classified as C-fibers and  $\geq 2$  m/s were classified as A-fibers. Since this study focused on C-fibers we did not further analyze A-fiber subclasses. The percentage of A-fibers versus C-fibers in the nerve was calculated by dividing the number of neurons in each fiber class by the total number of fibers that could be excited by electrical stimulation of the nerve. To determine the number of electrically excitable fibers in each fascicle, the amplitude of the electrical stimulus (0.5 ms, 0.25 Hz) was gradually increased so that the number of C-fibers present could be counted. This process was repeated for each fascicle using shorter duration (0.05 ms) and higher frequency (2.5 Hz) electrical stimulation to quantitate the number of myelinated A-fibers present in the fascicle.

#### *Spontaneous Activity*

To determine the percentage of spontaneously active fibers in the saphenous nerve of control and vincristine-treated rats, activity was monitored in at least 100 fibers for each animal. The percentage of spontaneously active fibers per nerve was calculated by dividing the number of different spontaneously active waveforms present by the total number of electrically excitable fibers observed. Each fascicle was monitored for 2 min, and the number of spontaneously active waveforms quantitated. For each spontaneously active waveform encountered, the rate of ongoing activity was measured for 3 consecutive, 2-min observation periods. These 3 values were averaged, and this number was considered the rate of spontaneous activity for that fiber. If the rate of spontaneous activity was greater than 100 AP/min, a heat lamp was directed towards the receptive field to verify that this

was a cold-sensitive fiber. In all fibers tested with a spontaneous activity rate greater than 100 AP/min, warming the foot decreased the rate of spontaneous activity. In these spontaneous activity experiments, the skin was never mechanically probed nor stimulated with a Peltier heating device to prevent any stimulation-induced afterdischarge from being misclassified as spontaneous activity. No attempt was made to identify the fiber class of the spontaneously active waveforms. In a subset of electrophysiological experiments on control and vincristine-treated rats, both the room temperature and the surface temperature of the contralateral hindpaw was measured using a thermocouple and a digital thermometer (Physitemp, Clifton, N.J.).

### *Characterization of C-fibers*

#### *Modality Classification*

The receptive fields of C-fibers were determined using a mechanical search stimulus, either a blunt probe or a ~60 g von Frey hair (VFH) which activates > 90 % of C-fibers in the saphenous nerve of the rat (Ahlgren et al. 1992, see Figure 4). C-fibers were required to show a slowed conduction velocity in response to electrical stimulation following mechanical stimulation of the receptive field (see Figure 1B). This test established that the mechanical receptive field under study was innervated by the C-fiber whose latency to electrical stimulation was shifted. The receptive fields of C-fibers were determined to be cutaneous if they were activated by lifting and squeezing the skin or if the mechanically sensitive spot moved to a new location when the skin was moved relative to the subcutaneous tissues. Fibers that did not meet this criterion, but were mechanically sensitive were classified as C-deep neurons. All other C-fiber categories were cutaneous. Fibers classified as C-mechanoheats (C-MH) responded to mechanical stimulation and heat stimulation. Fibers classified as C-mechanocolds (C-MC) responded to both mechanical stimulation and cold stimulation. Fibers classified as C-cold (C-C) responded only to cold stimulation. Fibers classified as C-mechanoheatcolds (C-MHC) responded to mechanical,

heat and cold stimulation; it was unclear whether the activation by cold was due to a mechanical alteration of the skin since these fibers always had mechanical thresholds less than 0.02 g. For fibers classified as C-silent, it was not possible to identify a mechanical receptive field; this category presumably included both sympathetic postganglionic neurons and mechanically-insensitive, silent fibers and was not further evaluated.

### *Mechanical Activation Threshold*

Mechanical activation thresholds were determined using a series of von Frey hairs that ranged in intensity from 0.02 - 263 grams (A. Ainsworth, London, England). The mechanical threshold was defined as the intensity in grams of the weakest VFH to which the fiber fired more than 2 AP's in 50% of the trials. Each trial consisted of a brief (~1 sec) application of a VFH to the center of the receptive field. VFH were applied in ascending order, and approximately 5-10 trials were performed for each VFH tested. Threshold was verified by alternately testing the strongest ineffective VFH and the weakest effective VFH. Such repeated mechanical testing of C-fibers does not cause a change in mechanical threshold (K.D. Tanner and J.D. Levine, unpublished observations, (Ahlgren et al., 1992)).

### *Heat Activation Threshold*

Heat activation thresholds were determined using a Peltier device (Thermal Devices Inc., Minneapolis, MN) that delivered a ramped heat stimulus from 30 to 58°C at a rate of 1°C / s. After the Peltier device was placed on the receptive field of a C-fiber, activity was monitored for 2 min to verify the absence of mechanically-induced activity. The heat threshold was defined as the temperature at which the C-fiber fired a second AP. Heat activation threshold was determined twice with a 10-min interstimulus interval. The average of these 2 measurements was the heat activation threshold for that fiber.

### *Cold Activation*

Cold responsiveness was determined using the Peltier device which delivered a ramped cold stimulus from 30 to 0°C at a rate of approximately 1°C / s. After the Peltier device was placed on the receptive field of a C-fiber, activity was monitored for 2 min to verify the absence of any mechanically induced activity. Cold-responsiveness was determined by the presence of an increase in the rate of ongoing activity in a fiber in response to cooling. Threshold was not determined in these fibers due to the presence of ongoing activity. Cold-responsiveness was verified by the presence of an increase in the rate of ongoing activity in a fiber in response to placing either ice or a cooled metal probe above or on the receptive field. In addition, cold-responsiveness was verified by the presence of a decrease in the rate of ongoing activity in a fiber in response to directing a radiant heat lamp towards the fiber's receptive field.

### *Sustained Mechanical Stimulation*

Sustained mechanical stimulation of receptive fields was accomplished by use of a mechanical stimulation device consisting of a force transducer (Entran Devices, Inc., Model ELF-TC500-1, Fairfield, NJ) with a response range of 1-400 g mounted in series with a receptacle that can interchangeably hold von Frey hair filaments (modified from a set of Stoelting VFHs, Wood Dale, IL) that deliver various gram weight stimuli. A 10 g mechanical stimulus was chosen to examine the response properties of nociceptive afferents because this stimulus is suprathreshold for >90 % of C-fibers in the saphenous nerve (see Figure 4). VFH's were used since they are able to compensate well for changes in tissue elasticity over time, unlike rigid probes. The VFH was applied to the receptive field, by hand, and maintained at the just-bent position for 1 min. The voltage output signal from the force transducer was a quantitative measure of the force applied to the receptive field and was sent to both a chart recorder and a VCR tape for display, storage, and off-line analysis.

For each fiber whose response to prolonged stimulation was studied, the conduction velocity, receptive field location, baseline spontaneous activity, and mechanical threshold were determined. Due to physical constraints, only C-fibers with receptive fields below the ankle were studied. To avoid inadvertently recording the response properties of slowed A $\delta$ -fibers (see Results, Figure 2), only C-fibers that conducted at less than 1 m/s were studied. Since some vincristine-treated fibers develop an afterdischarge following mechanical stimulation (see Table 3), we did not record from C-fibers that fired >5 AP/min during the 2-min observation period to avoid recording from those fibers that may have developed ongoing activity following mechanical search stimulation of the skin; these fibers comprised <10 % of the population. In general, the prolonged stimulation protocol consisted of 4 trials of sustained 1-min mechanical stimulation with a 10-min interstimulus interval between trials. The average of these 4 trials was the sustained mechanical stimulation response for that fiber and usually had a standard error of the mean of less than 10%. In a small number of cases included in the analysis, more trials were conducted to reduce the standard error or fewer trials were conducted because the fiber was lost. Activity was monitored for 5 min after the removal of the mechanical stimulus to quantitate afterdischarge.

### *Data Analysis*

Data are expressed as mean  $\pm$  standard error of the mean (SEM). Statistical analyses were done using Student's t-test, analysis of variance (ANOVA), Chi square analysis, or Mann-Whitney U test, as appropriate.

## Results

In this study, data were collected from 35 vincristine-treated rats and 30 control rats. Vincristine-treated rats did not gain weight normally during the course of the treatment, as has been described previously (Aley et al., 1996). There was an average decrease in body weight during vincristine treatment of  $5.6 \pm 1.8\%$ , although this varied substantially from rat to rat.

### *Vincristine causes a slowing of the conduction velocity of sensory neurons*

As shown in Figure 2A the mean conduction velocity of C-fibers in vincristine-treated rats ( $0.60 \pm 0.006$  m/s,  $n = 693$ ) is significantly ( $p < 0.001$ ) slower than that of C-fibers in control rats ( $0.67 \pm 0.01$  m/s,  $n = 401$ ). Similarly, as shown in Figure 2B, the mean conduction velocity of A-fibers in vincristine-treated rats ( $18.1 \pm 0.4$  m/s,  $n=561$ ) is significantly ( $p < 0.001$ ) slower than that of A-fibers in control rats ( $21.8 \pm 0.6$  m/s,  $n = 264$ ).

### *Vincristine does not increase spontaneous activity in sensory neurons*

As shown in Table 1, both the average rate of spontaneous activity and the percentage of spontaneously active fibers in vincristine-treated rats is lower than that in control rats. These differences, while not significant ( $p > 0.05$ , t-test), reflect a significant ( $p < 0.02$ , Chi square) decrease in the proportion of fibers that have rates of spontaneous activity  $>100$  AP/min. In both vincristine-treated and control rats, the distribution of rates of spontaneous activity was bimodal with peaks at  $<10$  AP/min and  $>100$  AP/min (data not shown). However, in vincristine-treated rats there were less than half as many fibers with firing rates  $>100$  AP/min than in control rats. In all cases tested, fibers with rates of spontaneous activity  $> 100$  AP / min were cold-sensitive. To verify that this difference in the spontaneous activity of cold-sensitive fibers was not due to differences in skin temperature, the paw temperatures of anesthetized vincristine-treated rats and control rats



were measured and averaged over the course of the recording session. There was no significant difference ( $p > 0.05$ ) between the paw temperature of control ( $24.6 \pm 0.7$  °C,  $n = 9$ ) and vincristine-treated rats ( $24.2 \pm 0.7$  °C,  $n = 9$ ).

*Vincristine does not cause a selective loss of A-fibers or C-fibers*

The proportion of A-fibers ( $44.6 \pm 1.4\%$ ,  $n = 14$  rats) and C-fibers ( $55.4 \pm 1.4\%$ ,  $n = 14$  rats) present in the saphenous nerve of vincristine-treated rats is similar ( $p > 0.05$ ) to the proportion of A-fibers ( $41.2 \pm 1.6\%$ ,  $n = 8$  rats) and C-fibers ( $58.8 \pm 1.6\%$ ,  $n = 8$  rats) in control rats.

*Vincristine does not alter the distribution of C-fibers among functional subclasses*

As shown in Table 2, vincristine-treated rats have a similar distribution of C-fiber afferents among functional subclasses (i.e. C-MH, C-M, C-MC, C-C, C-MHC, C-DEEP, and C-SILENT) to control rats ( $p > 0.05$ , Chi square). Of note, there is no clear decrease in the percentage of cold-responsive C-fibers in vincristine-treated rats as compared to control rats.

*Vincristine does not decrease the heat activation threshold of C-fibers*

In addition, as shown in Figure 3, the average heat thresholds of vincristine-treated C-fibers ( $48.3 \pm 1.1$ °C,  $n = 18$ ) are not statistically different ( $p > 0.05$ ) from those of control C-fibers ( $46.8 \pm 0.7$ °C,  $n = 29$ ).

*Vincristine does not decrease the mechanical activation threshold of C-fibers*

As shown in Figure 4, the average mechanical threshold for control C-fibers ( $2.6 \pm 0.9$  g,  $n = 44$ ) was higher than but not significantly different ( $p = 0.51$ , Mann-Whitney U test) from the average mechanical threshold for vincristine-treated C-fibers ( $4.5 \pm 1.8$  g,

n = 38).

*Vincristine increases responsiveness to sustained mechanical stimulation in a subset of C-fibers*

To assay responsiveness of C-fibers to sustained mechanical stimulation, a 10 g stimulus was delivered to the receptive field for 1 min. Figure 5 demonstrates the reproducibility of this sustained mechanical stimulus, as well as the reproducibility of the response of a C-fiber to this stimulus over the course of 4 trials, each of which was followed by a 10-min interstimulus interval.

Examples of responses of C-fibers from control and vincristine-treated rats are shown in Figure 6. Figure 6A shows the post-stimulus time histogram response of a representative C-fiber from a control rat that had a mechanical threshold of 1.7 g and a conduction velocity of 0.78 m/s. Figure 6B shows the post-stimulus time histogram response of an individual C-fiber from a vincristine-treated rat that also had a mechanical threshold of 1.7 g and a conduction velocity of 0.62 m/s. This vincristine-treated C-fiber fired more than twice as many APs as the control C-fiber and is representative of a subpopulation of hyperresponsive C-fibers found in vincristine-treated rats.

A histogram of the distribution of C-fiber responses to a 10 g, 1 min sustained mechanical stimulus is plotted for all C-fibers studied from control and vincristine-treated rats in Figure 7. Whereas the responses of C-fibers from control rats are clustered in a unimodal distribution in the 50-59 AP bin, the responses of C-fibers from vincristine-treated rats form 2 distinct clusters in a bimodal distribution with a cluster around the 50-59 AP / stimulus and another at the 100-109 AP / stimulus and greater. The responses of 55% of vincristine-treated C-fibers were similar to the responses of control C-fibers. This group of C-fibers, defined as those that fire less than 100 AP in response to sustained mechanical stimulation, will be referred to as "low-firing" C-fibers. The other 45% of vincristine-treated C-fibers were hyperresponsive (n = 9), firing approximately twice as many APs as

the response of a typical control C-fiber and will be referred to as "high-firing" C-fibers. Of 21 C-fibers studied from control rats, only 1 had a response similar to the subpopulation of high-firing, hyperresponsive C-fibers in vincristine-treated rats (see Figure 7). Interestingly, the responses of control C-fibers were quite similar to each other, regardless of their mechanical thresholds which ranged from 0.4 g to 4.6 g (see Figure 9C).

Figure 8 shows the time course of the average C-fiber responses to sustained mechanical stimulation in control and vincristine-treated rats. As seen in Figure 8A, the time course of the average response of all vincristine-treated C-fibers (■) to a sustained mechanical stimulus, including both low-firing and high-firing C-fibers, was significantly ( $p < 0.01$ ) greater than the average response of all control C-fibers (□). As seen in Figure 8B, when vincristine-treated C-fibers are considered as 2 distinct populations, the time course of the average response of low-firing vincristine-treated C-fibers (●) is indistinguishable ( $p > 0.05$ ) from that of all control C-fibers (□); however, the time course of the average response of high-firing vincristine-treated C-fibers (▲) was significantly increased ( $p < 0.0001$ ) compared to that of all control C-fibers (□). The hyperresponsiveness in vincristine-treated C-fibers occurs during the burst, but is more pronounced during the plateau phase of the C-fiber response (10 - 60 s after the onset of the stimulus).

As shown in Table 3, the increased responsiveness in high-firing vincristine-treated C-fibers was significant ( $p < 0.01$ ) both during the burst (first 10 sec) and the plateau (last 50 sec) of the 1 min response. Interestingly, there was also a significant afterdischarge in high-firing vincristine-treated C-fibers ( $p < 0.05$ ) that was not present in low-firing vincristine-treated or control C-fibers. It is important to note that this afterdischarge occurred in only a few of the high-firing vincristine-treated C-fibers. The single hyperresponsive, high-firing C-fiber seen in control rats had a response to sustained mechanical stimulation similar to that of the hyperresponsive vincristine-treated C-fibers (data not shown separately).

Lastly, as shown in Figure 9, hyperresponsiveness in the subpopulation of high-firing C-fibers in vincristine-treated rats does not correlate with receptive field location, conduction velocity, or mechanical threshold. The data presented in Figure 9 are from those C-fibers whose responses to sustained mechanical stimulation was studied. As shown in Figure 9A, high-firing C-fibers in vincristine-treated rats do not appear to be located in any specific skin regions of the dorsal hindpaw. As shown in Figure 9B, the average conduction velocity of all vincristine-treated C-fibers ( $0.75 \pm 0.02$  m/s,  $n = 20$ ) tended to be slower ( $p = 0.08$ ) than the average conduction velocity of all control C-fibers ( $0.80 \pm 0.02$  m/s,  $n = 21$ ), which was consistent with previous findings (see Figure 2A). The average conduction velocity of low-firing C-fibers ( $0.74 \pm 0.03$  m/s,  $n = 11$ ) in vincristine-treated rats was not different ( $p > 0.05$ ) from the average conduction velocity of hyperresponsive, high-firing C-fibers ( $0.76 \pm 0.03$  m/s,  $n = 9$ ) in vincristine-treated rats. As shown in Figure 9C, there was no significant difference between the average mechanical threshold of all control C-fibers ( $1.5 \text{ g} \pm 0.3$  m/s,  $n = 21$ ) and that of all vincristine-treated C-fibers ( $2.1 \text{ g} \pm 0.4$  m/s,  $n = 20$ ), though there was a trend ( $p = 0.18$ ) for vincristine-treated C-fibers to have higher mechanical thresholds, which was consistent with previous findings (see Figure 4). In addition, the average mechanical threshold of low-firing C-fibers ( $2.0 \text{ g} \pm 0.6$  m/s,  $n = 11$ ) in vincristine-treated rats was similar ( $p > 0.05$ ) to that of hyperresponsive, high-firing C-fibers ( $2.3 \text{ g} \pm 0.6$  m/s,  $n = 9$ ) in vincristine-treated rats.

## Discussion

The neural mechanisms underlying neuropathic pain following a wide variety of insults to peripheral nerves including metabolic disorders, traumatic injury, and neurotoxic drugs are largely unknown. Specifically, the neural mechanisms of chemotherapy-induced neuropathic pain that is caused by neurotoxic drugs such as vincristine and taxol and that occurs in cancer patients have not been investigated. In this study, we have characterized C-fiber function during the peak phase of vincristine-induced neuropathy in the rat. The finding that approximately half of vincristine-treated C-fibers exhibit a marked hyperresponsiveness to sustained mechanical stimulation while most other aspects of nociceptor function were unaffected is striking. There was no increase in C-fiber sensitivity as measured by mechanical and heat activation thresholds, rather there was a trend for the mechanical activation thresholds of C-fibers to be *higher* than that of controls. Interestingly, there was also no increase in the level of spontaneous activity, a change that has been reported in other models of neuropathic pain (Wall and Gutnick, 1974; Xie and Xiao, 1990; Kajander and Bennett, 1992; Devor, 1994). A significant slowing of conduction velocity was evident in sensory fibers from both the A-fiber and C-fiber classes, consistent with the magnitude of slowing seen in humans with vincristine-induced neuropathy ((McLeod and Penny, 1969; Casey et al., 1973) although see (Sandler et al., 1969)). Interestingly, a slowing of conduction velocity, often used clinically as a hallmark of peripheral neuropathy, did not correlate with C-fiber hyperresponsiveness to sustained mechanical stimulation (see Figure 9B). Finally, there was no change in the proportion of C-fibers in each class in vincristine-treated rats as compared to control rats. These data suggest that vincristine interferes with neural mechanisms underlying the evoked response to external stimulation, rather than causing a generalized alteration of C-fiber nociceptor function.

### Mechanism of vincristine-induced C-fiber hyperresponsiveness to sustained mechanical stimulation

The profile of electrophysiological changes suggests that vincristine affects mechanical transduction and/or mechanisms underlying adaptation during a response to sustained stimulation. The mechanisms of vincristine-induced hyperresponsiveness to mechanical stimulation are likely to involve its known actions on the microtubular cytoskeleton. Vincristine has been shown *in vitro* to cause the depolymerization of microtubules and *in vivo* to compromise axonal integrity and cause dissolution of the cytoskeletal structure in the peripheral nerve of a variety of species, including humans (Gottschalk et al., 1968; Shelanski and Wisniewski, 1969; Green et al., 1977; Sahenk et al., 1987). In fact, recent ultrastructural analysis of unmyelinated axons in the peripheral nerve of vincristine-treated rats during the peak phase of hyperalgesia revealed disorientation of microtubules and swelling of unmyelinated axons without any signs of axonal degeneration were evident (Tanner et al., 1997).

C-fiber hyperresponsiveness in vincristine-treated rats may be the result of an action of vincristine on mechanisms underlying transduction of mechanical stimuli. Although the mechanisms of mechanical transduction are unknown, a role for cytoskeletal elements has been postulated (Guharay and Sachs, 1984; Wang et al., 1993). In *C. elegans*, sensory neurons required for mechanosensation express a unique class of microtubules that are required for touch sensitivity (Chalfie, 1993). If the microtubular cytoskeleton is required for mechanotransduction in vertebrate somatic afferents, then vincristine-induced C-fiber hyperresponsiveness may be restricted to mechanical stimulation. Further characterization of the behavioral and electrophysiological responses of vincristine-treated rats to heat and chemical stimulation could reveal whether C-fiber hyperresponsiveness occurs in response to other stimulus modalities.

The C-fiber hyperresponsiveness we observed might also stem from an impairment of electrophysiological adaptation mechanisms. Several lines of evidence suggest that

cytoskeletal elements can regulate the subcellular localization and kinetics of ion channel activation (Srinivasan et al., 1988; Bigot and Hunt, 1990; Kirsch et al., 1991; Rosenmund and Westbrook, 1993). Hyperresponsiveness is most pronounced during the adaptation phase of the response, namely from 10-60 s after the stimulus is applied. If conductances involved in adaptation of mechanical responses were similarly regulated by the microtubular cytoskeleton, then vincristine might impair adaptation mechanisms in the nerve fiber terminal.

Several investigators have proposed that impairment of axonal transport might underlie vincristine-induced neuropathy (Shelanski and Wisniewski, 1969; Bradley et al., 1970; Casey et al., 1973; Weiss et al., 1974). Subsequent alteration of the complement of proteins present in the nerve terminal may contribute to changes in the excitability of C-fibers, as has been suggested for the axotomy model of neuropathy (Devor et al., 1993).

Lastly, although vincristine is thought to most profoundly affect peripheral neurons, it might also affect non-neuronal cells including muscle and epithelial tissues. Higher doses of vincristine have been shown to produce myopathy characterized by degeneration of muscle fibers when administered systemically in the rat (Slotwiner et al., 1966). Thus, vincristine might also alter sensory neuron function indirectly.

#### C-fiber dysfunction in vincristine-induced neuropathy is distinct from that seen in inflammation

The profile of changes seen in vincristine-treated C-fibers is markedly different from the profile seen following inflammation or the administration of a single inflammatory mediator. Following inflammatory insults, C-fibers characteristically have lower activation thresholds, as well as increased responsiveness to a sustained stimulus. In contrast, the mechanical activation thresholds of vincristine-treated C-fibers are not lowered. This suggests that the cellular mechanisms that underlie C-fiber nociceptor sensitization following inflammation may be distinct from those underlying C-fiber dysfunction

observed in neuropathy. Furthermore, the dissociation between changes in activation threshold and changes in stimulus-response properties suggests that these neuronal properties can be independently regulated and may have distinct underlying molecular mechanisms.

#### Relationship of C-fiber dysfunction in vincristine-induced neuropathy to that seen in other neuropathies

Interestingly, the C-fiber hyperresponsiveness to mechanical stimulation seen in vincristine-treated rats is similar to C-fiber dysfunction observed in a rat model of diabetic painful peripheral neuropathy (Ahlgren et al., 1992; Ahlgren and Levine, 1994). In diabetic neuropathy, protein kinase C (PKC) is involved in the hyperresponsiveness of C-fibers during mechanical stimulation (Ahlgren and Levine, 1994). If a similar mechanism underlies hyperresponsiveness in the vincristine-treated C-fibers, then PKC inhibitors should similarly reverse vincristine-induced hyperresponsiveness and hyperalgesia. The relationship between an action of vincristine on microtubules and a potential role for PKC in vincristine-induced neuropathy remains to be elucidated. One possibility is that  $Ca^{2+}$  entry via mechanotransducers (Lumpkin and Hudspeth, 1995) could couple changes in cytoskeletal function and cellular recruitment of PKC.

Electrophysiological properties of diabetic and vincristine-treated nerves are relatively normal with the exception of hyperresponsiveness and decreased adaptation to prolonged mechanical stimulation. These common alterations in C-fiber function in 2 models of painful peripheral neuropathy with very different etiologies suggests that there may be common underlying mechanisms of dysfunction following a wide variety of insults to nerves. It is not known if hyperresponsiveness to mechanical stimulation is a feature of other neuropathy models such as the chronic constriction injury model (Bennett and Xie, 1988) or the partial nerve transection model (Seltzer et al., 1990), although there is preliminary evidence of heat hyperresponsiveness of C-fibers in the former (Koltzenburg et



al., 1994). In these other neuropathy models, however, there are increases in the level of spontaneous or ectopic activity, originating in both A- and C-fibers (Wall and Gutnick, 1974; Xie and Xiao, 1990; Kajander and Bennett, 1992; Devor, 1994) which are not observed in either vincristine-induced or diabetic neuropathy (Ahlgren et al., 1992). The increase in spontaneous activity seen in these other models of neuropathic pain may reflect additional changes in peripheral nerve function that occur with more extensive damage of the nerve.

If common peripheral mechanisms exist for multiple classes of peripheral neuropathies (toxic, traumatic, and metabolic), then the underlying pathophysiology of peripheral nerve injury could be mechanistically dissected and treatment strategies could be more rationally designed. In addition, an understanding of common changes in peripheral nerve function in a variety of neuropathic states would facilitate the further dissection of central nervous system mechanisms which may also contribute to neuropathic pain.

#### Role of C-fiber hyperresponsiveness in vincristine-induced hyperalgesia and neuropathy

The hyperresponsive subpopulation of C-fibers that we have described could, in part, be the neural basis of vincristine-induced hyperalgesia in rat and early stage vincristine-induced painful neuropathy in humans. These hyperresponsive C-fibers could directly cause hyperalgesia by increasing nociceptive afferent input to the central nervous system. Increased afferent input has been shown to increase the responsiveness of spinal cord dorsal horn neurons which could also contribute to the behavioral hyperalgesia (for review see Woolf & Doubell 1994). In addition, hyperresponsive C-fibers could make a greater contribution to the behavioral reflex indirectly if the gain of their input to the spinal cord were potentiated by virtue of their hyperexcitability; thus, even though only 45% of vincristine-treated C-fibers are hyperresponsive, they may more effectively activate dorsal horn neurons and predominantly drive the behavioral reflex.

In conclusion, we have shown that C-fiber nociceptor responsiveness to sustained mechanical stimulation was profoundly enhanced during the peak phase of vincristine-induced mechanical hyperalgesia in the rat. This abnormality in C-fiber function could underlie, at least in part, the behavioral mechanical hyperalgesia observed in chronically vincristine-treated rats, as well as the paresthesias and dysesthesias experienced by patients receiving vincristine as a chemotherapeutic agent.

## References

Ahlgren SC, Levine JD (1994). Protein kinase C inhibitors decrease hyperalgesia and C-fiber hyperexcitability in the streptozotocin-diabetic rat. *J Neurophysiol* 72, 684-692.

Ahlgren SC, White DM, Levine JD (1992). Increased responsiveness of sensory neurons in the saphenous nerve of the streptozotocin-diabetic rat. *J Neurophysiol* 68, 2077-2085.

Aley KO, Reichling DB, Levine JD (1996). Vincristine hyperalgesia in the rat: a model of painful vincristine neuropathy in humans. *Neuroscience* 73, 259-265.

Bennett GJ, Xie YK (1988). A peripheral mononeuropathy in rat that produces disorders of pain sensation like those seen in man. *Pain* 33, 87-107.

Bigot D, Hunt SP (1990). Effect of excitatory amino acids on microtubule-associated proteins in cultured cortical and spinal neurones. *Neurosci Lett* 111, 275-280.

Bradley WG, Lassman LP, Pearce GW, Walton JN (1970). The neuromyopathy of vincristine in man. Clinical, electrophysiological and pathological studies. *J Neurol Sci* 10, 107-131.

Casey EB, Jelliffe AM, Le QP, Millett YL (1973). Vincristine neuropathy. Clinical and electrophysiological observations. *Brain* 96, 69-86.

Castle MC, Margileth DA, Oliverio VT (1976). Distribution and excretion of (3H)vincristine in the rat and the dog. *Cancer Res* 36, 3684-3689.

Chalfie M (1993). Touch receptor development and function in *Caenorhabditis elegans*. *J Neurobiol* 24, 1433-1441.

Devor M (1994). The pathophysiology of damaged peripheral nerves. In *Textbook of Pain*, PD Wall, R Melzack, ed. (Edinburgh: Churchill Livingstone), pp. 79-100.

Devor M, Govrin Lippmann R, Angelides K (1993). Na<sup>+</sup> channel immunolocalization in peripheral mammalian axons and changes following nerve injury and neuroma formation. *J Neurosci* 13, 1976-1992.

Gottschalk PG, Dyck PJ, Kiely JM (1968). Vinca alkaloid neuropathy: nerve biopsy studies in rats and in man. *Neurology* 18, 875-882.

Green LS, Donoso JA, Heller BI, Samson FE (1977). Axonal transport disturbances in vincristine-induced peripheral neuropathy. *Ann Neurol* 1, 255-262.

Greig NH, Soncrant TT, Shetty HU, Momma S, Smith QR, Rapoport SI (1990). Brain uptake and anticancer activities of vincristine and vinblastine are restricted by their low cerebrovascular permeability and binding to plasma constituents in rat. *Cancer Chemother Pharmacol* 26, 263-268.

Guharay F, Sachs F (1984). Stretch-activated single ion channel currents in tissue-cultured embryonic chick skeletal muscle. *J Physiol (Lond)* 352, 685-701.

Himes RH, Kersey RN, Heller BI, Samson FE (1976). Action of the vinca alkaloids vincristine, vinblastine, and desacetyl vinblastine amide on microtubules in vitro. *Cancer Res* 36, 3798-3802.

Holland JF, Scharlau C, Gailani S, Krant MJ, Olson KB, Horton J, Shnider BI, Lynch JJ, Owens A, Carbone PP, Colsky J, Grob D, Miller SP, Hall TC (1973). Vincristine treatment of advanced cancer: a cooperative study of 392 cases. *Cancer Res* 33, 1258-1264.

Kajander KC, Bennett GJ (1992). Onset of a painful peripheral neuropathy in rat: a partial and differential deafferentation and spontaneous discharge in A beta and A delta primary afferent neurons. *J Neurophysiol* 68, 734-744.

Kaplan RS, Wiernik PH (1982). Neurotoxicity of antineoplastic drugs. *Semin Oncol* 9, 103-130.

Kirsch J, Langosch D, Prior P, Littauer UZ, Schmitt B, Betz H (1991). The 93-kDa glycine receptor-associated protein binds to tubulin. *J Biol Chem* 266, 22242-22245.

Koltzenburg M, Kees S, Budweiser S, Ochs G, Toyka K (1994). The properties of unmyelinated nociceptive afferents change in a painful chronic constriction neuropathy. In *Proc 7th World Cong Pain*, G Gebhart, D Hammond, T Jensen, ed. (Seattle: IASP Press), pp. 511-522.

Lumpkin EA, Hudspeth AJ (1995). Detection of Ca<sup>2+</sup> entry through mechanosensitive channels localizes the site of mechano-electrical transduction in hair cells. *Proc Natl Acad Sci U S A* 92, 10297-10301.

McCarthy GM, Skillings JR (1992). Jaw and other orofacial pain in patients receiving vincristine for the treatment of cancer. *Oral Surg Oral Med Oral Pathol* 74, 299-304.

McLeod JG, Penny R (1969). Vincristine neuropathy: an electrophysiological and histological study. *J Neurol Neurosurg Psychiatry* 32, 297-304.

Olmsted JB, Borisy GG (1973). Microtubules. *Annu Rev Biochem* 42, 507-540.

Owellen RJ, Hartke CA, Dickerson RM, Hains FO (1976). Inhibition of tubulin-microtubule polymerization by drugs of the Vinca alkaloid class. *Cancer Res* 36, 1499-1502.

Rosenmund C, Westbrook GL (1993). Calcium-induced actin depolymerization reduces NMDA channel activity. *Neuron* 10, 805-814.

Sahenk Z, Brady ST, Mendell JR (1987). Studies on the pathogenesis of vincristine-induced neuropathy. *Muscle Nerve* 10, 80-84.

Sandler SG, Tobin W, Henderson ES (1969). Vincristine-induced neuropathy. A clinical study of fifty leukemic patients. *Neurology* 19, 367-374.

Seltzer Z, Dubner R, Shir Y (1990). A novel behavioral model of neuropathic pain disorders produced in rats by partial sciatic nerve injury. *Pain* 43, 205-218.

Shelanski ML, Wisniewski H (1969). Neurofibrillary degeneration induced by vincristine therapy. *Arch Neurol* 20, 199-206.

Slotwiner P, Song SK, Anderson PJ (1966). Spheromembranous degeneration of muscle induced by vincristine. *Arch Neurol* 15, 172-176.

Srinivasan Y, Elmer L, Davis J, Bennett V, Angelides K (1988). Ankyrin and spectrin associate with voltage-dependent sodium channels in brain. *Nature* 333, 177-180.

Tanner K, Levine J, Topp K (1997). Microtubule disorientation and axonal swelling in unmyelinated sensory axons during vincristine-induced painful neuropathy in rat. *J. Neurosci.* *submitted*.

Wall PD, Gutnick M (1974). Ongoing activity in peripheral nerves: the physiology and pharmacology of impulses originating from a neuroma. *Exp Neurol* 43, 580-593.

Wang N, Butler JP, Ingber DE (1993). Mechanotransduction across the cell surface and through the cytoskeleton. *Science* 260, 1124-1127.

Weiss HD, Walker MD, Wiernik PH (1974). Neurotoxicity of commonly used antineoplastic agents (second of two parts). *N Engl J Med* 291, 127-133.

Woolf CJ, Doubell TP (1994). The pathophysiology of chronic pain--increased sensitivity to low threshold A beta-fibre inputs. *Curr Opin Neurobiol* 4, 525-534.

Xie YK, Xiao WH (1990). Electrophysiological evidence for hyperalgesia in the peripheral neuropathy. *Sci China [b]* 33, 663-672.

Zhou XJ, Martin M, Placidi M, Cano JP, Rahmani R (1990). In vivo and in vitro pharmacokinetics and metabolism of vincaalkaloids in rat. II. Vinblastine and vincristine. *Eur J Drug Metab Pharmacokinet* 15, 323-332.



**Figure 1: Experimental paradigm and electrophysiological recording period.**

**A:** Schematic of the experimental timeline. Rats were injected i.v. with 100  $\mu\text{g}/\text{kg}$  vincristine sulfate (V) on days 1-5 and days 8-12. The magnitude of mechanical hyperalgesia in vincristine-treated rats is shown schematically above the timeline (Aley et al., 1996). The arrow in the figure shows the period during which electrophysiological recordings were made from sensory fibers in the saphenous nerves of vincristine-treated rats, namely on days 13-17, during the peak of behavioral mechanical hyperalgesia. All recordings on day 13 occurred more than 24 hours after the final dose of the drug. Data from the 5 recording days were pooled. **B:** Each C-fiber studied was required to show a slowed conduction velocity in response to electrical stimulation following mechanical stimulation of the receptive field. This "collision test" established that the mechanical receptive field under study was innervated by the C-fiber whose latency to electrical stimulation was shifted. The top trace shows the activation of a C-fiber with a latency of 46 ms in response to electrical stimulation of the whole nerve. The bottom trace shows electrical activation of the same C-fiber, now with a latency of 56 ms, following mechanical stimulation of its receptive field. This C-fiber had a conduction velocity of 0.70 m/s and a mechanical threshold of 1.7 g. Note that another fiber conducted at 16 ms both before and after the collision test.

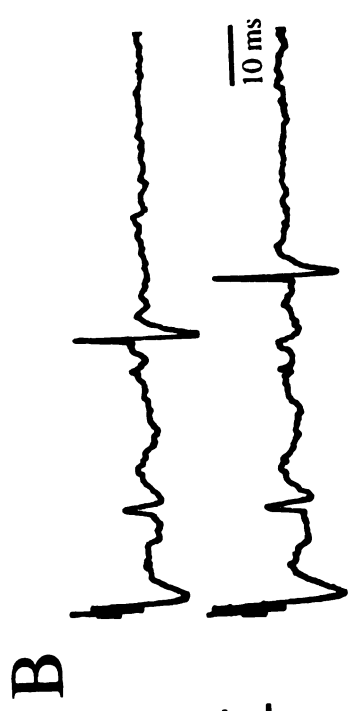
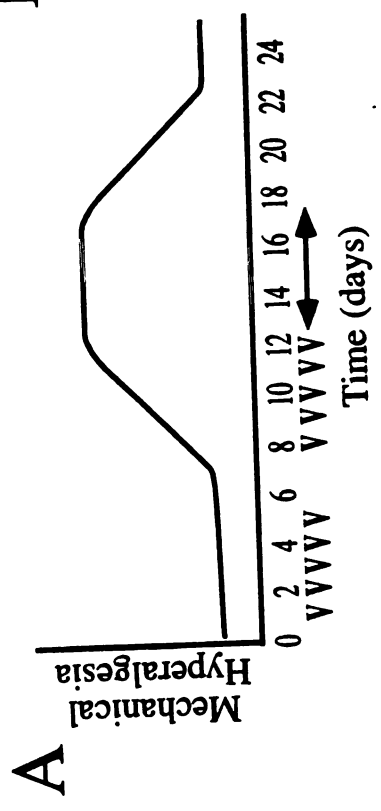


**Figure 2: Vincristine causes a slowing of the conduction velocity of both A-fibers and C-fibers.** Conduction velocities were determined by dividing the distance between the recording and stimulating electrodes by the latency of an individual AP from an afferent following an electrical stimulus to the whole nerve. The filled bars represent data from vincristine-treated rats and the open bars represent data from control rats. **A:** The distribution of C-fiber conduction velocities is shown in the histogram on the left for 693 vincristine-treated C-fibers and 401 control C-fibers. Binwidth is 0.1 m/s. The average C-fiber conduction velocity in control and vincristine-treated rats is depicted in the bar graph on the right; these averages were calculated from the values in the histogram on the left. Error bars in this and subsequent figures represent standard error of the mean (SEM). **B:** The distribution of A-fiber conduction velocities is shown in the histogram on the left for 561 vincristine-treated A-fibers and 264 control A-fibers. Binwidth is 2 m/s. The average A-fiber conduction velocity in control and vincristine-treated rats is depicted in the bar graph on the right; these averages were calculated from the values in the histogram on the left.

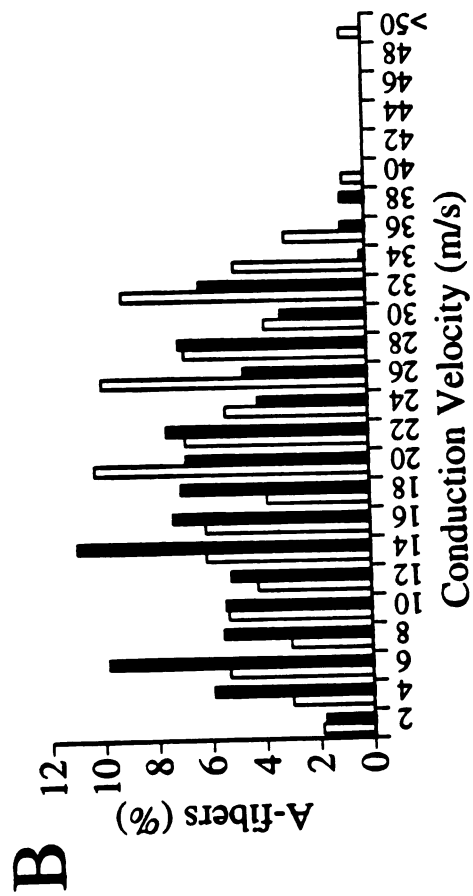
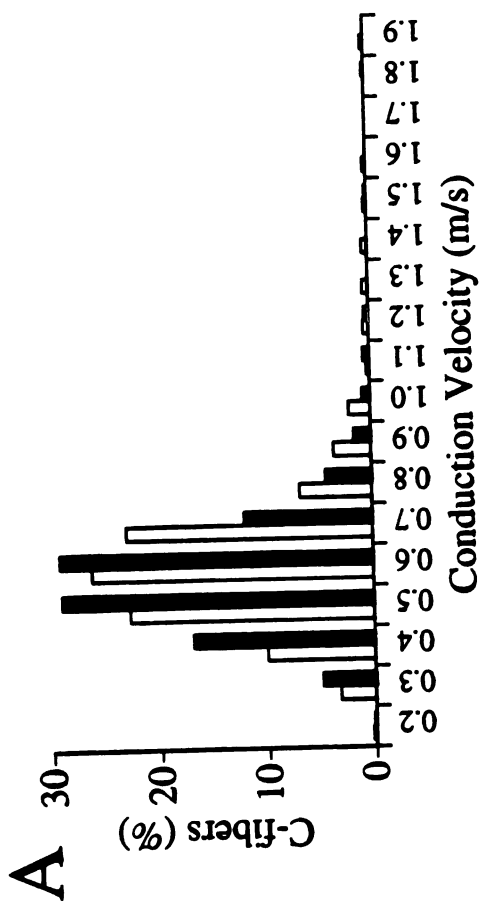
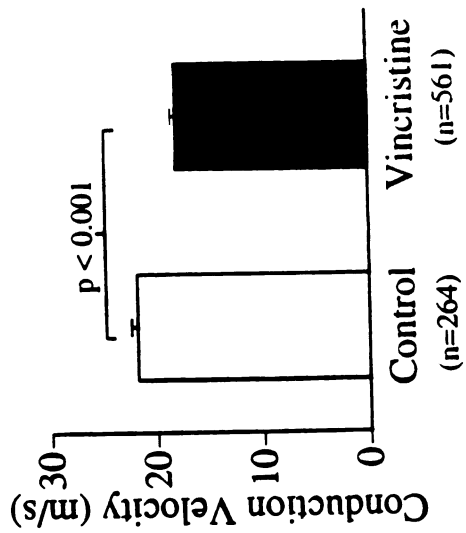
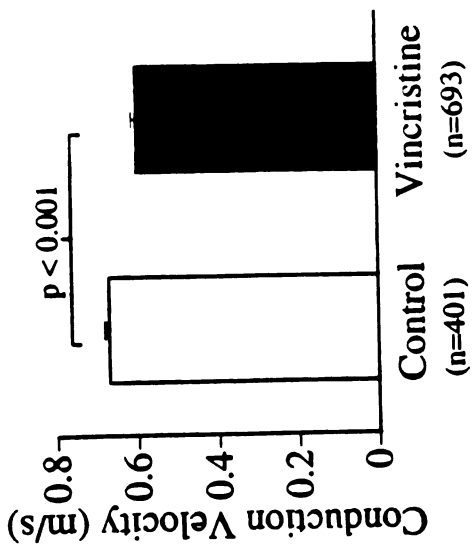


**Figure 3: Vincristine does not decrease the heat activation threshold of C-fibers.** Heat activation thresholds were determined using a Peltier device that delivered a ramped heat stimulus from 30 to 58°C at a rate of 1°C/ s. Heat threshold was defined as the temperature at which the C-fiber fired a second AP. Each heat activation threshold was the average of 3 trials with a 10 min interstimulus interval between trials. **A:** The distribution of C-fiber heat activation thresholds is shown in the histogram for 18 vincristine-treated C-fibers and 29 control C-fibers. Binwidth is 2°C. **B:** The average heat activation threshold for control C-fibers is shown by the open bar and for vincristine-treated C-fibers is shown by the filled bar.

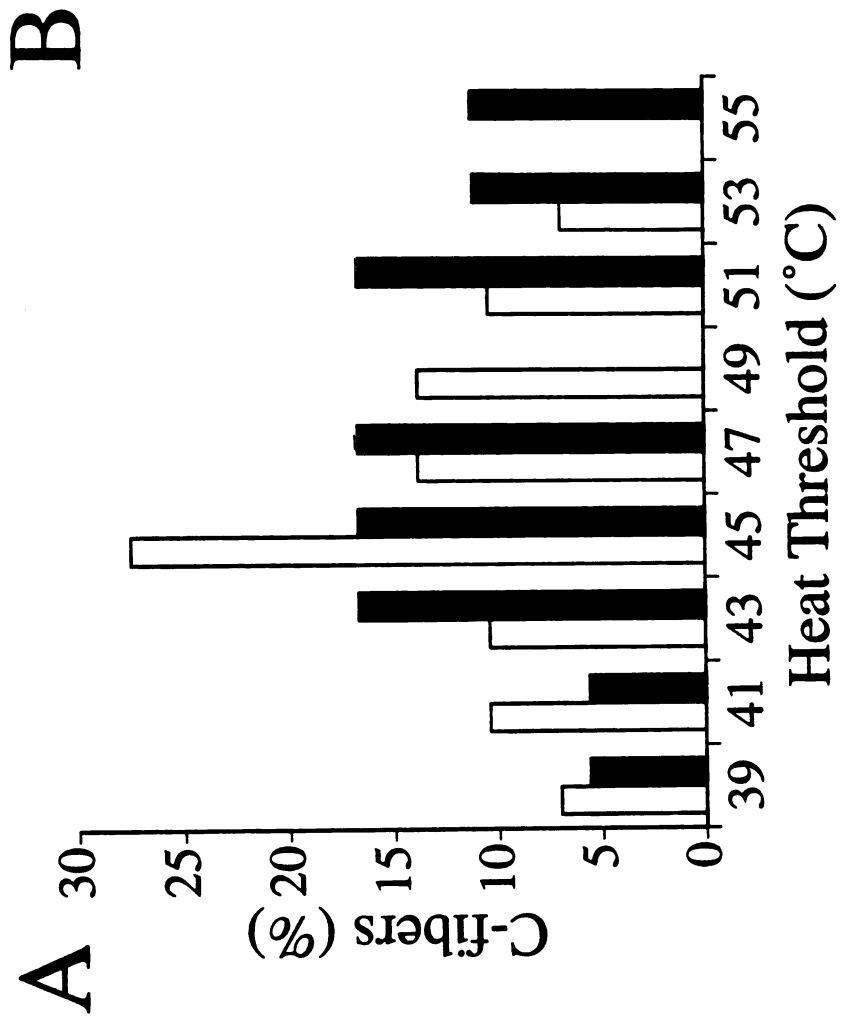
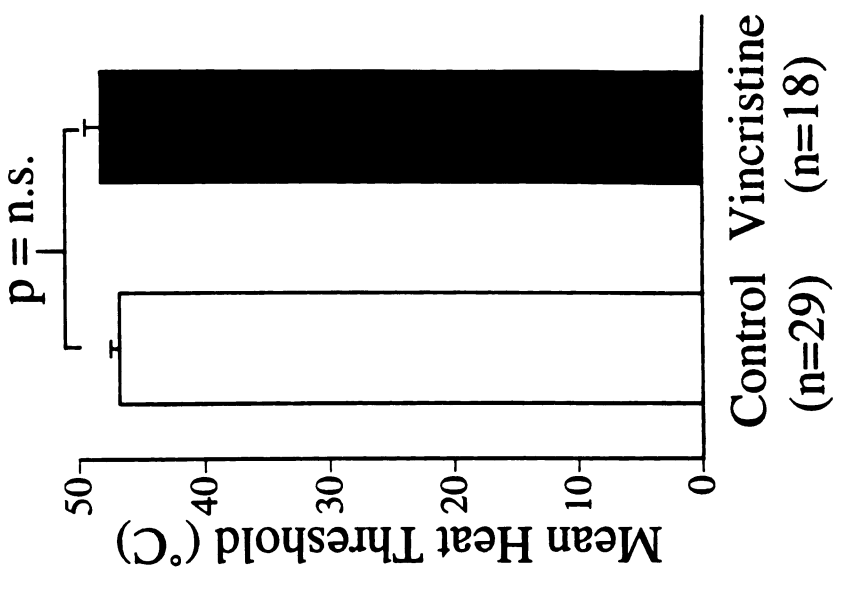
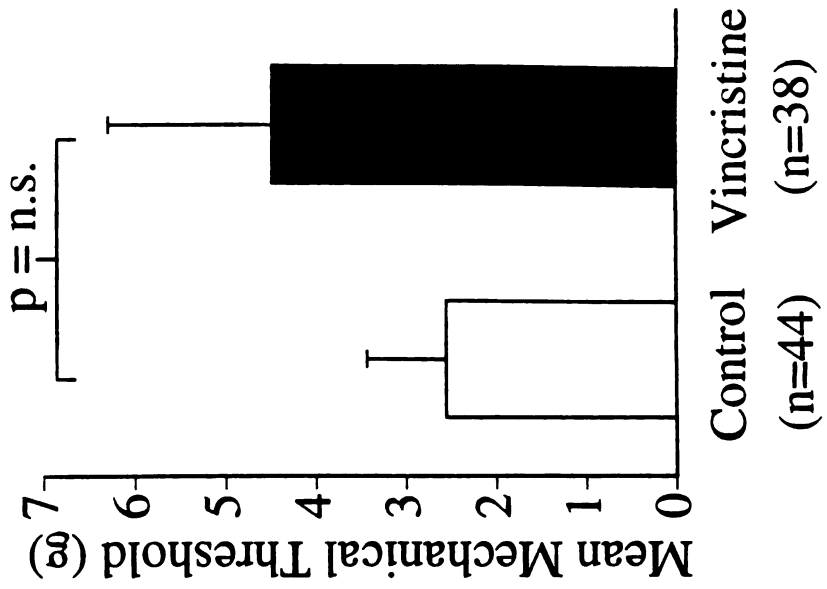
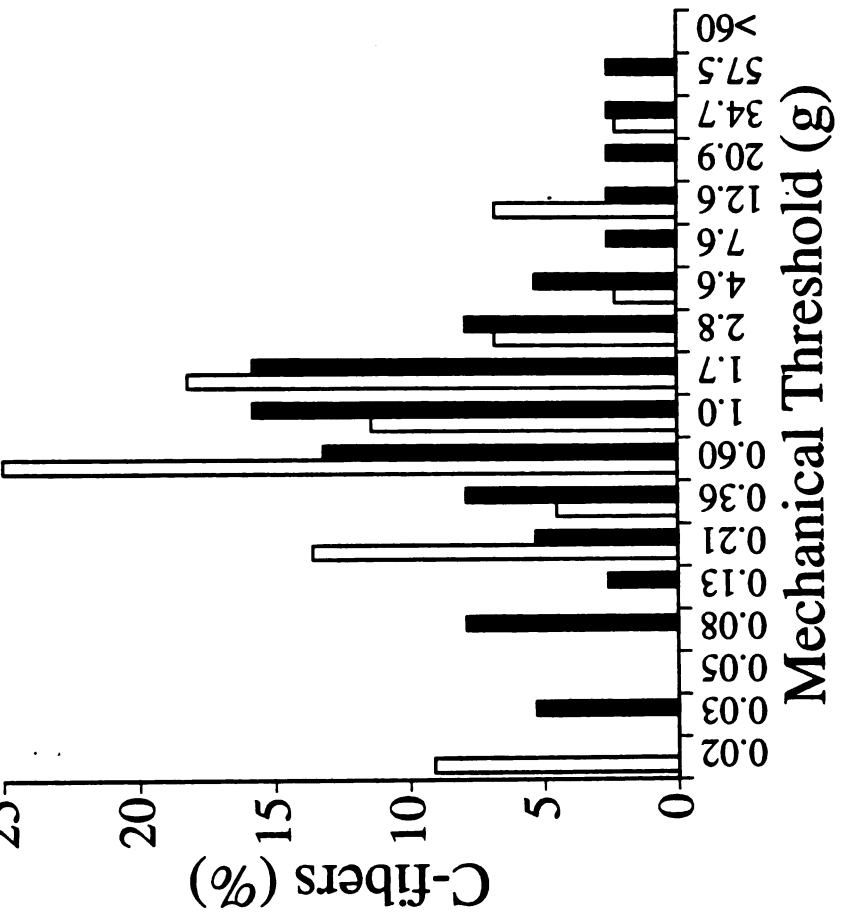


**Figure 4: Vincristine does not decrease the mechanical activation threshold of C-fibers.** Mechanical activation thresholds were determined using a series of von Frey hairs. The mechanical threshold was defined as the gram weight value of the lowest intensity VFH to which the neuron fired more than 2 APs in 50% of the trials. **A:** The distribution of C-fiber mechanical thresholds is shown in the histogram for 38 vincristine-treated C-fibers and 44 control C-fibers. Each bin on the x-axis is the intensity in grams of a VFH used to test C-fiber mechanical threshold, with the exception of the “> 60” bin which combines all VFHs of intensities greater than 60 grams. **B:** The average mechanical activation threshold for control C-fibers is shown by the open bar and for vincristine-treated C-fibers is shown by the filled bar.

**B**



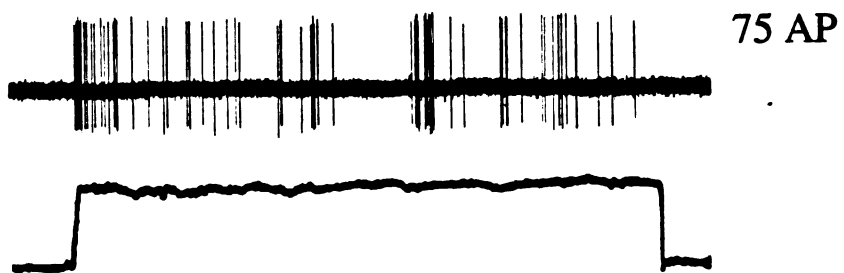
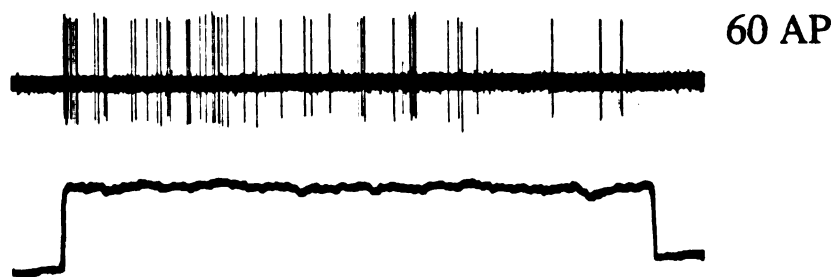
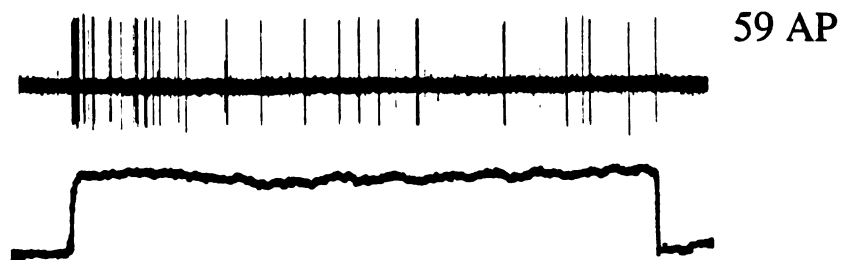
**A**



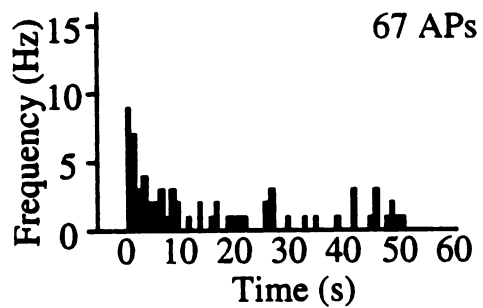
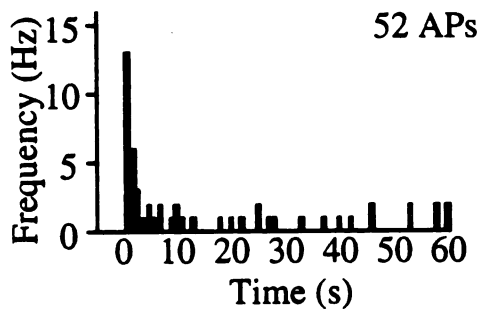
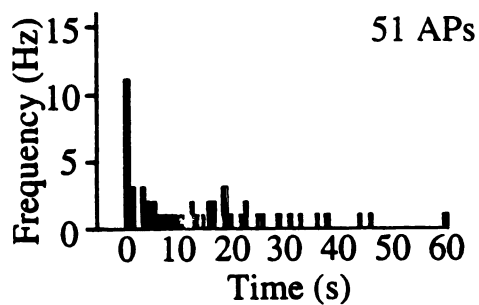
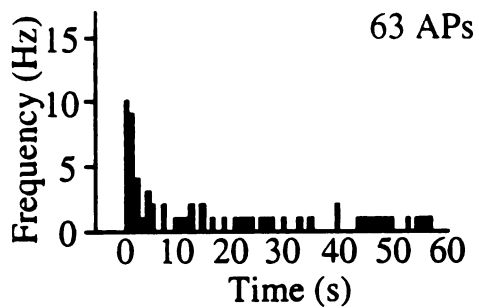
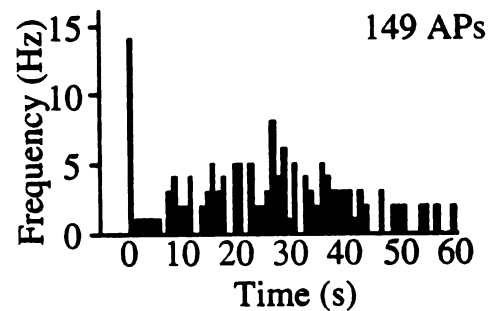
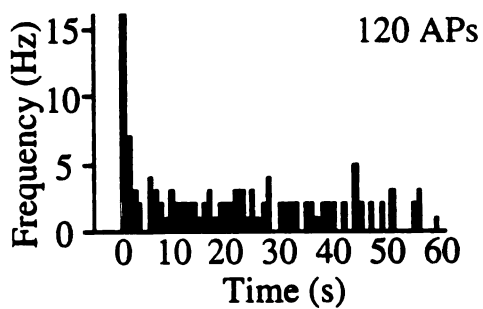
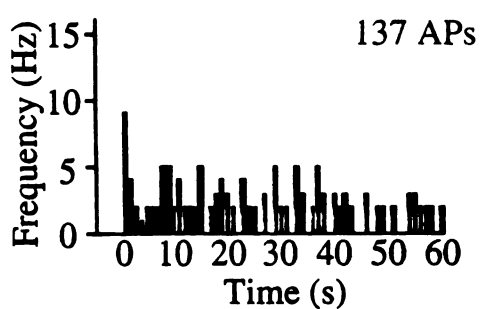
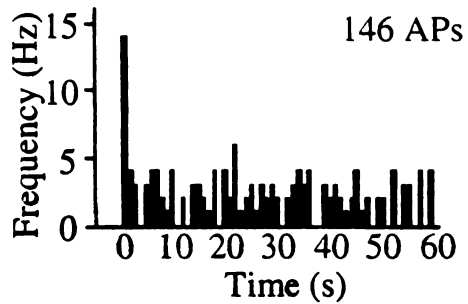


**Figure 5: C-fiber responses to sustained mechanical stimulation are reproducible.**

The responses of a C-fiber with a mechanical threshold of 0.6 g and a conduction velocity of 0.71 m/s to 4 trials of 1 min, 10 g stimulation are shown in the order in which they were performed. The interstimulus interval was 10 min. This C-fiber fired 59 APs in trial 1, 60 APs in trial 2, 75 APs in trial 3, and 50 APs in trial 4. The average response for the 4 trials of sustained mechanical stimulation was  $61 \pm 5.2$  APs.



**Figure 6: Vincristine causes increased responsiveness to sustained mechanical stimulation in a subset of C-fibers.** Activity was recorded from each fiber for 2 min prior to stimulation. Then, a 10 g VFH was applied to the center of the fiber's receptive field for 1 min, from 0 - 60 s. Binwidth is 1 s. **A:** The response of a C-fiber from a control rat. This fiber had a conduction velocity of 0.78 m/s, a mechanical threshold of 1.7 g, and fired no APs during the 2 min immediately preceding stimulation (only the last 10 s is shown here). The fiber fired 63, 51, 52, and 67 APs during the 4 stimulation trials for an average of  $58.3 \pm 4.0$  AP / stimulation. The peak firing frequency during the burst for the 4 trials was 10, 11, 13, and 9 Hz, respectively. **B:** The response of a hyperresponsive C-fiber from a vincristine-treated rat. This fiber had a conduction velocity of 0.62 m/s, a mechanical threshold of 1.7 g, and fired no APs during the 2 min immediately preceding stimulation. The fiber fired 146, 137, 120, and 149 APs during the 4 stimulation trials for an average of  $138 \pm 6.5$  AP / stimulation. The peak firing frequency during the burst for the 4 trials was 14, 9, 16, and 14 Hz, respectively.

**A****Control****B****Vincristine**

**Figure 7: The responses to sustained mechanical stimulation in vincristine-treated rats are bimodal.** The total number of APs fired in response to 1 min of 10 g stimulation of the receptive field is plotted for 21 control C-fibers (open bars) and 20 vincristine-treated C-fibers (filled bars). The percentage of C-fibers that fired greater than 100 APs in response to the 1 min 10 g stimulus, referred to as high-firing C-fibers, is 4.8% of control C-fibers (1/21) and 45% of vincristine-treated C-fibers (9/20).

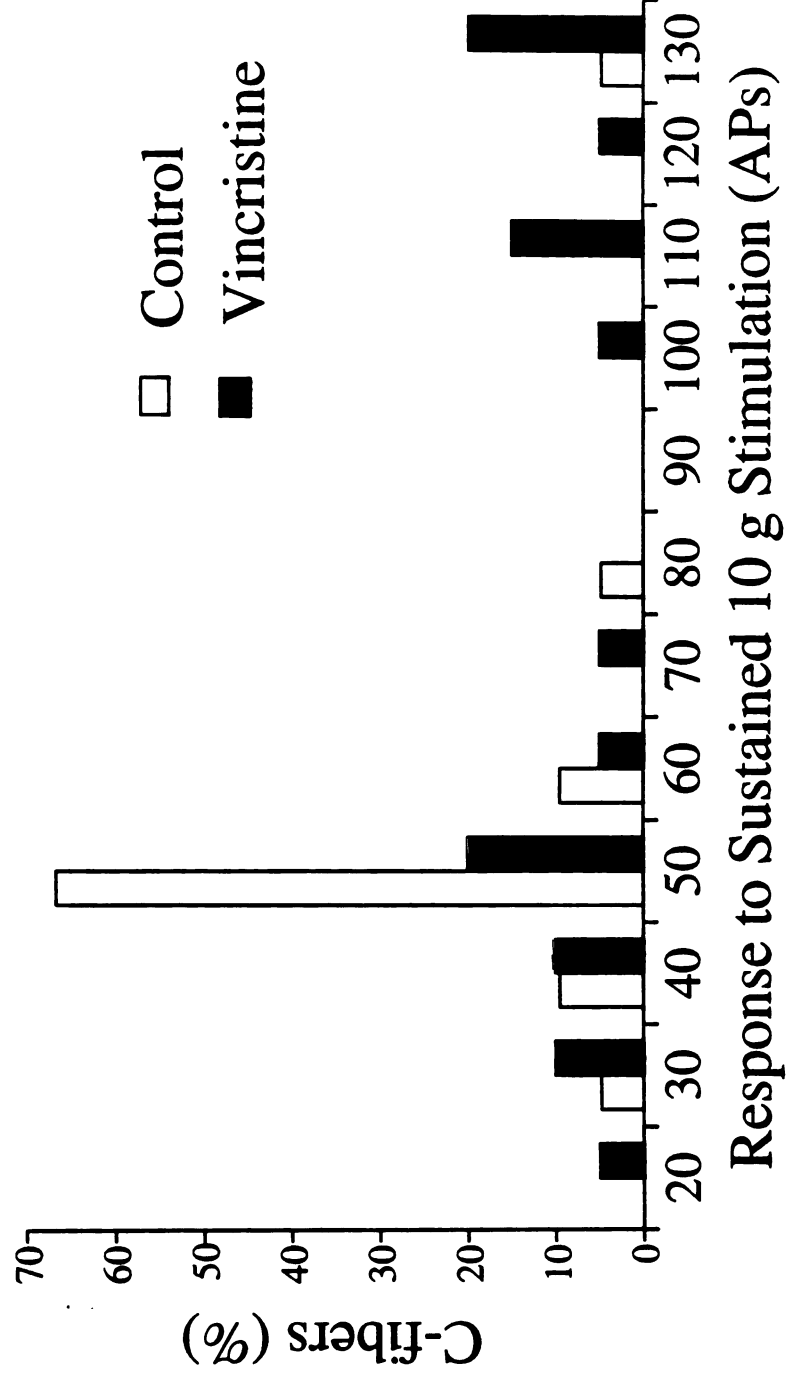


**Figure 8: Time course of responses to sustained mechanical stimulation in control and vincristine-treated C-fibers.** **A:** The average time course of the response of C-fibers to 1 min of 10 g stimulation to the receptive field is plotted for all control ( $\square$ ,  $n = 21$ ) and all vincristine-treated ( $\blacksquare$ ,  $n = 20$ ) C-fibers. **B:** The average time course of the response to 1 min of 10 g stimulation to the receptive field is plotted for high-firing vincristine-treated C-fibers firing more than 100 APs during stimulation ( $\blacktriangle$ ,  $n = 9$ ), low-firing vincristine-treated C-fibers firing less than 100 APs during stimulation ( $\bullet$ ,  $n = 11$ ), and all control C-fibers ( $\square$ ,  $n = 21$ ). Binwidth is 10 s. Some error bars are contained within the symbols.

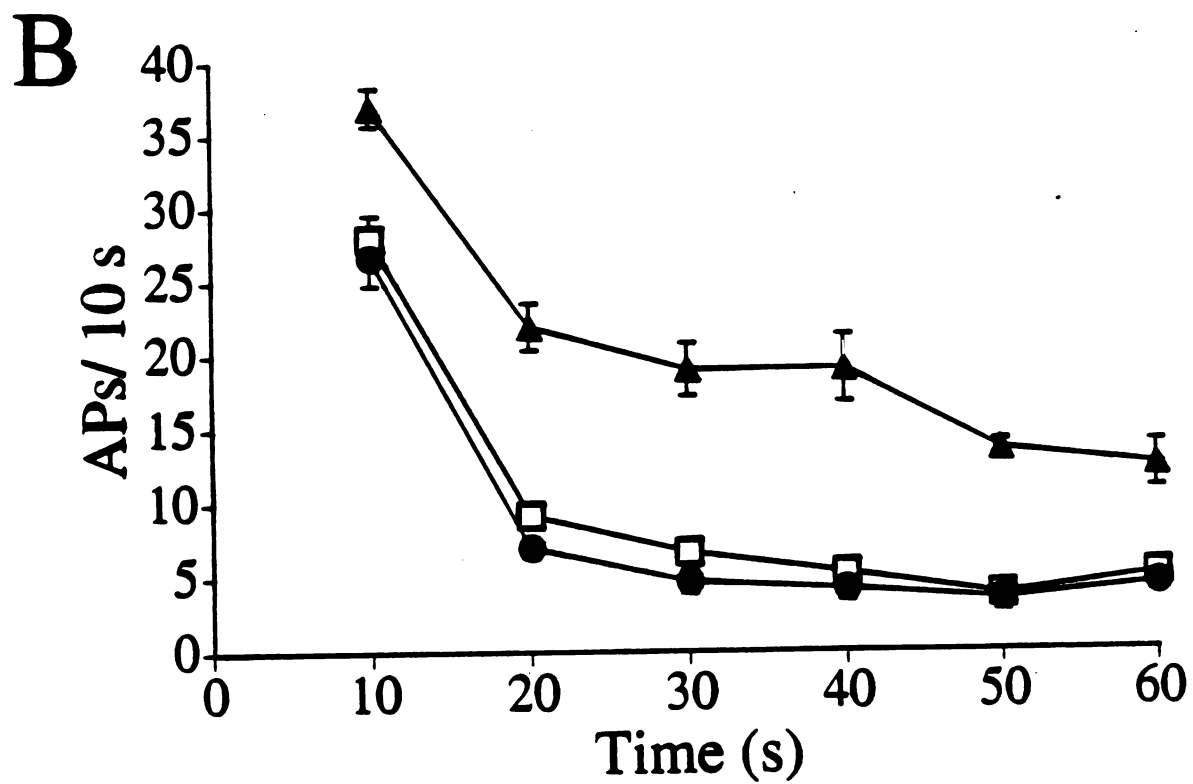
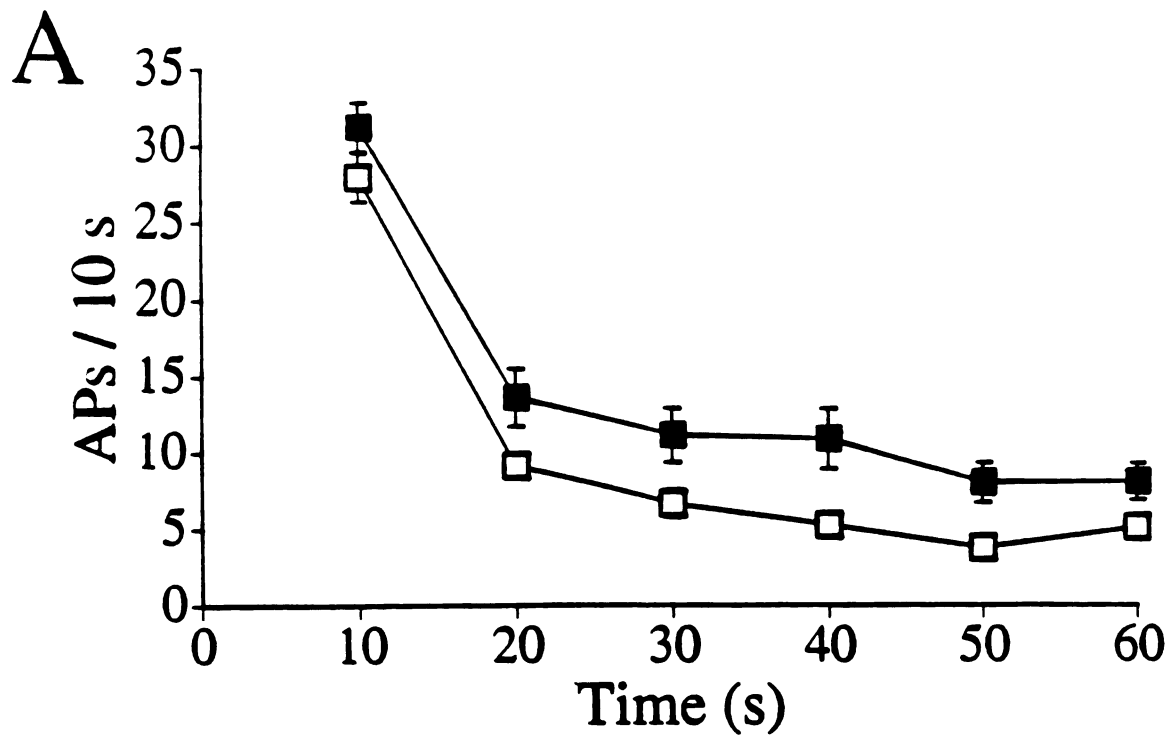




**Figure 9: Hyperresponsiveness in C-fibers is not correlated with receptive field location, conduction velocity, or mechanical threshold.** **A:** The receptive field locations for all C-fibers studied for responsiveness to sustained mechanical stimulation is shown on the left for control C-fibers and on the right for vincristine-treated C-fibers. C-fibers that fired less than 100 APs during stimulation are represented by the symbol ○. C-fibers that fired more than 100 APs during stimulation are represented by the symbol ⊙. In this drawing of the left hindpaw, top is medial and bottom is lateral. **B:** The average conduction velocity for all control C-fibers studied (n = 21) is shown in the open bars. The average conduction velocity for all vincristine-treated C-fibers studied (n = 20), vincristine-treated C-fibers firing less than 100 APs during stimulation (n = 11), and vincristine-treated C-fibers firing more than 100 APs during stimulation (n = 9) is shown in the filled bars. **C:** The average mechanical threshold for all control C-fibers studied (n = 21) is shown in the open bars. The average mechanical threshold for all vincristine-treated C-fibers studied (n = 20), vincristine-treated C-fibers firing less than 100 APs during stimulation (n = 11), and vincristine-treated C-fibers firing more than 100 APs during stimulation (n = 9) is shown in the filled bars. There are no significant differences between the groups.



Table 1: *Spontaneous activity in the saphenous nerve of control and vincristine-treated rats*

	Spontaneously Active Neurons (%)	Rate of Spontaneous Activity ( APs / min )	Spontaneously Active Neurons with > 100 AP / min (%)	Skin Surface Temperature (°C)
Control	7.0 ± 0.8 (8†)	120.5 ± 24.4 (61)	34.4 (21)	24.6 ± 0.7 (9†)
Vincristine	5.7 ± 0.6 (14†)	85.6 ± 23.4 (84)	16.7* (14)	24.2 ± 0.7 (9†)

There was no significant difference in the percentage or firing rate of spontaneously active neurons in vincristine-treated rats as compared to controls (t-test). \* represents  $p < 0.01$  (chi square analysis) as compared to control. In parentheses are the n values. † These n values refer to the number of rats studied. In all other cases the n value refers to the number of neurons studied. See methods for further details.

Table 2: *Distribution of C-fiber classes in the saphenous nerve of control and vincristine-treated rats*

	n	C-MH	C-deep	C-MHC	C-silent	C-C	C-MC	C-M
Control	43	62.8% (27)	16.3% (7)	7.0% (3)	4.7% (2)	2.3% (1)	4.7% (2)	2.3% (1)
Vincristine	33	57.6% (19)	18.2% (6)	0% (0)	9.1% (3)	6.1% (2)	3.0% (1)	6.1% (2)

C-fibers were classified as C-mechanoheat (C-MH), C-deep, C-mechanoheatcold (C-MHC), C-silent, C-cold (C-C), C-mechanocold (C-MC), or C-mechanical (C-M). In parentheses are the number of C-fibers that were classified as being in each category. The n values refer to the total number of C-fibers classified in control and vincristine-treated rats. There were no significant differences in the distribution of vincristine-treated C-fibers as compared to controls (chi square).

**Table 3: Responses of C-fibers in the saphenous nerve of control and vincristine-treated rats to sustained mechanical stimulation**

	n	Total Response (APs)	Burst Response (APs)	Plateau Response (APs)	Post-Stimulus Discharge (APs)
Control: All	21	58.5 ± 4.2	28.0 ± 1.6	30.3 ± 3.6	2.5 ± 0.4
Vincristine: All	20	83.3 ± 8.8*	31.3 ± 1.6	52.1 ± 7.7*	5.0 ± 1.9
Vincristine: Low-firing	11	50.3 ± 3.5	26.7 ± 1.9	23.9 ± 3.1	2.8 ± 0.4
Vincristine: High-firing	9	123.7 ± 4.8*	37.0 ± 1.2*	86.6 ± 5.3*	7.7 ± 4.1*

The average number of APs fired in response to a sustained mechanical stimulus (10 g, 60 s) is shown for each group. See Results section for definition of groups.

\* represents  $p < 0.05$  as compared to the mean response for all control C-fibers.

### **Chapter III:**

**Nociceptors in vincristine-induced painful neuropathy in rat  
are hyperresponsive to multiple stimulus modalities**

## Abstract

Neuropathic pain accompanies peripheral nerve injury following a wide variety of insults including metabolic disorders, trauma, and neurotoxic drugs. Vincristine, a widely used chemotherapeutic agent that inhibits microtubule dynamics, produces a painful peripheral neuropathy in humans (Sandler et al., 1969; Holland et al., 1973) and mechanical hyperalgesia in rats (Aley et al., 1996). Approximately half of C-fiber nociceptors in vincristine-treated rats are markedly hyperresponsive to mechanical stimulation. The mechanisms underlying this nociceptor hyperresponsiveness are unknown. Vincristine could specifically interfere with cellular mechanisms that are involved specifically in mechanotransduction. Alternatively, vincristine might impair general cellular adaptation mechanisms and produce hyperresponsiveness to multiple modalities of stimulation. To distinguish between these possibilities and gain insight into mechanisms of nociceptor hyperresponsiveness, we used *in vivo* extracellular recordings to examine the responses of vincristine-treated nociceptors to heat stimulation. Based on their response to mechanical stimulation, nociceptors from vincristine-treated rats could be classified as either hyperresponsive or non-hyperresponsive, as described previously (Tanner et al., 1997b). Vincristine does indeed cause heat hyperresponsiveness in vincristine-treated nociceptors that are also hyperresponsive to mechanical stimulation. As a population, high-firing vincristine-treated C-fibers had significantly greater responses to heat stimulation than low-firing vincristine-treated or control C-fibers. Thus, mechanisms of vincristine-induced nociceptor hyperresponsiveness involve general cellular adaptation mechanisms that contribute to nociceptor responses to multiple stimulus modalities. Heat hyperresponsiveness was pronounced in only a subset of mechanically hyperresponsive nociceptors and was never detected in the absence of mechanical hyperresponsiveness. These data suggest that vincristine may also specifically alter mechanotransduction.

## **Introduction**

Chemotherapy-induced pain is a form of neuropathic pain caused by neurotoxic drugs such as vincristine and taxol and is characterized by painful paresthesias and dysesthesias. The clinical antineoplastic efficacy of vincristine is limited by the development of a dose-dependent sensorimotor neuropathy (Sandler et al., 1969; Holland et al., 1973). Vincristine is thought to exert its antineoplastic effects by inhibiting microtubule dynamics in mitotic spindles, and thus preventing cell division (Olmsted and Borisy, 1973; Himes et al., 1976; Owellen et al., 1976; Jordan et al., 1992; Lobert et al., 1996). The neuropathy observed in patients treated with vincristine has been hypothesized to result from effects of vincristine on neuronal microtubules resulting in impaired axonal transport or other microtubule-dependent functions in peripheral neurons (Shelanski and Wisniewski, 1969; Bradley et al., 1970; Casey et al., 1973; Weiss et al., 1974).

The recent development of an animal model of vincristine-induced painful neuropathy (Aley et al., 1996) provides the opportunity to investigate the mechanisms underlying this form of nerve injury. Rats treated systemically with vincristine (100  $\mu\text{g}/\text{kg}$ ) develop mechanical hyperalgesia during the second week of vincristine administration that persists for more than a week following the final injection of the drug. Electrophysiological recordings during the peak of mechanical hyperalgesia revealed that approximately half of the C-fiber nociceptors in the saphenous nerves of vincristine-treated rats are markedly hyperresponsive to suprathreshold mechanical stimulation (Tanner et al., 1997b). In addition, the mean conduction velocities of A-fibers and C-fibers were significantly slowed.

Although the mechanisms that underlie vincristine-induced nociceptor hyperresponsiveness to mechanical stimulation are unknown, they likely involve actions of vincristine on the microtubular cytoskeleton. We have recently shown that vincristine causes disorganization of the axonal microtubule cytoskeleton in vincristine-treated rats during the peak phase of mechanical hyperalgesia (Tanner et al., 1997b). This axonal



cytoskeletal disorganization may also occur in the nerve terminal since vincristine is thought to act on labile microtubules which are enriched in the nerve terminal (Binet et al., 1990; Ahmad et al., 1993). Since cytoskeletal elements in the nerve terminal may be involved in mechanotransduction, vincristine could specifically interfere with nociceptor responses to mechanical stimulation. Alternatively, since the cytoskeleton is involved in the anchoring of ion channels and receptors and can contribute to adaptation and desensitization of these proteins following activation (Srinivasan et al., 1988; Bigot and Hunt, 1990; Kirsch et al., 1991; Rosenmund and Westbrook, 1993), then vincristine might produce hyperresponsiveness to multiple modalities of stimulation. Since the majority of primary afferent nociceptors are polymodal, responding to mechanical, heat, and chemical stimuli (Bessou and Perl, 1969; Martin et al., 1987; Tanner et al., 1997b), an investigation of their responses to other modalities of stimulation might lend insight into the mechanisms of vincristine-induced hyperresponsiveness.

To determine whether nociceptor hyperresponsiveness is restricted to mechanical stimuli or generalizes to multiple modalities of stimulation, we employed *in vivo* single-unit electrophysiology to measure the responses of C-fiber nociceptors to heat stimulation in rats treated with vincristine.

## Methods

### *Animals*

Experiments were performed on 250-350 g male Sprague-Dawley rats (Bantin and Kingman, Fremont, CA). Rats were housed in a temperature- and humidity-controlled environment and were maintained on a 12 hour light/dark cycle. Food and water were available *ad libitum*. Experiments were approved by the Committee on Animal Research at UCSF.

### *Vincristine Treatment*

Vincristine sulfate (Sigma, St. Louis, MO) was dissolved in saline to a stock concentration of 1 mg/ml, and was between pH 4.5 and 5.2. Vincristine was then diluted daily in saline to a concentration of 100  $\mu\text{g/ml}$  that was administered intravenously into the tail vein at a dose of 100  $\mu\text{g/kg}$  followed by 0.5 ml of saline. Treatments occurred daily (Monday through Friday) for 2 weeks with the dosage calculated on daily body weight. This dosage regimen was chosen because it produced maximal hyperalgesia in the absence of motor impairment in most rats (Aley et al., 1996). Paresthesias occur in humans receiving 12.5-75  $\mu\text{g/kg}$  vincristine administered weekly (McLeod and Penny, 1969; Sandler et al., 1969; Holland et al., 1973). Vincristine-treated rats weighed  $294 \pm 5$  g (n=14) at the time of electrophysiological recording. Control rats were weight-matched,  $307 \pm 7$  g (n=12), and untreated; previous behavioral experiments demonstrated that repeated intravenous saline injections had no effect on behavioral nociceptive threshold (Aley et al., 1996). Experimental rats were used for electrophysiological recordings during the peak phase of chronic vincristine-induced hyperalgesia that occurred in the absence of the drug, that is from 1-5 days following the final injection of vincristine (Figure 1). This recording window was chosen based on behavioral data which showed that the mechanical withdrawal threshold of > 90% of vincristine-treated rats was decreased >15% during these 5 days (K.O. Aley and J.D. Levine, unpublished observations). Vincristine-treated rats did

not gain weight normally during the course of the treatment, as has been described previously (Aley et al., 1996). There was an average decrease in body weight during vincristine treatment of  $10.8 \pm 1.6$  %. At this dose of vincristine, 18% of rats were euthanized prior to electrophysiological recording because of the development of motor impairment.

### *In vivo single unit electrophysiology*

The single-unit electrophysiological recording techniques employed have been described previously (White and Levine, 1991; Ahlgren et al., 1992). Briefly, rats were anesthetized with pentobarbital sodium (65 mg/kg, i.p.) and additional anesthetic was administered throughout the experiment to maintain areflexia. Recordings were made from the saphenous nerve, the cutaneous nerve that innervates the medial-dorsal hindpaw where mechanical hyperalgesia was characterized in awake rats (Aley et al., 1996). The skin overlying the saphenous nerve was retracted at mid-thigh level. The nerve was exposed and dissected free from surrounding tissue and vessels and maintained in a pool of 37°C mineral oil. Bipolar electrodes were placed under the nerve at a distal site to enable electrical stimulation (Stimulator S-88, Grass Medical Instruments, Quincy, MA and Stimulus Isolator NL-800, Neurolog, Medical Systems Corp., Greenvale, NY) of peripheral neurons. At a proximal site, a portion of the nerve was desheathed to expose axons. The nerve was crushed proximal to the recording site to prevent the elicitation of flexor reflexes during electrical stimulation of the nerve. Fine fascicles of axons were then dissected from the nerve with sharpened jeweler's forceps and placed on a silver wire recording electrode. Action potentials (APs) from individual fibers were amplified and filtered (Neurolog, Medical Systems Corp., Greenvale, NY) and then stored on tape (Video Cassette Recorder 420K, A. R. Vetter Co., Rebersburg, PA), as well as being discriminated by amplitude (Winston Electronics Co., San Francisco, CA) and displayed on a chart recorder on-line. The animal was sacrificed by pentobarbital overdose at the end of the recording session.

### Characterization of C-fiber nociceptors

#### *Conduction velocity*

Conduction velocity was determined by dividing the distance between the recording and stimulating electrodes, which measured between 20 and 33 mm, by the latency of the AP following an electrical stimulus to the whole nerve. Neurons that conducted at  $< 2$  m/s were classified as C-fibers and  $\geq 2$  m/s were classified as A-fibers (Lynn and Carpenter, 1982; Leem et al., 1993). Since previous experiments have shown that vincristine-treated sensory neurons of all classes have slowed conduction velocities, only C-fibers that conducted at less than 1 m/s were studied to avoid inadvertently recording the response properties of slowed A $\delta$ -fibers (Tanner et al., 1997b).

#### *Receptive field*

The receptive fields of C-fibers were determined using a mechanical search stimulus, either a blunt probe or a ~60 g von Frey hair (VFH) which activates  $> 90$  % of C-fibers in the saphenous nerve of the rat (Lynn and Carpenter, 1982; Ahlgren et al., 1992). C-fibers were required to show a slowed conduction velocity in response to electrical stimulation following mechanical stimulation of the receptive field. This latency shift test established that the mechanical receptive field under study was innervated by the C-fiber whose latency to electrical stimulation was shifted. The receptive fields of C-fibers were determined to be cutaneous if they were activated by lifting and squeezing the skin or if the mechanically sensitive spot moved to a new location when the skin was moved relative to the subcutaneous tissues. Neurons that did not meet this criterion were not further evaluated.

### *Mechanical Activation Threshold*

Mechanical activation thresholds were determined using a series of von Frey hairs that ranged in intensity from 0.02 - 263 g (A. Ainsworth, London, England). The mechanical threshold was defined as the intensity in grams of the weakest VFH to which the neuron fired more than 2 APs in 50% of the trials. Each trial consisted of a brief (~1 sec) application of a VFH to the center of the receptive field. VFH were applied in ascending order, and approximately 5-10 trials were performed for each VFH tested. Threshold was verified by alternately testing the strongest ineffective VFH and the weakest effective VFH. Such repeated mechanical testing of C-fibers does not cause a change in mechanical threshold (K.D. Tanner and J.D. Levine, unpublished observations, (Reeh et al., 1987; Ahlgren et al., 1992)).

### *Sustained Mechanical Stimulation*

Sustained mechanical stimulation of receptive fields was accomplished by use of a mechanical stimulation device consisting of a force transducer (Entran Devices, Inc., Model ELF-TC500-1, Fairfield, NJ) with a response range of 1-400 g mounted in series with a receptacle that can interchangeably hold von Frey hair filaments (modified from a set of Stoelting VFHs, Wood Dale, IL) that deliver various gram weight stimuli. VHF's were used since they are able to compensate well for changes in tissue elasticity over time, unlike rigid probes. The VFH is applied to the receptive field, by hand, and maintained at the just-bent position for 1 min. The voltage output signal from the force transducer is a quantitative measure of the force applied to the receptive field and is sent to both a chart recorder and a VCR tape for display, storage, and off-line analysis.

A 10 g mechanical stimulus was chosen to examine the response properties of nociceptive afferents because this stimulus is suprathreshold for >90 % of C-fibers in the saphenous nerve. For each neuron whose response to prolonged stimulation was studied, the conduction velocity, receptive field location, baseline spontaneous activity, and

mechanical threshold were determined. In general, the prolonged stimulation protocol consisted of 4 trials of sustained 1-min mechanical stimulation with a 10-min interstimulus interval between trials. The average of these 4 trials was the sustained mechanical stimulation response for that neuron and usually had a standard error of the mean of less than 10%. In a small number of cases included in the analysis, more trials were conducted to reduce the standard error. Activity was monitored for 5 min after the removal of the mechanical stimulus to quantitate afterdischarge.

#### *Classification of Vincristine-Treated Nociceptors*

Vincristine increases responsiveness to sustained mechanical stimulation in a subset of C-fiber nociceptors (Tanner et al., 1997b). Whereas the responses of C-fibers from control rats are clustered in a unimodal distribution in the range of 50-59 AP / stimulus, the responses of C-fibers from vincristine-treated rats form 2 distinct clusters in a bimodal distribution with a cluster around 50-59 AP/stimulus and another around 100-109 AP/stimulus and greater (Tanner et al., 1997b). Vincristine-treated C-fibers that fired less than 100 AP in response to sustained mechanical stimulation were categorized as "low-firing" C-fibers. Vincristine-treated C-fibers that fired more than 100 AP in response to sustained mechanical stimulation were categorized as "high-firing" C-fibers. The hyperresponsiveness in high-firing vincristine-treated C-fibers occurs both during the burst (first 10 s) and the plateau (last 50 s) phases of the response to mechanical stimulation (see Table 1). Hyperresponsiveness in the subpopulation of high-firing C-fibers in vincristine-treated rats does not correlate with receptive field location, conduction velocity, or mechanical threshold (Tanner et al., 1997b).

#### *Heat Activation Threshold*

Heat activation thresholds were determined using a Peltier device (Thermal Devices Inc., Minneapolis, MN) that delivered a ramped heat stimulus from 30 to 58°C at a rate of

1°C/s. Activity was monitored for 2 min following mechanical stimulation and prior to any heat stimulation to determine the presence of spontaneous activity. After the Peltier device was placed on the receptive field of a C-fiber, activity was monitored again for 2 min to verify the absence of activity induced mechanically by the Peltier device. The heat threshold was defined as the temperature at which the C-fiber fired a second AP. Heat activation threshold was determined twice with a 10-min interstimulus interval. The average of these two measurements was the heat activation threshold for that fiber.

### *Suprathreshold Heat Stimulation*

Suprathreshold heat stimulation of receptive fields consisted of a ramp from 30°C to a maximum of ~53°C at a rate of 1°C / s. This ramped heat stimulation protocol was chosen because square wave heat stimuli resulted in profound inactivation of C-fiber responses during even a 10-s trial. Preliminary experiments showed that C-fiber responses were most reproducible to ramped heat stimuli at this stimulation rate and maximum temperature (K.D. Tanner and J.D. Levine, unpublished observations). After the determination of heat threshold, three heat ramp stimuli were delivered to the receptive field of each fiber at an interstimulus interval of 20 min. Unfortunately, even at this long interstimulus interval, there was partial desensitization of the heat response with subsequent trials in many neurons. Thus, heat responses were not averaged, and the response to only the first heat stimulus was used in all analyses.

For each neuron whose response to prolonged mechanical and heat stimuli was studied, the conduction velocity, receptive field location, baseline spontaneous activity, and mechanical threshold were determined. Due to physical constraints related to the size of the Peltier thermal stimulator, only C-fibers with receptive fields distal to the ankle were studied. Since some vincristine-treated neurons develop an afterdischarge following mechanical stimulation (see Table 3), we did not record from C-fibers that fired > 5 AP/min during the 2-min observation period to avoid recording from those neurons that may have

developed ongoing activity following mechanical search stimulation of the skin. These fibers were <10 % of the population.

### *Data Analysis*

Data are expressed as mean  $\pm$  standard error of the mean (SEM). As noted in the text, statistical analyses were done using Student's t-test, analysis of variance (ANOVA), Chi square analysis, or Mann-Whitney U test.



## Results

### *Vincristine does not decrease heat activation threshold in nociceptors*

As we have shown in previous experiments, vincristine does not decrease heat thresholds in C-fiber nociceptors (Tanner et al., 1997b). To verify that this is the case for nociceptors in this study, we determined the average heat activation thresholds for control and vincristine-treated nociceptors. As shown in Figure 2, the average heat thresholds of vincristine-treated C-fibers ( $45.6 \pm 1.0^\circ\text{C}$ ,  $n = 19$ ) are not statistically different ( $p > 0.05$ ) from those of control C-fibers ( $45.5 \pm 1.0^\circ\text{C}$ ,  $n = 16$ ).

### *Vincristine causes heat hyperresponsiveness in high-firing vincristine-treated nociceptors*

We tested the hypothesis that high-firing vincristine-treated nociceptors, which are hyperresponsive to mechanical stimulation, are also hyperresponsive to heat stimulation. Figure 3 shows examples of responses to mechanical stimulation (1 min, 10 g) and heat stimulation (ramp from  $30^\circ\text{C}$  to  $53^\circ\text{C}$  at  $1^\circ\text{C/s}$ ) for a control nociceptor and a low-firing and a high-firing vincristine-treated nociceptor that had similar mechanical and heat activation thresholds. This high-firing vincristine-treated nociceptor fired more than twice as many APs than control or low-firing vincristine-treated nociceptors for both mechanical and heat stimulation. Thus, high-firing vincristine-treated nociceptors can be hyperresponsive to both mechanical and heat stimulation

### *Heat hyperresponsiveness occurs in high-firing but not low-firing vincristine-treated nociceptors.*

The average responses to mechanical stimulation are plotted for all control C-fibers and all vincristine-treated C-fibers, as well as for low-firing vincristine-treated C-fibers and high-firing vincristine-treated C-fibers separately. As previously reported (Tanner et al., 1997b), the averaged response to mechanical stimulation for all vincristine-treated C-fibers

is significantly greater than for control C-fibers (Figure 4A,  $p < 0.05$ ). In addition, the averaged response of high-firing vincristine-treated C-fibers to mechanical stimulation is significantly greater compared to the averaged response for either low-firing vincristine-treated C-fibers ( $p < 0.01$ ) or control C-fibers ( $p < 0.01$ ). Although a similar pattern is seen when the average responses to heat stimulation are plotted in Figure 4B, the response to heat stimulation for all vincristine-treated C-fibers is not significantly greater than for control C-fibers ( $p > 0.05$ ). High-firing vincristine-treated C-fibers do, however, have a significantly greater response to heat stimulation when compared to either low-firing vincristine-treated C-fibers ( $p < 0.01$ ) or control C-fibers ( $p < 0.01$ ).

*Heat hyperresponsiveness occurs in some, but not all, high-firing vincristine-treated nociceptors.*

Although heat hyperresponsiveness can accompany mechanical hyperresponsiveness in high-firing vincristine-treated nociceptors, this is not always the case. The magnitude of the heat response is plotted against the mechanical response for each nociceptor studied in Figure 5A. Whereas the mechanical responses of high-firing vincristine-treated nociceptors are all clearly much higher than control or low-firing vincristine-treated nociceptors, only a subset of the heat responses of high-firing vincristine-treated nociceptors exceed those of control and low-firing vincristine-treated nociceptors. However, since the magnitude of the heat response is correlated with the neuron's heat activation threshold (Figure 5B), those high-firing vincristine-treated nociceptors that do not appear to have heat responses higher than controls in Figure 4A could simply have higher heat thresholds. To determine whether this could account for the apparent lack of heat hyperresponsiveness in some high-firing vincristine-treated nociceptors, we plotted the response to heat stimulation against heat threshold for each neuron (Figure 5B). Note that some high-firing vincristine-treated nociceptors have heat responses greater than or at the high end of control and low-firing vincristine-treated

nociceptors with similar heat thresholds; however, the remaining high-firing vincristine-treated nociceptors are well within the range of heat responses of control and low-firing vincristine-treated nociceptors. Thus, the range of heat thresholds in high-firing vincristine-treated nociceptors are unlikely to account for the lack of heat hyperresponsiveness in some high-firing vincristine-treated nociceptors.

*Hyperresponsiveness in nociceptors is not correlated with receptive field location, conduction velocity, mechanical threshold, or heat threshold.*

Lastly, as shown in Figure 6, hyperresponsiveness in vincristine-treated C-fibers, defined by their responsiveness to mechanical stimulation, does not correlate with receptive field location, conduction velocity, mechanical threshold, or heat activation threshold. As shown in Figure 6A, high-firing C-fibers in vincristine-treated rats do not appear to be located in any specific skin regions of the dorsal hindpaw. As shown in Figure 6B, the average conduction velocity of all vincristine-treated C-fibers ( $0.77 \pm 0.02$  m/s,  $n = 19$ ) was not significantly different than that of all control C-fibers ( $0.74 \pm 0.02$  m/s,  $n = 16$ ). The average conduction velocity of low-firing C-fibers ( $0.79 \pm 0.02$  m/s,  $n = 12$ ) in vincristine-treated rats was not different ( $p > 0.05$ ) from the average conduction velocity of hyperresponsive, high-firing C-fibers ( $0.75 \pm 0.03$  m/s,  $n = 7$ ) in vincristine-treated rats. As shown in Figure 6C, the average mechanical threshold of all vincristine-treated C-fibers ( $2.2 \text{ g} \pm 0.4 \text{ g}$ ,  $n = 19$ ) was not significantly different than that of all control C-fibers ( $2.0 \text{ g} \pm 0.3 \text{ g}$ ,  $n = 16$ ). The average mechanical threshold of low-firing C-fibers ( $1.9 \text{ g} \pm 0.4 \text{ g}$ ,  $n = 12$ ) in vincristine-treated rats was not different ( $p > 0.05$ ) from the average mechanical threshold of hyperresponsive, high-firing C-fibers ( $2.7 \text{ g} \pm 0.7 \text{ g}$ ,  $n = 7$ ) in vincristine-treated rats. As shown in Figure 6D, the average heat threshold of all vincristine-treated C-fibers ( $45.6 \pm 1.0^\circ\text{C}$ ,  $n = 19$ ) was not significantly different than that of all control C-fibers ( $45.5 \pm 1.0^\circ\text{C}$ ,  $n = 16$ ). The average heat threshold of low-firing C-fibers ( $46.3 \pm 1.4^\circ\text{C}$ ,  $n = 12$ ) in vincristine-treated rats was not different ( $p > 0.05$ ) from the average mechanical

## **Discussion**

The neural mechanisms underlying neuropathic pain following a wide variety of insults including metabolic disorders, trauma, and neurotoxins are largely unknown. Specifically, the neural mechanisms of chemotherapy-induced neuropathic pain that is caused by neurotoxic drugs such as vincristine and taxol have not been investigated. In a previous electrophysiological study, we found that approximately half of C-fibers in vincristine-treated rats exhibited marked hyperresponsiveness to sustained mechanical stimulation. Other than a slowing of conduction velocity in all classes of sensory neurons, all other aspects of nociceptor function assayed were unaffected. These data suggested that vincristine does not alter all the functions of nociceptors, but rather enhances nociceptor responses to sustained mechanical stimulation.

The mechanisms of vincristine-induced mechanical hyperresponsiveness are unknown. Vincristine could interfere with cellular mechanisms that are involved specifically in mechanotransduction. Alternatively, vincristine might impair general cellular adaptation mechanisms and produce hyperresponsiveness to multiple modalities of stimulation. To distinguish between these possibilities, we examined the responses of vincristine-treated nociceptors to heat stimulation. Vincristine does indeed cause heat hyperresponsiveness in vincristine-treated nociceptors that are also hyperresponsive to mechanical stimulation. As a population, high-firing vincristine-treated C-fibers had significantly greater responses to heat stimulation than low-firing vincristine-treated or control C-fibers. Thus, mechanisms of vincristine-induced nociceptor hyperresponsiveness involve general cellular adaptation mechanisms that contribute to nociceptor responses to multiple stimulus modalities. Heat hyperresponsiveness was pronounced in only a subset of mechanically hyperresponsive nociceptors and was never detected in the absence of mechanical hyperresponsiveness. These data suggest that vincristine may also specifically alter mechanotransduction.

### Relationship between mechanical and heat hyperresponsiveness in vincristine-treated nociceptors

As a population, high-firing vincristine-treated nociceptors have significantly greater responses to heat stimulation than control or low-firing vincristine-treated nociceptors. However, not every mechanically hyperresponsive vincristine-treated nociceptor was also heat hyperresponsive. Of seven mechanically hyperresponsive high-firing vincristine-treated C-fibers examined, only two were profoundly heat hyperresponsive. The mechanical responses of these heat hyperresponsive nociceptors were not exceptional compared to other mechanically hyperresponsive vincristine-treated nociceptors. The remaining five nociceptors had heat responses in the range of control and low-firing vincristine-treated nociceptors with comparable heat thresholds. Compared to control nociceptors, there was no decrease in heat activation threshold for either the whole population of vincristine-treated nociceptors or those that exhibited mechanical hyperresponsiveness. However, all those vincristine-treated nociceptors that exhibited heat hyperresponsiveness had thresholds less than 45.5°C, the average heat activation threshold of all nociceptors studied. Heat hyperresponsiveness may be correlated with a lower heat activation threshold; however, a larger heat hyperresponsive population of vincristine-treated nociceptors would be required to address this hypothesis. Alternatively, since neurons with lower heat thresholds have more opportunity to fire during a heat ramp stimulus, it might be technically difficult to reveal heat hyperresponsiveness in C-fibers with high heat thresholds. This potential technical impediment is compounded by the inability to average heat responses across several trials. Unlike analysis of mechanical hyperresponsiveness which has the benefit of averaging the neuronal response across several trials, prominent desensitization following heat stimulation of polymodal nociceptors decreases the reliability of the measured heat responses. Assuming heat

hyperresponsiveness was equally detectable among all nociceptors studied, our data is compatible with the suggestion that mechanical hyperresponsiveness can occur both independently of and in conjunction with heat hyperresponsiveness.

There were no examples in our data of vincristine-treated nociceptors that exhibited heat hyperresponsiveness in the absence of mechanical hyperresponsiveness. In no case did low-firing vincristine-treated nociceptors have exacerbated responses to heat stimulation. These data are compatible with the suggestion that while vincristine can alter mechanisms that contribute only to mechanical responsiveness, it cannot affect mechanisms that contribute only to heat responsiveness.

#### Mechanisms of vincristine-induced nociceptor mechanical and heat hyperresponsiveness

The mechanisms by which vincristine causes both heat and mechanical hyperresponsiveness in nociceptors are likely to involve its actions on the microtubular cytoskeleton. In fact, recent ultrastructural analysis of unmyelinated axons in the peripheral nerve of vincristine-treated rats revealed disorientation of microtubules during the period of nociceptor hyperresponsiveness (Tanner et al., 1997a). Since vincristine-treated nociceptors can be hyperresponsive to both heat and mechanical stimulation and perhaps to mechanical stimulation only, vincristine may cause multiple changes in the cellular physiology of nociceptors.

#### *Mechanisms of hyperresponsiveness to multiple stimulus modalities*

Hyperresponsiveness to multiple stimulus modalities might occur due to alterations in axonal transport, as has been previously hypothesized (Shelanski and Wisniewski, 1969; Bradley et al., 1970; Casey et al., 1973; Weiss et al., 1974). Although axonal microtubules are known to support fast and slow axonal transport of cellular components both anterogradely and retrogradely (Sheetz et al., 1989; Allan et al., 1991; Cleveland and Hoffman, 1991; Sheetz and Martenson, 1991; Hirokawa, 1993), the extent to which the disorientation observed in axonal microtubules in vincristine-induced neuropathy would

affect axonal transport is unclear. If axonal transport was impaired, cytoskeletal disorganization could produce alterations of the complement of proteins present in the nerve terminal and secondarily cause changes in the excitability of nociceptors that are independent of stimulus modality, as has been suggested for the axotomy model of neuropathy (Devor et al., 1993).

In addition, vincristine-induced disorientation of nerve terminal microtubules could disrupt adaptation mechanisms that occur during neuronal responses to all modalities of suprathreshold stimulation. Several lines of evidence suggest that the cytoskeleton is involved generally in the anchoring of ion channels and receptors, as well as in the desensitization of some of these receptors following activation (Srinivasan et al., 1988; Bigot and Hunt, 1990; Kirsch et al., 1991; Rosenmund and Westbrook, 1993). If conductances involved in adaptation in polymodal nociceptors were regulated by the microtubular cytoskeleton, then vincristine might impair general adaptation mechanisms in the nerve fiber terminal and produce hyperresponsiveness.

Lastly, preliminary analysis of the temporal structure of the responses of mechanically hyperresponsive vincristine-treated nociceptors revealed that these nociceptors fired in one of two distinct modes: a variable frequency firing pattern with the majority of ISIs less than 100 msec or a constant frequency firing pattern with the majority of ISIs in the range of 100-300 msec (K.D. Tanner and J.D. Levine, unpublished observations). Both vincristine-treated nociceptors that were hyperresponsive to heat and mechanical stimulation fired in a constant frequency mode to sustained mechanical stimulation. These data suggest that vincristine-induced hyperresponsiveness that is independent of stimulus modality may involve cellular mechanisms on the time-scale of 100-300 ms.

#### *Mechanisms of hyperresponsiveness to only mechanical stimulation*

Although vincristine-treated nociceptors can be hyperresponsive to both mechanical and heat stimulation, most mechanically hyperresponsive nociceptors studied did not

exhibit detectable hyperresponsiveness to heat stimulation. These data suggest that vincristine may also affect mechanisms of mechanotransduction without affecting general mechanisms of nociceptor responsiveness.

Hyperresponsiveness only to mechanical stimulation could occur due to alterations in axonal transport, perhaps stranding dysfunctional proteins involved in mechanotransduction. This would require that proteins involved in mechanotransduction degrade, are transported, and/or replenished on a different time-scale than those involved in heat transduction. For axotomized C-fiber afferents, the neuroma tip of the axon develops both novel heat and mechanical sensitivity on approximately the same time-scale, within hours of transection (Michaelis et al., 1995; Blenk et al., 1996).

More likely, modality-specific hyperresponsiveness may result from direct effects of vincristine on the mechanotransduction apparatus. Cytoskeletal disorganization and microtubule disorientation occurs in unmyelinated axons when nociceptors are hyperresponsive and may also occur in nociceptive nerve terminals (Tanner et al., 1997a). Although the mechanisms of mechanical transduction are unknown in vertebrate somatic afferents, a role for cytoskeletal elements has been postulated (Guharay and Sachs, 1984; Wang et al., 1993). In *C. elegans*, sensory neurons required for mechanosensation express a unique class of microtubules that are required for touch sensitivity (Chalfie, 1993). In addition, these touch cells express sodium channels that share homology with epithelial sodium channels found in the kidney that are thought to be involved in osmotic regulation (Chalfie, 1993; Canessa et al., 1994). Interestingly, these putative sodium channel osmo/mechano-transducers can be regulated by the cytoskeleton (Berdiev et al., 1995).

#### Nociceptor hyperresponsiveness in other models of neuropathic pain

In all neuropathic pain models in which the transduction properties of nociceptors have been studied, hyperresponsiveness to heat or mechanical stimulation is a common alteration. In diabetic neuropathy, mechanical hyperresponsiveness is observed, but heat



responsiveness has not been examined (Ahlgren et al., 1992; Ahlgren and Levine, 1994). In the chronic constriction injury model, heat hyperresponsiveness is observed, but mechanical responsiveness has not been studied (Koltzenburg et al., 1994). Our data suggest that both heat and mechanical hyperresponsiveness can occur during vincristine-induced neuropathy. In each of these models, heat or mechanical hyperresponsiveness occurs in the absence of a reduction in heat or mechanical activation thresholds and a subset of C-fibers exhibit pronounced afterdischarges following removal of the stimulus (Ahlgren et al., 1992; Koltzenburg et al., 1994; Tanner et al., 1997b). Taken together, these studies are compatible with the suggestion that common peripheral mechanisms of nociceptor hyperresponsiveness may exist for multiple classes of peripheral neuropathies (toxic, traumatic, and metabolic).

In conclusion, vincristine treatment can cause heat hyperresponsiveness in nociceptors that are also hyperresponsive to mechanical stimulation. As a population, high-firing vincristine-treated C-fibers have significantly greater responses to heat stimulation than low-firing vincristine-treated or control C-fibers. Thus, mechanisms of vincristine-induced nociceptor hyperresponsiveness involve general cellular mechanisms that contribute to nociceptor responses to multiple stimulus modalities. Since heat hyperresponsiveness was pronounced in only a subset of mechanically hyperresponsive nociceptors and was never detected in the absence of mechanical hyperresponsiveness, vincristine may also specifically alter mechanotransduction. These multiple mechanisms may contribute to behavioral mechanical hyperalgesia observed in rats treated with vincristine, as well as paresthesias and dysesthesias experienced by patients receiving vincristine as a chemotherapeutic agent.

## References

Ahlgren SC, Levine JD (1994). Protein kinase C inhibitors decrease hyperalgesia and C-fiber hyperexcitability in the streptozotocin-diabetic rat. *J Neurophysiol* 72, 684-692.

Ahlgren SC, White DM, Levine JD (1992). Increased responsiveness of sensory neurons in the saphenous nerve of the streptozotocin-diabetic rat. *J Neurophysiol* 68, 2077-2085.

Ahmad FJ, Pienkowski TP, Baas PW (1993). Regional differences in microtubules dynamics in the axon. *J Neurosci* 13, 856-866.

Aley KO, Reichling DB, Levine JD (1996). Vincristine hyperalgesia in the rat: a model of painful vincristine neuropathy in humans. *Neuroscience* 73, 259-265.

Allan V, Vale R, Navone F (1991). Microtubule-based organelle transport in neurons. In *The Neuronal Cytoskeleton*, R Burgoyne, ed. (New York: Wiley-Liss), pp. 257-282.

Berdiev BK, Prat AG, Cantiello HF, Ausiello DA, Fuller CM, Jovov B, Benos DJ, Ismailov II (1995). Regulation of epithelial sodium channels by short actin filaments. *Prog Brain Res* 105, 179-182.

Bessou P, Perl ER (1969). Response of cutaneous sensory units with unmyelinated fibers to noxious stimuli. *J Neurophysiol* 32, 1025-43.

Bigot D, Hunt SP (1990). Effect of excitatory amino acids on microtubule-associated proteins in cultured cortical and spinal neurones. *Neurosci Lett* 111, 275-280.

Binet S, Chaineau E, Fellous A, Lataste H, Krikorian A, Couzinier J-P, Meininger V (1990). Immunofluorescence study of the action of navelbine, vincristine and vinblastine on mitotic and axonal microtubules. *Int J Cancer* 46, 262-266.

Blenk K, Michaelis M, Vogel C, Janig W (1996). Thermosensitivity of acutely axotomized sensory nerve fibers. *J Neurophysiol* 76, 743-752.

Bradley WG, Lassman LP, Pearce GW, Walton JN (1970). The neuromyopathy of vincristine in man. Clinical, electrophysiological and pathological studies. *J Neurol Sci* 10, 107-131.

Canessa CM, Schild L, Buell G, Thorens B, Gautschi I, Horisberger JD, Rossier BC (1994). Amiloride-sensitive epithelial Na<sup>+</sup> channel is made of three homologous subunits. *Nature* 367, 470-473.

Casey EB, Jellife AM, Le QP, Millett YL (1973). Vincristine neuropathy. Clinical and electrophysiological observations. *Brain* 96, 69-86.

Chalfie M (1993). Touch receptor development and function in *Caenorhabditis elegans*. *J Neurobiol* 24, 1433-1441.

Cleveland D, Hoffman P (1991). Slow axonal transport models come full circle: Evidence that microtubule sliding mediates axon elongation and tubulin transport. *Cell* 67, 453-456.

Devor M, Govrin Lippmann R, Angelides K (1993). Na<sup>+</sup> channel immunolocalization in peripheral mammalian axons and changes following nerve injury and neuroma formation. *J Neurosci* 13, 1976-1992.

Guharay F, Sachs F (1984). Stretch-activated single ion channel currents in tissue-cultured embryonic chick skeletal muscle. *J Physiol (Lond)* 352, 685-701.

Himes RH, Kersey RN, Heller BI, Samson FE (1976). Action of the vinca alkaloids vincristine, vinblastine, and desacetyl vinblastine amide on microtubules in vitro. *Cancer Res* 36, 3798-3802.

Hirokawa N (1993). Axonal transport and the cytoskeleton. *Current Opinion Neurobiol* 3, 724-731.

Holland JF, Scharlau C, Gailani S, Krant MJ, Olson KB, Horton J, Shnider BI, Lynch JJ, Owens A, Carbone PP, Colsky J, Grob D, Miller SP, Hall TC (1973). Vincristine treatment of advanced cancer: a cooperative study of 392 cases. *Cancer Res* 33, 1258-1264.

Jordan M, Thrower D, Wilson L (1992). Effects of vinblastine, podophyllotoxin and nocodazole on mitotic spindles. *J Cell Sci* 102, 401-416.

Kirsch J, Langosch D, Prior P, Littauer UZ, Schmitt B, Betz H (1991). The 93-kDa glycine receptor-associated protein binds to tubulin. *J Biol Chem* 266, 22242-22245.

Koltzenburg M, Kees S, Budweiser S, Ochs G, Toyka K (1994). The properties of unmyelinated nociceptive afferents change in a painful chronic constriction neuropathy. In Proc 7th World Cong Pain, G Gebhart, D Hammond, T Jensen, ed. (Seattle: IASP Press), pp. 511-522.

Leem JW, Willis WD, Chung JM (1993). Cutaneous sensory receptors in the rat foot. *J Neurophysiol* 69, 1684-1699.

Lobert S, Vulevic B, Correia JJ (1996). Interaction of vinca alkaloids with tubulin: A comparison of vinblastine, vincristine, and vinorelbine. *Biochemistry* 35, 6806-6814.

Lynn B, Carpenter SE (1982). Primary afferent units from the hairy skin of the rat hind limb. *Brain Res* 238, 29-43.

Martin HA, Basbaum AI, Kwiat GC, Goetzl EJ, Levine JD (1987). Leukotriene and prostaglandin sensitization of cutaneous high-threshold C- and A-delta mechanonociceptors in the hairy skin of rat hindlimb. *Neuroscience* 22, 651-659.

McLeod JG, Penny R (1969). Vincristine neuropathy: an electrophysiological and histological study. *J Neurol Neurosurg Psychiatry* 32, 297-304.

Michaelis M, Blenk KH, Jänig W, Vogel C (1995). Development of spontaneous activity and mechanosensitivity in axotomized afferent nerve fibers during the first hours after nerve transection in rats. *J Neurophysiol* 74, 1020-1027.

Olmsted JB, Borisy GG (1973). Microtubules. *Annu Rev Biochem* 42, 507-540.

Owellen RJ, Hartke CA, Dickerson RM, Hains FO (1976). Inhibition of tubulin-microtubule polymerization by drugs of the Vinca alkaloid class. *Cancer Res* 36, 1499-1502.

Reeh PW, Bayer J, Kocher L, Handwerker HO (1987). Sensitization of nociceptive cutaneous nerve fibers from the rat's tail by noxious mechanical stimulation. *Exp Brain Res* 65, 505-512.

Rosenmund C, Westbrook GL (1993). Calcium-induced actin depolymerization reduces NMDA channel activity. *Neuron* 10, 805-814.

Sandler SG, Tobin W, Henderson ES (1969). Vincristine-induced neuropathy. A clinical study of fifty leukemic patients. *Neurology* 19, 367-374.

Sheetz M, Martenson C (1991). Axonal transport: beyond kinesin and cytoplasmic dynein. *Current Opinion Neurobiol* 1, 393-398.

Sheetz M, Steuer E, Schroer T (1989). The mechanism and regulation of fast axonal transport. *Trends Neurosci.* 12, 474-478.

Shelanski ML, Wisniewski H (1969). Neurofibrillary degeneration induced by vincristine therapy. *Arch Neurol* 20, 199-206.

Srinivasan Y, Elmer L, Davis J, Bennett V, Angelides K (1988). Ankyrin and spectrin associate with voltage-dependent sodium channels in brain. *Nature* 333, 177-180.

Tanner K, Levine J, Topp K (1997a). Microtubule disorientation and axonal swelling in unmyelinated sensory axons during vincristine-induced painful neuropathy in rat. *J. Neurosci. submitted.*

Tanner KD, Reichling DB, Levine JD (1997b). Mechanical hyperresponsiveness of nociceptors in vincristine-induced neuropathy in rat. *submitted.*

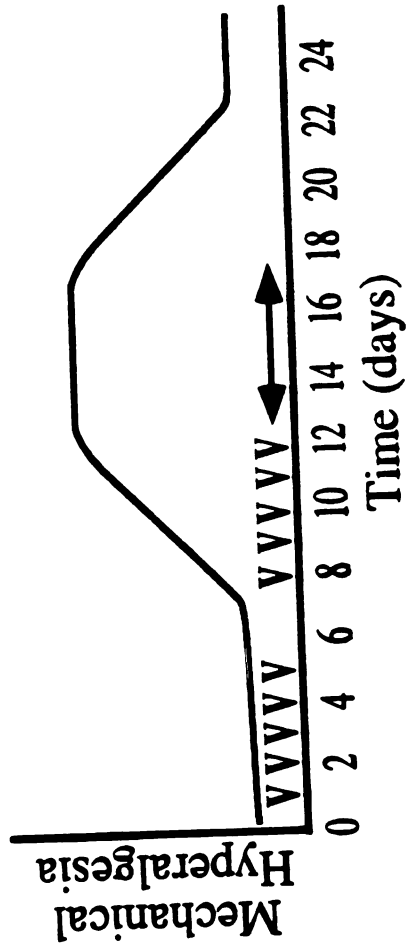
Wang N, Butler JP, Ingber DE (1993). Mechanotransduction across the cell surface and through the cytoskeleton. *Science* 260, 1124-1127.

Weiss HD, Walker MD, Wiernik PH (1974). Neurotoxicity of commonly used antineoplastic agents (second of two parts). *N Engl J Med* 291, 127-133.

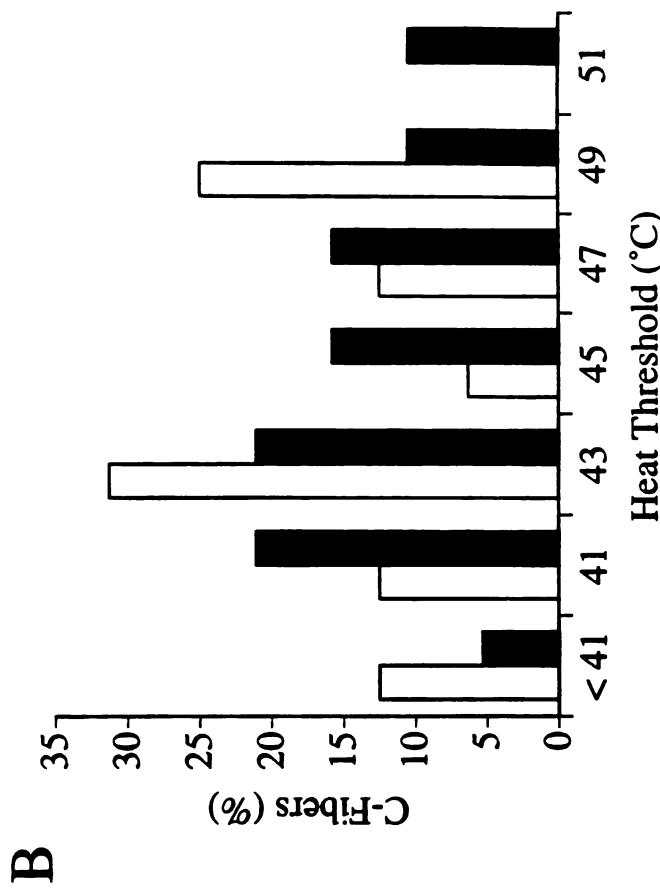
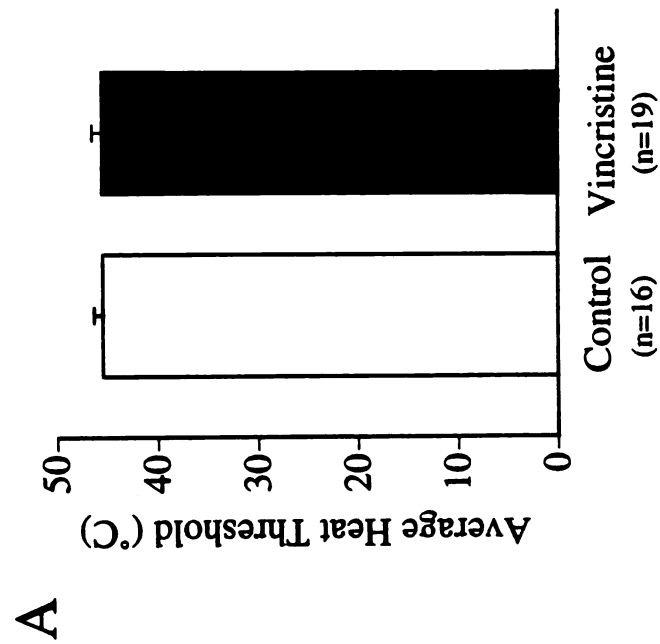
White DM, Levine JD (1991). Different mechanical transduction mechanisms for the immediate and delayed responses of rat C-fiber nociceptors. *J Neurophysiol* 66, 363-368.

**Figure 1: Schematic of experimental timeline.** Rats were injected intravenously with 100  $\mu\text{g}/\text{kg}$  vincristine sulfate (V) on days 1-5 and days 8-12. The magnitude of mechanical hyperalgesia in vincristine-treated rats is shown schematically above the timeline (Aley et al., 1996). Electrophysiological recordings performed during the time period indicated by the arrow have demonstrated that unmyelinated sensory neurons are hyperresponsive to mechanical stimulation (Tanner et al., 1997b). The mechanical withdrawal threshold of >90% of vincristine-treated rats was decreased >15% during the time period indicated by the arrow (K.O. Aley and J.D. Levine, unpublished observations).



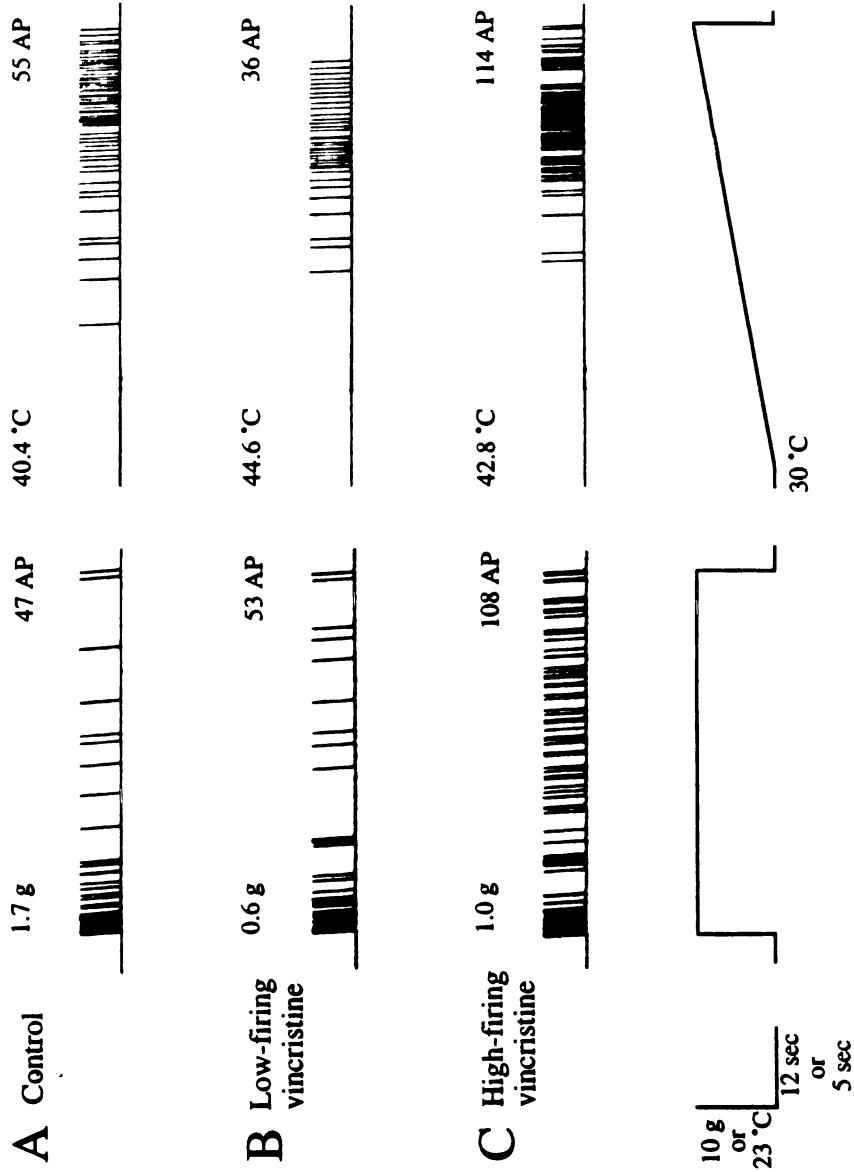


**Figure 2: Vincristine does not decrease the heat activation threshold of nociceptors.** Heat activation thresholds were determined using a Peltier device that delivered a ramped heat stimulus from 30 to 58°C at a rate of 1°C/ s. Heat threshold was defined as the temperature at which the C-fiber fired a second AP. Each heat activation threshold was the average of 2 trials with a 10 min interstimulus interval between trials. **A:** The average heat activation threshold for control C-fibers is shown by the open bar and for vincristine-treated C-fibers is shown by the filled bar. **B:** The distribution of C-fiber heat activation thresholds is shown in the histogram for 16 vincristine-treated C-fibers and 19 control C-fibers. Binwidth is 2°C.

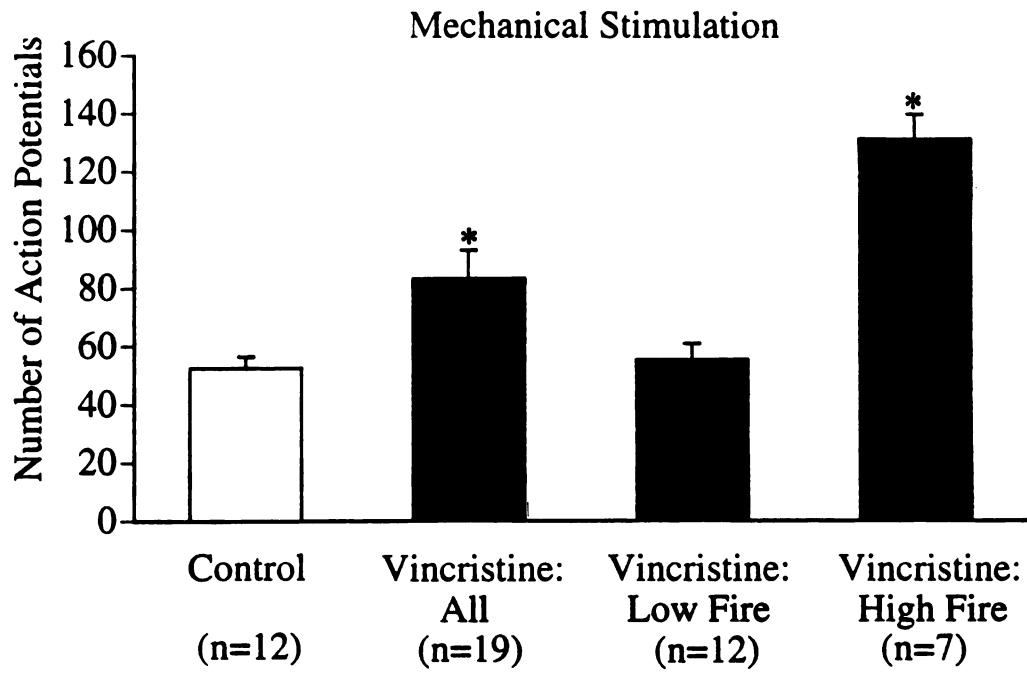
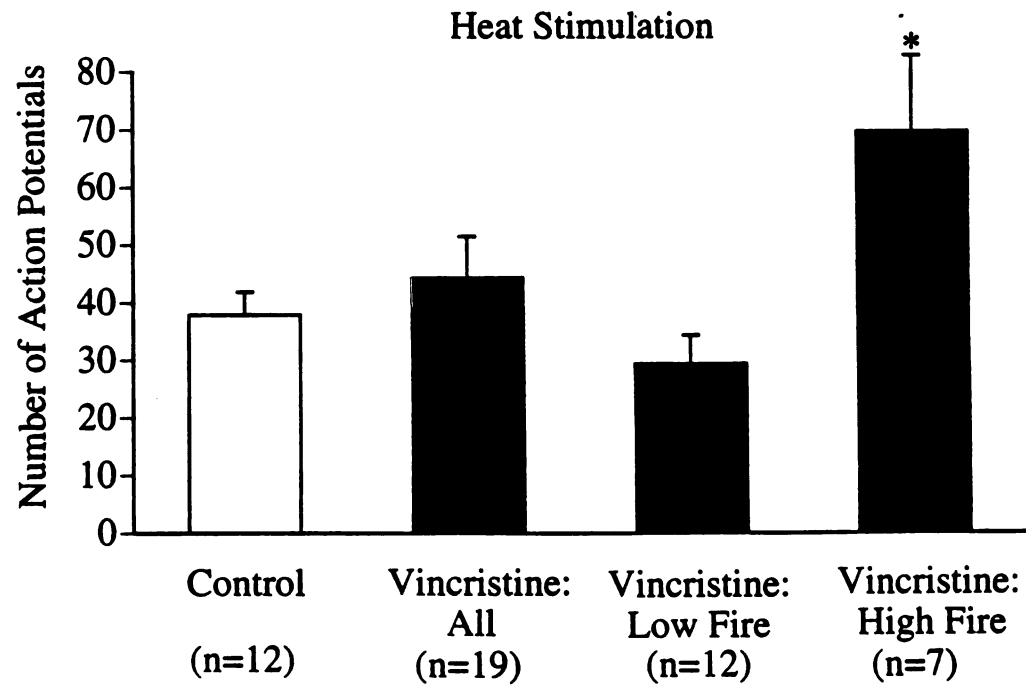


**Figure 3: Vincristine causes heat hyperresponsiveness in high-firing vincristine-treated nociceptors.** Example responses to mechanical stimulation (1 min, 10 g) and heat stimulation (ramp from 30°C to 53°C at 1°C / s) for **A:** a C-fiber from a control rat with a mechanical threshold of 1.7 g and a heat threshold of 40.4°C, **B:** a low-firing C-fiber from a vincristine-treated rat with a mechanical threshold of 0.6 g and a heat threshold of 44.6°C, and **C:** a high-firing C-fiber from a vincristine-treated rat with a mechanical threshold of 1.0 g and a heat threshold of 42.8°C. The number of APs fired during each stimulation trial is shown in the upper right of each trial. Note that this high-firing vincristine-treated nociceptor fired more than twice as many APs than control or low-firing vincristine-treated nociceptors for both mechanical and heat stimulation.

Mechanical responsiveness      Heat responsiveness



**Figure 4: Heat hyperresponsiveness occurs in high-firing but not low-firing vincristine-treated nociceptors.** **A:** The average response to mechanical stimulation (10 g, 1 min) for all control C-fibers studied (n = 16) is shown in the open bars. The average response to mechanical stimulation for all vincristine-treated C-fibers studied (n = 19), low-firing vincristine-treated C-fibers (n = 12), and high-firing vincristine-treated C-fibers (n = 7) is shown in the filled bars. **B:** The average response to heat stimulation (ramp from 30°C to 53°C at 1°C / s) for all control C-fibers studied (n = 16) is shown in the open bars. The average response to heat stimulation for all vincristine-treated C-fibers studied (n = 19), low-firing vincristine-treated C-fibers (n = 12), and high-firing vincristine-treated C-fibers (n = 7) is shown in the filled bars. \* p < 0.05.

**A****B**

**Figure 5: Heat hyperresponsiveness occurs in some, but not all, high-firing vincristine-treated nociceptors.** **A:** The response to mechanical stimulation (10 g, 1 min) for all control C-fibers studied (n = 16) is plotted against the response to heat stimulation (ramp from 30°C to 53°C at 1°C / s) of that nociceptor for control C-fibers (n = 19, □), low-firing vincristine-treated C-fibers (n = 12, ●), and high-firing vincristine-treated C-fibers (n = 7, ▲). Note that high-firing vincristine-treated nociceptors can have greater heat responses than control or low-firing vincristine-treated nociceptors. **B:** The response to heat stimulation is plotted against the heat threshold of that nociceptor for control C-fibers (n = 19, □), low-firing vincristine-treated C-fibers (n = 12, ●), and high-firing vincristine-treated C-fibers (n = 7, ▲). The regression line for control data is shown for reference. Note that high-firing vincristine-treated nociceptors can have greater heat responses than control or low-firing vincristine-treated nociceptors with comparable heat thresholds.



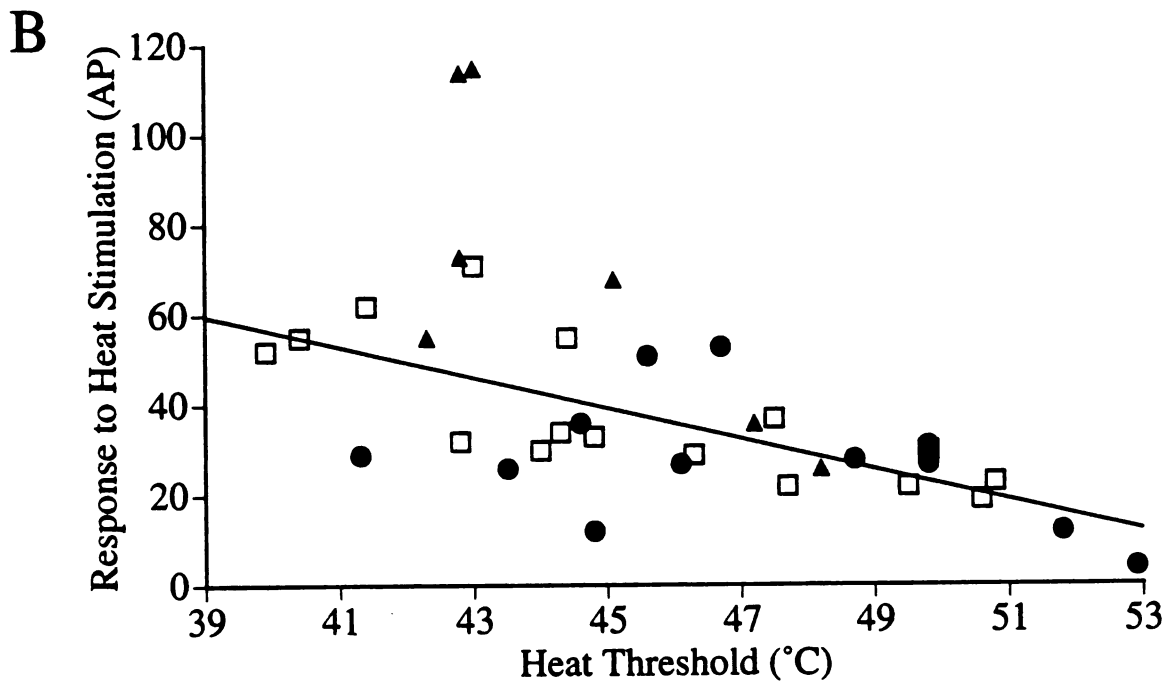
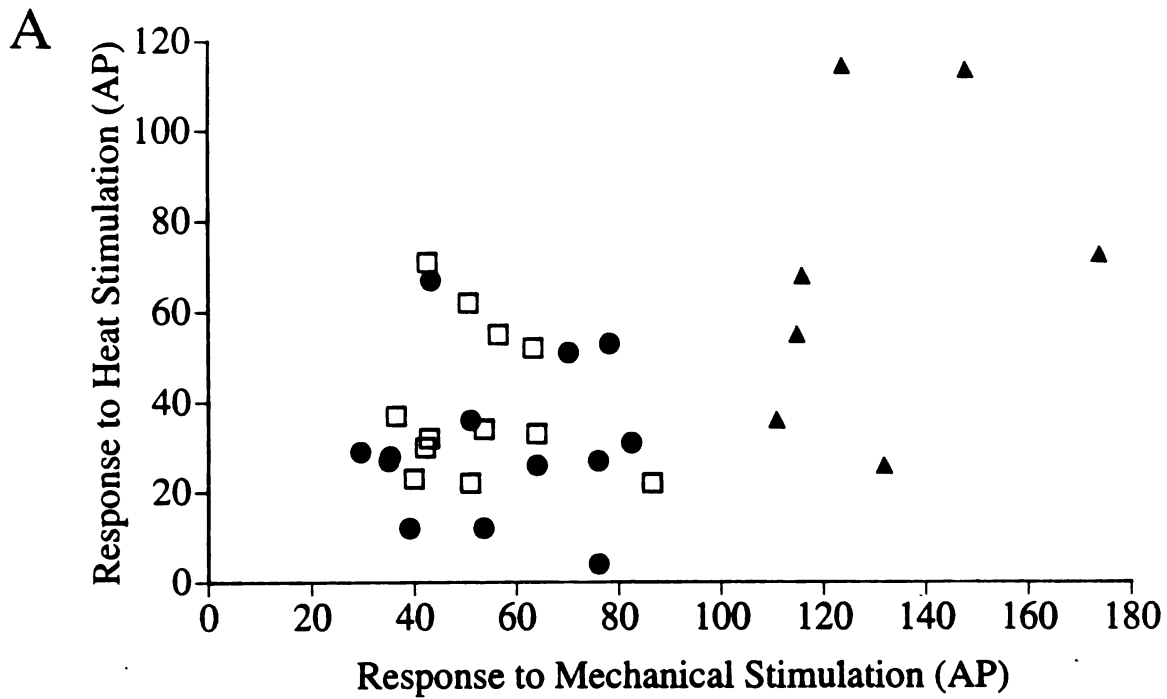
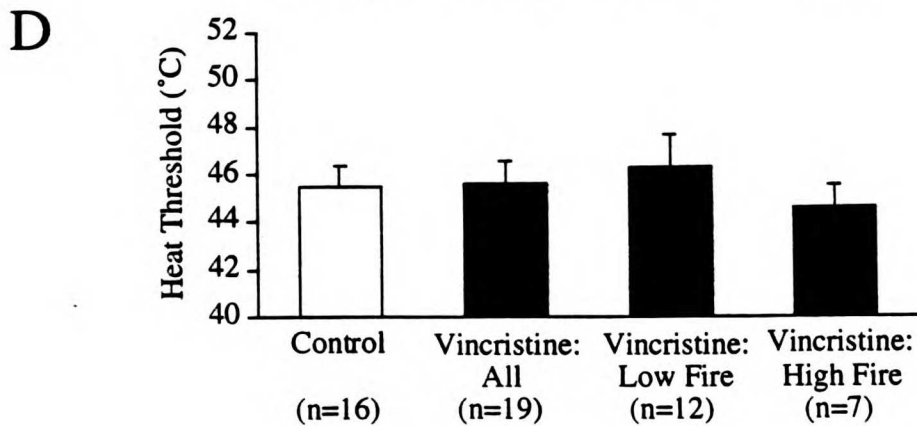
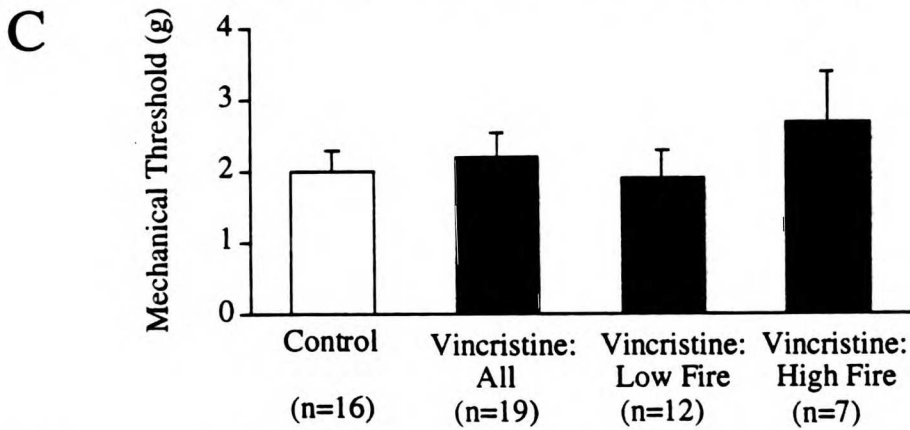
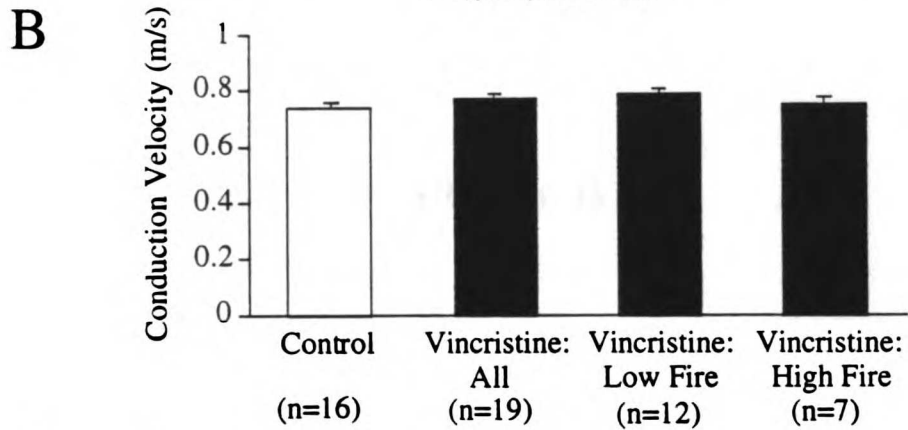
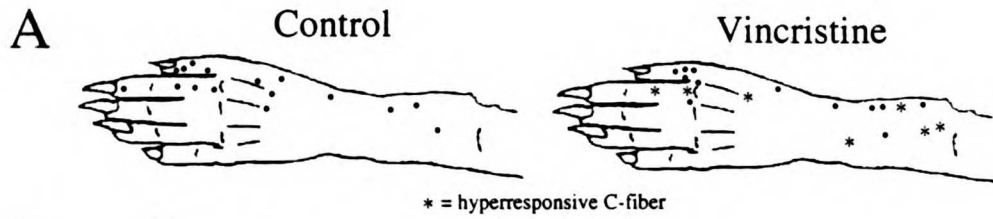


**Figure 6: Hyperresponsiveness in nociceptors is not correlated with receptive field location, conduction velocity, mechanical threshold, or heat threshold.** **A:** The receptive field locations for all C-fibers studied is shown on the left for control C-fibers and on the right for vincristine-treated C-fibers. Low-firing vincristine-treated nociceptors are represented by the symbol (●) and high-firing, mechanically hyperresponsive vincristine-treated nociceptors are represented by the symbol (\*). In this drawing of the left hindpaw, top is medial and bottom is lateral. **B:** The average conduction velocity for all control C-fibers studied (n = 16) is shown in the open bars. The average conduction velocity for all vincristine-treated C-fibers studied (n = 19), low-firing vincristine-treated C-fibers (n = 12), and high-firing vincristine-treated C-fibers (n = 7) is shown in the filled bars. **C:** The average mechanical threshold for all control C-fibers studied (n = 16) is shown in the open bars. The average mechanical threshold for all vincristine-treated C-fibers studied (n = 19), low-firing vincristine-treated C-fibers (n = 12), and high-firing vincristine-treated C-fibers (n = 7) is shown in the filled bars. **D:** The average heat threshold for all control C-fibers studied (n = 16) is shown in the open bars. The average mechanical threshold for all vincristine-treated C-fibers studied (n = 19), low-firing vincristine-treated C-fibers (n = 12), and high-firing vincristine-treated C-fibers (n = 7) is shown in the filled bars. There are no significant differences between the groups.



## **Chapter IV:**

### **Temporal analysis of nociceptor hyperresponsiveness during vincristine-induced painful neuropathy in rat**

## **Abstract**

Pain is associated with a variety of insults to peripheral nerve including metabolic disorders, trauma, and neurotoxic drugs. Vincristine, a chemotherapeutic agent that is thought to exert its antineoplastic effects by depolymerizing microtubules, produces neuropathy in humans characterized by painful paresthesias and dysesthesias. Systemic administration of vincristine (100  $\mu\text{g}/\text{kg}$ ) in rat produces mechanical hyperalgesia during which approximately half of C-fiber nociceptors are markedly hyperresponsive to mechanical stimulation. In addition to firing more than twice as many action potentials as control nociceptors, these hyperresponsive vincristine-treated nociceptors also appeared to fire in distinct temporal patterns that were not seen in the responses of control or low-firing vincristine-treated nociceptors. An investigation of the characteristics of these temporal firing patterns may yield insight into mechanisms of nociceptor hyperresponsiveness. To analyze this change in firing pattern, the distribution of interspike intervals and plots of instantaneous frequency were constructed for the responses to mechanical stimulation of vincristine-treated and control nociceptors. Instantaneous frequency plots reveal that hyperresponsive vincristine-treated nociceptors fired in one of two characteristic firing patterns. One mode was a variable frequency firing pattern with alternating periods of high and low firing frequency, whereas the second mode was a constant frequency firing pattern. The variable frequency mode is correlated with a preponderance of ISIs less than 100 msec, whereas the constant frequency mode is correlated with a preponderance of ISIs in the range of 100-300 msec. In addition, hyperresponsive nociceptors that fire in constant frequency mode have significantly higher mechanical thresholds compared to both those that fire in variable frequency mode and control nociceptors; there was no difference in the conduction velocities of these populations. These data suggest that multiple cellular mechanisms may contribute to vincristine-induced hyperresponsiveness in nociceptors, that the time scale of these mechanisms may be different, and that the temporal characteristics of hyperresponsiveness are correlated with the mechanical threshold of the nociceptor.

## **Introduction**

The neural mechanisms underlying neuropathic pain following a wide variety of insults including metabolic disorders, trauma, and neurotoxic drugs are largely unknown. Chemotherapy-induced pain is a form of neuropathic pain associated with neurotoxic drugs such as vincristine and taxol and is characterized by painful paresthesias and dysesthesias (Sandler et al., 1969; Holland et al., 1973). The vinca alkaloid vincristine is a widely used antineoplastic agent that is thought to exert its effects by disruption of the cytoskeleton in mitotically active cells. The clinical efficacy of vincristine is limited by the development of a mixed sensorimotor neuropathy (Sandler et al., 1969; Holland et al., 1973). Recently, we established an animal model of vincristine-induced painful neuropathy in rat (Aley et al., 1996). Mechanical hyperalgesia, measured 24 hours after vincristine administration, develops when 10 daily vincristine injections (100  $\mu\text{g}/\text{kg}$ ) are administered intravenously over a 2-week period that persists for more than a week following the final injection of vincristine.

During the peak phase of mechanical hyperalgesia, approximately half of C-fiber nociceptors in the peripheral nerves of vincristine-treated rats are markedly hyperresponsive to suprathreshold mechanical stimulation (Tanner et al., 1997b). In contrast, mechanical activation thresholds are not decreased; rather there is a trend towards higher mechanical thresholds in vincristine-treated nociceptors. In addition, the mean conduction velocities of A-fibers and C-fibers in vincristine-treated rats are significantly slowed. All other aspects of peripheral nerve function assayed appear unaffected (Tanner et al., 1997b). Together these data suggest that vincristine predominantly affects neural mechanisms underlying the evoked response to external stimulation without causing generalized impairment of neuronal function.

Although the mechanisms of vincristine-induced hyperresponsiveness to mechanical stimulation are unknown, they likely involve vincristine-induced changes in the microtubular cytoskeleton. Recent ultrastructural analysis of unmyelinated axons during

vincristine-induced hyperalgesia revealed disorientation of microtubules without any signs of axonal degeneration (Tanner et al., 1997a). Since the cytoskeleton is involved in the anchoring of ion channels and receptors and can contribute to adaptation and desensitization of these proteins (Srinivasan et al., 1988; Bigot and Hunt, 1990; Kirsch et al., 1991; Rosenmund and Westbrook, 1993), vincristine-induced disorientation of microtubules in the nerve terminal might contribute to nociceptor hyperresponsiveness by modulating the kinetics of ion channels involved in responses to external stimulation.

Hyperresponsive vincristine-treated nociceptors appeared to fire in distinct temporal patterns, often in bursts of several action potentials, that are not seen in control or low-firing vincristine-treated nociceptors. An investigation of the characteristics of these temporal firing patterns may yield insight into the ionic mechanisms that contribute to nociceptor hyperresponsiveness. To determine the characteristics of nociceptor firing patterns, we constructed histograms of the distribution of interspike intervals and plots of instantaneous frequency for the responses of vincristine-treated nociceptors and control nociceptors to mechanical stimulation. In addition, we correlated the conduction velocity, mechanical threshold, and receptive field location of hyperresponsive nociceptors to determine if any of these characteristics were predictive of distinct temporal firing patterns.

## Methods

### *Animals*

Experiments were performed on 200-400 g male Sprague-Dawley rats (Bantin and Kingman, Fremont, CA). Rats were housed in a temperature- and humidity-controlled environment and were maintained on a 12 hour light/dark cycle. Food and water were available *ad libitum*. Experiments were approved by the Committee on Animal Research at UCSF.

### *Vincristine Treatment*

Vincristine sulfate (Sigma, St. Louis, MO) was dissolved in saline to a stock concentration of 1 mg/ml, pH between 4.5 and 5.2. The drug was then diluted daily, just prior to use, in saline to a concentration of 100 µg/ml that was administered intravenously into the tail vein at a dose of 100 µg/kg followed by 0.5 ml of saline. Treatments occurred daily (Monday through Friday) for 2 weeks with the dosage calculated on daily body weight. This dosage regimen was chosen because it produced maximal hyperalgesia in the absence of motor impairment in most rats (Aley et al., 1996). Paresthesias occur in humans receiving 12.5-75 µg/kg vincristine administered weekly (McLeod and Penny, 1969; Sandler et al., 1969; Holland et al., 1973). Vincristine-treated rats weighed  $293 \pm 9$  g (n=17) at the time of electrophysiological recording. Control rats were weight-matched,  $296 \pm 7$  g (n=10), and untreated; previous behavioral experiments demonstrated that repeated intravenous saline injections had no effect on behavioral nociceptive threshold (Aley et al., 1996). Experimental rats were used for electrophysiological recordings during the peak phase of chronic vincristine-induced hyperalgesia that occurred in the absence of the drug, that is from 1-5 days following the final injection of vincristine. This recording window was chosen based on behavioral data which showed that the mechanical withdrawal threshold of >90% of vincristine-treated rats was decreased >15% during these 5 days (K.O. Aley and J.D. Levine, unpublished observations). Vincristine-treated rats did



not gain weight normally during the course of the treatment, as has been described previously (Aley et al., 1996). There was an average decrease in body weight during vincristine treatment of  $11 \pm 2\%$ , although this varied substantially from rat to rat. At this dose of vincristine, 18% of rats were euthanized prior to electrophysiological recording because of the development of motor impairment.

#### *In vivo single unit electrophysiology*

The single-unit electrophysiological recording techniques employed have been described previously (White and Levine, 1991; Ahlgren et al., 1992). Briefly, rats were anesthetized with pentobarbital sodium (65 mg/kg i.p.) and additional anesthetic was administered throughout the experiment to maintain areflexia. Recordings were made from the saphenous nerve, the cutaneous nerve that innervates the medial-dorsal hindpaw where mechanical hyperalgesia to vincristine was characterized (Aley et al., 1996). The skin overlying the saphenous nerve was retracted at mid-thigh level. The nerve was exposed and dissected free from surrounding tissue and vessels and maintained in a pool of 37°C mineral oil. Bipolar stimulating electrodes were placed under the nerve at a distal site to enable electrical stimulation (Stimulator S-88, Grass Medical Instruments, Quincy, MA and Stimulus Isolator NL-800, Neurolog, Medical Systems Corp., Greenvale, NY) of peripheral neurons. At a proximal site, a portion of the nerve was desheathed to expose axons. The nerve was crushed proximal to the recording site to prevent the elicitation of flexor reflexes during electrical stimulation of the nerve. Fine fascicles of axons were then dissected from the nerve with sharpened jeweler's forceps and placed on a silver wire recording electrode. Action potentials (APs) from individual fibers were amplified and filtered (Neurolog, Medical Systems Corp., Greenvale, NY) and then stored on tape (Video Cassette Recorder 420K, A. R. Vetter Co., Rebersburg, PA), as well as being discriminated by amplitude (Winston Electronics Co., San Francisco, CA) and displayed

on a chart recorder. The animal was sacrificed by pentobarbital overdose at the end of the recording session.

### *Characterization of C-fiber nociceptors*

#### *Conduction velocity*

Conduction velocity was determined by dividing the distance between the recording and stimulating electrodes, which measured between 20 and 33 mm, by the latency of the AP following an electrical stimulus to the whole nerve. Neurons that conducted at  $<2$  m/s were classified as C-fibers and  $\geq 2$  m/s were classified as A-fibers (Lynn and Carpenter, 1982; Leem et al., 1993).

#### *Receptive field*

The receptive fields of C-fibers were determined using a mechanical search stimulus, either a blunt probe or a ~60 g von Frey hair (VFH) which activates  $>90\%$  of C-fibers in the saphenous nerve of the rat (Lynn and Carpenter, 1982; Ahlgren et al., 1992). C-fibers were required to show a slowed conduction velocity in response to electrical stimulation following mechanical stimulation of the receptive field. This latency shift test established that the mechanical receptive field under study was innervated by the C-fiber whose latency to electrical stimulation was shifted. The receptive fields of C-fibers were determined to be cutaneous if they were activated by lifting and squeezing the skin or if the mechanically sensitive spot moved to a new location when the skin was moved relative to the subcutaneous tissues. Neurons that did not meet this criterion were not further evaluated.

#### *Mechanical Activation Threshold*

Mechanical activation thresholds were determined using a series of von Frey hairs that ranged in intensity from 0.02 - 263 g (A. Ainsworth, London, England). The

mechanical threshold was defined as the intensity in grams of the weakest VFH to which the neuron fired more than 2 APs in 50% of the trials. Each trial consisted of a brief (~1 s) application of a VFH to the center of the receptive field. VFH were applied in ascending order, and approximately 5-10 trials were performed for each VFH tested. Threshold was verified by alternately testing the strongest ineffective VFH and the weakest effective VFH. Such repeated mechanical testing of C-fibers does not cause a change in mechanical threshold (K.D. Tanner and J.D. Levine, unpublished observations, (Reeh et al., 1987; Ahlgren et al., 1992).

#### *Sustained Mechanical Stimulation*

Sustained mechanical stimulation of receptive fields was accomplished by use of a mechanical stimulation device consisting of a force transducer (Entran Devices, Inc., Model ELF-TC500-1, Fairfield, NJ) with a response range of 1-400 g mounted in series with a receptacle that can interchangeably hold von Frey hair filaments (modified from a set of Stoelting VFHs, Wood Dale, IL) that deliver various gram weight stimuli. VFHs were used since they are able to compensate well for changes in tissue elasticity over time, unlike rigid probes. The VFH is applied to the receptive field, by hand, and maintained at the just-bent position for 1 min. The voltage output signal from the force transducer is a quantitative measure of the force applied to the receptive field and is sent to both a chart recorder and a VCR tape for storage and off-line analysis.

A 10-g mechanical stimulus was chosen to examine the response properties of nociceptive afferents because this stimulus is suprathreshold for >90 % of C-fibers in the saphenous nerve. For each neuron whose response to prolonged stimulation was studied, the conduction velocity, receptive field location, baseline spontaneous activity, and mechanical threshold were determined. In general, the prolonged stimulation protocol consisted of 4 trials of sustained 1-min mechanical stimulation with a 10-min interstimulus interval between trials. The average of these 4 trials was the sustained mechanical

stimulation response for that neuron and usually had a standard error of the mean of less than 10%. In a small number of cases included in the analysis, more trials were conducted to reduce the standard error or fewer trials were conducted because the neuron was lost. Activity was monitored for 5 min after the removal of the mechanical stimulus to quantitate afterdischarge.

Due to physical constraints in applying the sustained mechanical stimulus, only C-fibers with receptive fields below the ankle were studied. Since vincristine treatment causes slowing of the conduction velocity of all afferents, only C-fibers that conducted at less than 1 m/s were studied to avoid inadvertently recording the response properties of slowed A $\delta$ -fibers. In addition, since some vincristine-treated neurons develop an afterdischarge following mechanical stimulation, we did not record from C-fibers that fired >5 AP/min during the 2-min observation period to avoid recording from those neurons that may have developed ongoing activity following mechanical search stimulation of the skin; this was <10 % of the C-fibers population studied.

#### *Classification of vincristine-treated nociceptors*

Vincristine causes hyperresponsiveness to sustained mechanical stimulation in approximately half of C-fiber nociceptors (Tanner et al., 1997b). Whereas the responses of C-fibers from control rats are clustered in a unimodal distribution in the range of 50-59 AP/min stimulus, the responses of C-fibers from vincristine-treated rats form 2 distinct clusters in a bimodal distribution with a cluster in the range of 50-59 AP/min stimulus and another in the range of 100-109 AP/min stimulus and greater (Tanner et al., 1997b). Vincristine-treated C-fibers that fired <100 AP in response to sustained mechanical stimulation were categorized as "low-firing" C-fibers. Vincristine-treated C-fibers that fired >100 AP in response to sustained mechanical stimulation were categorized as hyperresponsive or "high-firing" C-fibers.

### *Instantaneous Frequency Plots*

To display the temporal profile of nociceptor responses to mechanical stimulation, instantaneous frequency plots were constructed by taking the inverse of each interspike interval and plotting these values against time along the x-axis for each mechanical stimulation trial for each neuron studied. Visual inspection of instantaneous frequency plots allowed high-firing vincristine-treated nociceptors to be further classified as firing in either a constant frequency mode or a variable frequency mode (see Figure 3). Of note, no constant frequency or variable frequency mode subclasses were evident in examining the instantaneous frequency plots of control or low-firing vincristine-treated nociceptors.

### *Interspike Interval (ISI) Analysis*

Interspike interval (ISI) analysis was used to quantitate the temporal characteristics of the responses of nociceptors to mechanical stimulation. The ISIs for each nociceptor response to mechanical stimulation (10 g, 1 min) were determined using Maclab Chart software (New South Wales, Australia). ISIs were grouped into 100 ms bins that ranged from 0 to 2.9 s with all interspike intervals greater than or equal to 3 s binned together. For each trial of mechanical stimulation, the number of ISIs in each interval bin was divided by the total number of interspike intervals for that trial. Thus, the distribution of ISIs was expressed as the percentage of ISIs in each interval bin for a given trial (see Figures 4, 5, and 6). This trial by trial normalization procedure allowed ISI distributions from several trials and several neurons to be averaged together. In addition, the ISI distribution just for the burst period of the response (first 10 sec) and just for the plateau period of the response (final 50 sec) were also determined in the manner described above.

### *Statistical Analysis*

Data are expressed as mean  $\pm$  standard error of the mean (SEM). Mann-Whitney U nonparametric analysis was used to compare the mechanical thresholds of C-fiber populations.

## Results

### *High-firing vincristine-treated nociceptors fire in distinct temporal patterns*

To assay responsiveness of C-fibers to sustained mechanical stimulation, a 10-g stimulus was delivered to the receptive field for 1 min. As shown previously (Tanner et al., 1997b), a subset of vincristine-treated C-fiber nociceptors are hyperresponsive (high-firing), firing more than twice as many APs in response to 10-g mechanical stimulation as control or non-hyperresponsive (low-firing) vincristine-treated C-fiber nociceptors. As shown in Table 1, the increased responsiveness in high-firing vincristine-treated C-fibers was significant ( $p < 0.01$ ) both during the burst (first 10 sec) and the plateau (last 50 sec), as well as the whole response (1 min). There were no significant differences between the conduction velocities and mechanical thresholds of high-firing vincristine-treated nociceptors compared to control or to low-firing vincristine-treated nociceptors (Table 1), although we have previously noticed a trend for high-firing vincristine-treated nociceptors to have higher mechanical thresholds (Tanner et al., 1997b). In addition, high-firing nociceptors do not appear to be located in any specific skin region of the dorsal hindpaw (Figure 7) (Tanner et al., 1997b).

High-firing vincristine-treated nociceptors fired in distinct temporal patterns not seen in the responses of control or low-firing vincristine-treated nociceptors. Examples of response to mechanical stimulation (10 g, 1 min) is shown in Figure 1A for a control nociceptor, Figure 1B for a low-firing vincristine-treated nociceptor, and Figure 1C for a high-firing vincristine-treated nociceptor. The control and the low-firing vincristine-treated nociceptors fire a burst of APs at the onset of the stimulus and then adapt, firing single APs irregularly for the duration of the stimulus. In contrast, this high-firing vincristine-treated nociceptor continues to fire clusters of 2-7 APs during the stimulus.

*High-firing vincristine-treated nociceptors fire in one of two modes during a mechanical response*

To emphasize the temporal structure of each response to mechanical stimulation, the data from each stimulation trial, such as those shown in Figure 1, were plotted as instantaneous frequency plots. Figure 2 shows the instantaneous frequency plot for one trial of stimulation for five different control nociceptors (Figure 2A) and five different low-firing vincristine-treated nociceptors (Figure 2B). Both control and low-firing vincristine-treated nociceptors usually fired a burst of APs in the first 10 sec and then adapted to very low levels of activity, firing single APs irregularly. Higher frequency events, reflecting doublet firing, can be seen in control and low-firing vincristine-treated nociceptors, but are infrequent (see lower panels, Figure 2A and 2B).

Visual inspection of the instantaneous frequency plots of high-firing vincristine-treated nociceptors revealed that they fired in two distinct temporal patterns (Figure 3). One mode was a variable frequency firing pattern with alternating periods of high and low firing frequency, whereas the second mode was a constant frequency firing pattern at an intermediate firing frequency. Examples of five constant frequency high-firing and five variable frequency high firing are shown in Figure 3A and 3B, respectively. Regardless of the temporal pattern of their response, all high-firing vincristine-treated nociceptors fired similar numbers of APs in response to mechanical stimulation (10 g, 1 min), such that their average firing frequency was not significantly different (Table 2).

It should be noted that although most neurons fired predominantly in either one mode or the other, rarely a high-firing vincristine-treated nociceptor would fire in one mode during one stimulus trial and in another mode during all other stimulus trials. There were no examples of a nociceptor that appeared to switch between firing modes within a single stimulus trial.



*Variable frequency high-firing vincristine-treated nociceptors are most likely to fire action potentials less than 100 msec apart and constant frequency high-firing vincristine-treated nociceptors are most likely to fire action potentials between 100 and 300 msec apart during a mechanical response*

To quantitate these two distinctive temporal firing patterns of high-firing vincristine-treated nociceptor responses, the average ISI distribution for mechanical stimulation (10 g, 1 min) was constructed for control nociceptors (n=21), low-firing vincristine-treated nociceptors (n=11), and high-firing vincristine-treated nociceptors (n=18) (Figure 4). There was a shift in the ISI distribution for both classes of high-firing vincristine-treated nociceptors. Variable frequency mode high-firing vincristine-treated nociceptors fired such that a preponderance of their ISIs were <100 msec long, whereas constant frequency mode high-firing vincristine-treated nociceptors fired such that a preponderance of their ISIs were between 100-300 msec long.

The temporal characteristics of the response of high-firing vincristine-treated nociceptors could result from their higher average firing frequency (Table 1) and not be related to effects of vincristine. If the temporal characteristics of nociceptor responsiveness are caused by an increased average firing frequency, the ISI distribution for the burst and the plateau for each population of nociceptors studied should be different since the burst response has an average firing frequency 4-5 times higher than that of the plateau phase. The ISI distributions for the burst (Figure 5) and plateau (Figure 6) periods were similar to the ISI distribution for the whole trial for all groups of nociceptors studied. The characteristic ISI distributions of seen for the whole stimulation trial for variable frequency mode high-firing vincristine-treated nociceptors and constant frequency mode high-firing vincristine-treated nociceptors is also seen in the ISI distributions for the burst period only and the plateau period only.

*Constant frequency mode high-firing vincristine-treated nociceptors have higher mechanical thresholds than variable frequency mode high-firing vincristine-treated nociceptors*

To determine whether other physiological characteristics of high-firing vincristine-treated nociceptors correlated with their temporal firing mode, we compared the conduction velocities and mechanical thresholds, as well as the number of APs in the total, burst, and plateau responses to mechanical stimulation of the two classes of high-firing vincristine-treated nociceptors. As shown in Table 2, there were no statistically significant differences between the characteristics of constant frequency mode and variable frequency mode high-firing vincristine-treated nociceptors, with the exception of mechanical threshold. The mechanical threshold of constant frequency mode high-firing vincristine-treated nociceptors ( $3.1 \pm 0.5$  g) was significantly greater ( $p < 0.05$ , Mann-Whitney U test) than that of both variable frequency mode high-firing vincristine-treated nociceptors ( $1.3 \pm 0.5$  g) and well as control nociceptors ( $1.5 \pm 0.3$  g).

To verify that temporal firing pattern was not correlated with skin properties on different regions of the paw, we compared the receptive field locations for all control and vincristine-treated nociceptors (Figure 7). There was no apparent difference in the distribution of receptive fields between control, low-firing vincristine-treated, and high-firing vincristine-treated nociceptors or between constant frequency mode and variable frequency mode high-firing vincristine-treated nociceptors.

## **Discussion**

In addition to firing more than twice as many action potentials as control nociceptors, we observed that hyperresponsive vincristine-treated nociceptors also fire in distinct temporal patterns in response to a sustained mechanical stimulus. An investigation of the characteristics of these temporal firing patterns may yield insight into the ionic mechanisms that contribute to nociceptor hyperresponsiveness. Instantaneous frequency plots revealed that hyperresponsive vincristine-treated nociceptors fired in one of two characteristic firing patterns. One mode was a variable frequency firing pattern with alternating periods of high and low firing frequency, whereas the second mode was a constant frequency firing pattern. The variable frequency mode was correlated with a majority of ISIs less than 100 msec, whereas the constant frequency mode was correlated with a majority of ISIs in the range of 100-300 msec. Hyperresponsive nociceptors that fired in constant frequency mode have significantly higher mechanical thresholds compared to both those that fire in variable frequency mode and control nociceptors; there was no difference in the conduction velocities of these populations. These data suggest that multiple cellular mechanisms may contribute to vincristine-induced hyperresponsiveness in nociceptors, that the time scale of these mechanisms is different, and that the temporal characteristics of hyperresponsiveness are correlated with the mechanical threshold of the nociceptor.

### Are shifts in high-firing ISI distributions simply a function of firing more action potentials?

Distinctive temporal firing patterns may not be caused by vincristine-induced alterations in function, but rather due to high-firing vincristine-treated nociceptors firing at twice the average firing frequency of control or low-firing vincristine-treated nociceptors. Since it is difficult to drive control nociceptors to fire at as high an average firing frequency as high-firing vincristine-treated nociceptors, even at higher intensities of mechanical stimulation, it is difficult to address this issue experimentally. However, several lines of

evidence suggest this is not the case. Firstly, the distribution pattern of ISIs was the same for the whole trial, the burst phase, and the plateau phase of the trial for each population of nociceptors examined. Since the average firing frequency of the burst period is 4-5 times higher than the plateau period for each class of nociceptors studied, large differences in average firing frequency do not appear to cause dramatic shifts in the ISI distributions. Secondly, if the shifts in the ISI distribution were solely due to the higher average firing frequency of high-firing vincristine-treated nociceptors, then the ISI distributions for constant frequency mode and variable frequency mode high-firing vincristine-treated nociceptors should appear the same. This is not, in fact, the case. Constant frequency mode nociceptors have a characteristic peak in the ISI distribution between 100-300 msec, whereas variable frequency mode nociceptors have a characteristic peak in the ISI distribution less than 100 msec. Lastly, preliminary temporal analysis of sensitized nociceptor responses following PGE<sub>2</sub>, which produces approximately a 40% increase in the average firing frequency, does not reveal two distinctive temporal firing patterns or the distribution of ISIs for (XJ Chen, KD Tanner, JD Levine, unpublished observations). These data suggest that an increase in average firing frequency is not sufficient to cause the shift in temporal structure and ISI distribution observed in high-firing vincristine-treated nociceptors. Therefore, the distinctive ISI distributions of high-firing vincristine-treated nociceptors are unlikely to be secondary to their increased average firing frequency, but rather arise from distinctive temporal firing patterns exhibited by these neurons.

#### Origins of characteristic temporal firing patterns: constant frequency mode vs. variable frequency mode

Since both constant frequency and variable frequency high-firing vincristine-treated nociceptors fire the same number of action potentials, the distinctive temporal firing patterns observed must stem from other differences between these nociceptors. These

temporal firing patterns might have their origins in different underlying nociceptor phenotypes or rather be due to multiple mechanisms of vincristine action.

Constant frequency and variable frequency high-firing vincristine-treated nociceptors could arise from two phenotypic populations of nociceptors expressing distinct complements of ion channels that influence the temporal patterns of firing. However, instantaneous frequency plots for control nociceptor and low-firing nociceptor responses to mechanical stimulation did not reveal two firing modes as are seen in the high-firing vincristine-treated nociceptors. If phenotypic differences in nociceptors underlie these two temporal firing modes, then they may only become apparent when nociceptors fire at higher average frequencies. In preliminary analyses, increasing the firing frequency of nociceptors by 40% with the inflammatory mediator PGE<sub>2</sub>, does not reveal distinct temporal firing patterns and shifts in the ISI distribution of nociceptors into constant frequency or variable frequency firing mode (XJ Chen, KD Tanner, JD Levine, unpublished observations).

Alternatively, the two temporal firing patterns in high-firing vincristine-treated C-fibers could result from vincristine-induced changes in nociceptor function. The mechanisms by which vincristine causes hyperresponsiveness in nociceptors are likely to involve its actions on the microtubular cytoskeleton. Recent ultrastructural analysis of unmyelinated axons in the peripheral nerve of vincristine-treated rats during the peak phase of hyperalgesia revealed disorientation of microtubules and swelling of unmyelinated axons without any signs of axonal degeneration (Tanner et al., 1997a).

Hyperresponsiveness may occur due to alterations in axonal transport secondary to cytoskeletal disorganization, as has been previously hypothesized (Shelanski and Wisniewski, 1969; Bradley et al., 1970; Casey et al., 1973; Weiss et al., 1974). Impairment of axonal transport could produce imbalances in the complement of ion channels present in the nerve terminal and changes in the dynamics of excitability in the nerve terminal. The degree of impairment of axonal transport might produce different

profiles of current imbalance in different nociceptors, subsequently causing altered firing patterns.

In addition, several lines of evidence suggest that the cytoskeleton is involved generally in the anchoring of ion channels and receptors, as well as in the desensitization of some of these receptors following activation (Srinivasan et al., 1988; Bigot and Hunt, 1990; Kirsch et al., 1991; Rosenmund and Westbrook, 1993). If conductances involved in the responsiveness of polymodal nociceptors were regulated by the microtubular cytoskeleton, then vincristine-induced disorientation of microtubules in the nerve terminal of nociceptors could disrupt ion channel localization and kinetics and produce altered firing patterns. Although adaptation mechanisms may be impaired in both classes of high-firing vincristine-treated nociceptors, the complement of ion channels involved may be quite different either because of the phenotype of the nociceptor or alterations in axonal transport. *In vitro* studies of sensory neurons have shown that nociceptive neurons express a variety of currents that contribute to their responsiveness (Leal et al., 1993; Weinreich, 1995; Gold et al., 1996a; Gold et al., 1996b). For example, blockade of Ca<sup>2+</sup>-activated potassium currents that repolarize the neuron following action potential firing can result in repetitive firing behavior that resembles hyperresponsiveness (Gold et al., 1996b). *In vitro* analysis of nociceptive dorsal root ganglion neurons harvested from vincristine-treated rats during the phase of nociceptor hyperresponsiveness and behavioral hyperalgesia might determine whether the kinetics or density of specific currents are altered.

#### Mechanical threshold is correlated with temporal firing pattern in high-firing vincristine-treated nociceptors

High-firing vincristine-treated nociceptors that fire in constant frequency mode have elevated mechanical thresholds compared to both variable frequency mode high-firing vincristine-treated nociceptors and control nociceptors. If the different temporal firing patterns have their origins in different underlying nociceptor phenotypes which are revealed

by vincristine, then higher mechanical thresholds may occur in a subpopulation of nociceptors with a particular complement of ion channels. Alternatively, vincristine may alter both adaptation mechanisms and mechanotransduction mechanisms in constant frequency high-firing vincristine-treated nociceptors. If mechanotransduction in nociceptors involves the microtubular cytoskeleton, vincristine might directly impair mechanotransduction. This difference in mechanical threshold in a subset of high-firing vincristine-treated nociceptors may explain the previously reported trend for high-firing vincristine-treated nociceptors in general to have a higher mechanical threshold than control or low-firing vincristine-treated nociceptors (Tanner et al., 1997b).

#### Temporal structure of nociceptor responses in other models of neuropathy and inflammation

This study is the first examination of temporal firing patterns of the responses abnormal nociceptors to external stimulation during neuropathic hyperalgesia. Nociceptors in both diabetic neuropathy and chronic constriction injury have been reported to be hyperresponsive to mechanical and heat stimuli, respectively (Ahlgren et al., 1992; Koltzenburg et al., 1994). Analysis of the characteristics of the temporal structure of hyperresponsive nociceptors in these other neuropathic pain models might reveal whether there are common underlying mechanisms of nociceptor dysfunction in neuropathy models of diverse etiology.

Following inflammatory insults, C-fibers characteristically have lower activation thresholds, as well as increased responsiveness to external stimuli. In the neuropathy models that have been examined, heat or mechanical hyperresponsiveness occurs strikingly in the absence of a reduction in heat or mechanical activation thresholds (Ahlgren et al., 1992; Koltzenburg et al., 1994; Tanner et al., 1997b), suggesting that the cellular mechanisms that underlie nociceptor sensitization following inflammation may be distinct from those underlying nociceptor hyperresponsiveness in neuropathy. Preliminary analysis

of the temporal structure of the responses nociceptors during inflammation did not exhibit constant and variable frequency firing modes or shifts in ISI distributions (XJ Chen, KD Tanner, JD Levine, unpublished observations). This novel analysis of the structure of nociceptive responses may further suggest that the cellular mechanisms that modulate nociceptor function under these conditions may differ.

In conclusion, hyperresponsive vincristine-treated nociceptors have distinctive ISI distributions that are likely to arise from the characteristic temporal firing patterns exhibited by these neurons. High-firing vincristine-treated nociceptors fired in either a variable frequency mode where APs are most likely to occur less than 100 msec apart or a constant frequency mode where APs are most likely to occur 100-300 msec apart. Interestingly, constant frequency mode high-firing vincristine-treated nociceptors have elevated mechanical thresholds. These data suggest that multiple cellular mechanisms may contribute to vincristine-induced hyperresponsiveness in nociceptors, that the time scale of these mechanisms is different, and that the temporal characteristics of hyperresponsiveness are correlated with the mechanical threshold of the nociceptor. These data provide hypotheses for future *in vitro* investigations of hyperresponsive vincristine-treated nociceptors which may provide insight into ionic mechanisms of the behavioral mechanical hyperalgesia observed in rats treated with vincristine, as well as paresthesias and dysesthesias experienced by patients receiving vincristine as a chemotherapeutic agent.



## References

Ahlgren SC, White DM, Levine JD (1992). Increased responsiveness of sensory neurons in the saphenous nerve of the streptozotocin-diabetic rat. *J Neurophysiol* 68, 2077-2085.

Aley KO, Reichling DB, Levine JD (1996). Vincristine hyperalgesia in the rat: a model of painful vincristine neuropathy in humans. *Neuroscience* 73, 259-265.

Bigot D, Hunt SP (1990). Effect of excitatory amino acids on microtubule-associated proteins in cultured cortical and spinal neurones. *Neurosci Lett* 111, 275-280.

Bradley WG, Lassman LP, Pearce GW, Walton JN (1970). The neuromyopathy of vincristine in man. Clinical, electrophysiological and pathological studies. *J Neurol Sci* 10, 107-131.

Casey EB, Jelliffe AM, Le QP, Millett YL (1973). Vincristine neuropathy. Clinical and electrophysiological observations. *Brain* 96, 69-86.

Gold MS, Dastmalchi S, Levine JD (1996a). Co-expression of nociceptor properties in dorsal root ganglion neurons from the adult rat in vitro. *Neuroscience* 71, 265-75.

Gold MS, Shuster MJ, Levine JD (1996b). Role of a Ca<sup>2+</sup>-dependent slow afterhyperpolarization in prostaglandin E<sub>2</sub>-induced sensitization of cultured rat sensory neurons. *Neurosci Lett* 205, 161-4.

Holland JF, Scharlau C, Gailani S, Krant MJ, Olson KB, Horton J, Shnider BI, Lynch JJ, Owens A, Carbone PP, Colsky J, Grob D, Miller SP, Hall TC (1973). Vincristine

treatment of advanced cancer: a cooperative study of 392 cases. *Cancer Res* 33, 1258-1264.

Kirsch J, Langosch D, Prior P, Littauer UZ, Schmitt B, Betz H (1991). The 93-kDa glycine receptor-associated protein binds to tubulin. *J Biol Chem* 266, 22242-22245.

Koltzenburg M, Kees S, Budweiser S, Ochs G, Toyka K (1994). The properties of unmyelinated nociceptive afferents change in a painful chronic constriction neuropathy. In *Proc 7th World Cong Pain*, G Gebhart, D Hammond, T Jensen, ed. (Seattle: IASP Press), pp. 511-522.

Leal CH, Koschorke GM, Taylor G, Weinreich D (1993). Electrophysiological properties and chemosensitivity of acutely isolated nodose ganglion neurons of the rabbit. *J Auton Nerv Syst* 45, 29-39.

Leem JW, Willis WD, Chung JM (1993). Cutaneous sensory receptors in the rat foot. *J Neurophysiol* 69, 1684-1699.

Lynn B, Carpenter SE (1982). Primary afferent units from the hairy skin of the rat hind limb. *Brain Res* 238, 29-43.

McLeod JG, Penny R (1969). Vincristine neuropathy: an electrophysiological and histological study. *J Neurol Neurosurg Psychiatry* 32, 297-304.

Reeh PW, Bayer J, Kocher L, Handwerker HO (1987). Sensitization of nociceptive cutaneous nerve fibers from the rat's tail by noxious mechanical stimulation. *Exp Brain Res* 65, 505-512.

Rosenmund C, Westbrook GL (1993). Calcium-induced actin depolymerization reduces NMDA channel activity. *Neuron* 10, 805-814.

Sandler SG, Tobin W, Henderson ES (1969). Vincristine-induced neuropathy. A clinical study of fifty leukemic patients. *Neurology* 19, 367-374.

Shelanski ML, Wisniewski H (1969). Neurofibrillary degeneration induced by vincristine therapy. *Arch Neurol* 20, 199-206.

Srinivasan Y, Elmer L, Davis J, Bennett V, Angelides K (1988). Ankyrin and spectrin associate with voltage-dependent sodium channels in brain. *Nature* 333, 177-180.

Tanner K, Levine J, Topp K (1997a). Microtubule disorientation and axonal swelling in unmyelinated sensory axons during vincristine-induced painful neuropathy in rat. *J. Neurosci. submitted.*

Tanner KD, Reichling DB, Levine JD (1997b). Mechanical hyperresponsiveness of nociceptors in vincristine-induced neuropathy in rat. *submitted.*

Weinreich D (1995). Cellular mechanisms of inflammatory mediators acting on vagal sensory nerve excitability. *Pulm Pharmacol* 8, 173-9.

Weiss HD, Walker MD, Wiernik PH (1974). Neurotoxicity of commonly used antineoplastic agents (second of two parts). *N Engl J Med* 291, 127-133.

White DM, Levine JD (1991). Different mechanical transduction mechanisms for the immediate and delayed responses of rat C-fiber nociceptors. *J Neurophysiol* 66, 363-368.

**Figure 1: Examples of control, low-firing vincristine, and high-firing vincristine nociceptor response patterns to sustained mechanical stimulation.** A 10 g VFH was applied to the center of the neuron's receptive field for 1 min. The temporal characteristics of the response to mechanical stimulation is shown for **A**: a control C-fiber with a mechanical threshold of 0.6 g, **B**: a low-firing vincristine-treated C-fiber with a mechanical threshold of 0.6 g, and **C**: a high-firing vincristine-treated C-fiber with a mechanical threshold of 0.6 g. The instantaneous frequency plot for each trial is shown to the right.

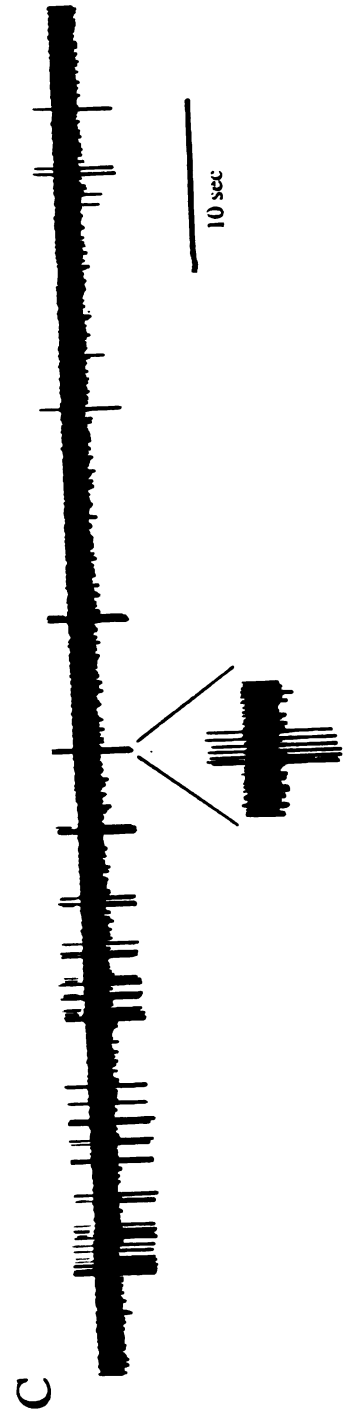
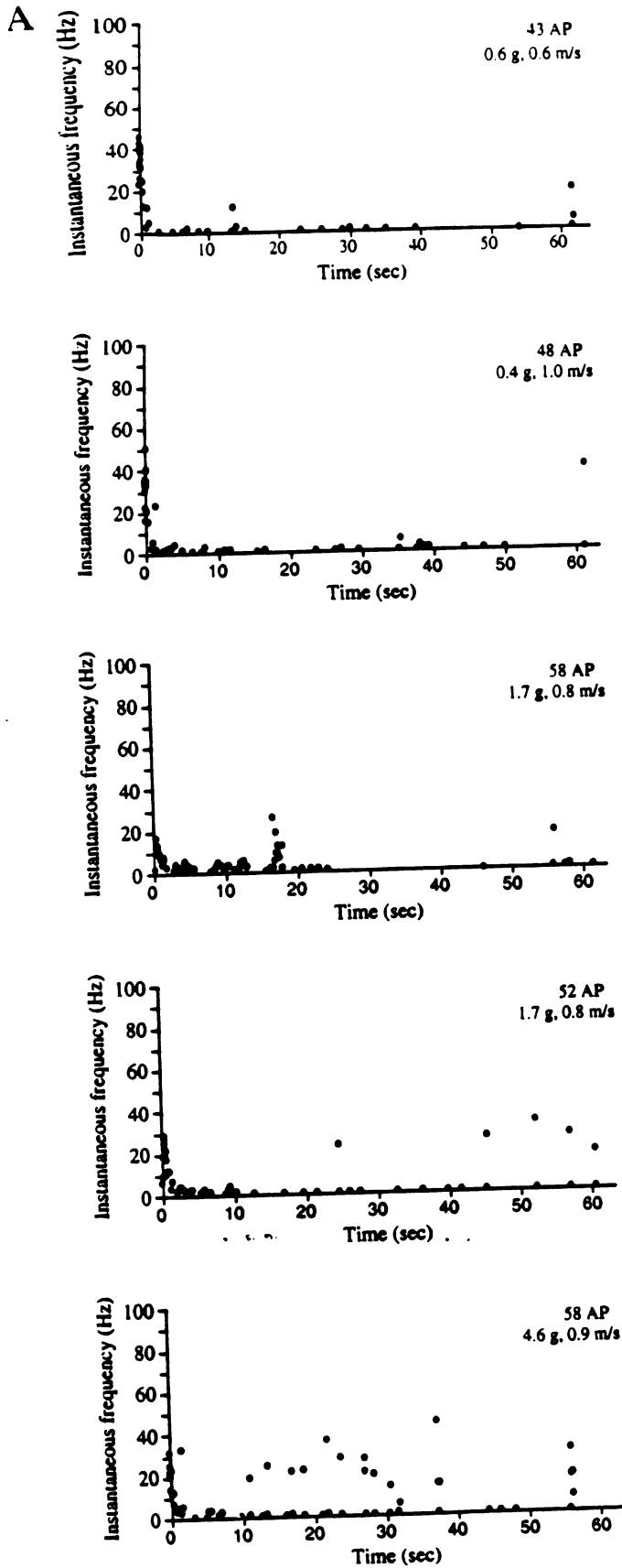


**Figure 2: Temporal characteristics of the responses of control and low-firing vincristine-treated nociceptors.** The temporal characteristics of the response to mechanical stimulation is shown for five different control nociceptors in **A** and for five different low-firing vincristine-treated nociceptors in **B**.

Control C-fibers



Low-firing vincristine C-fibers

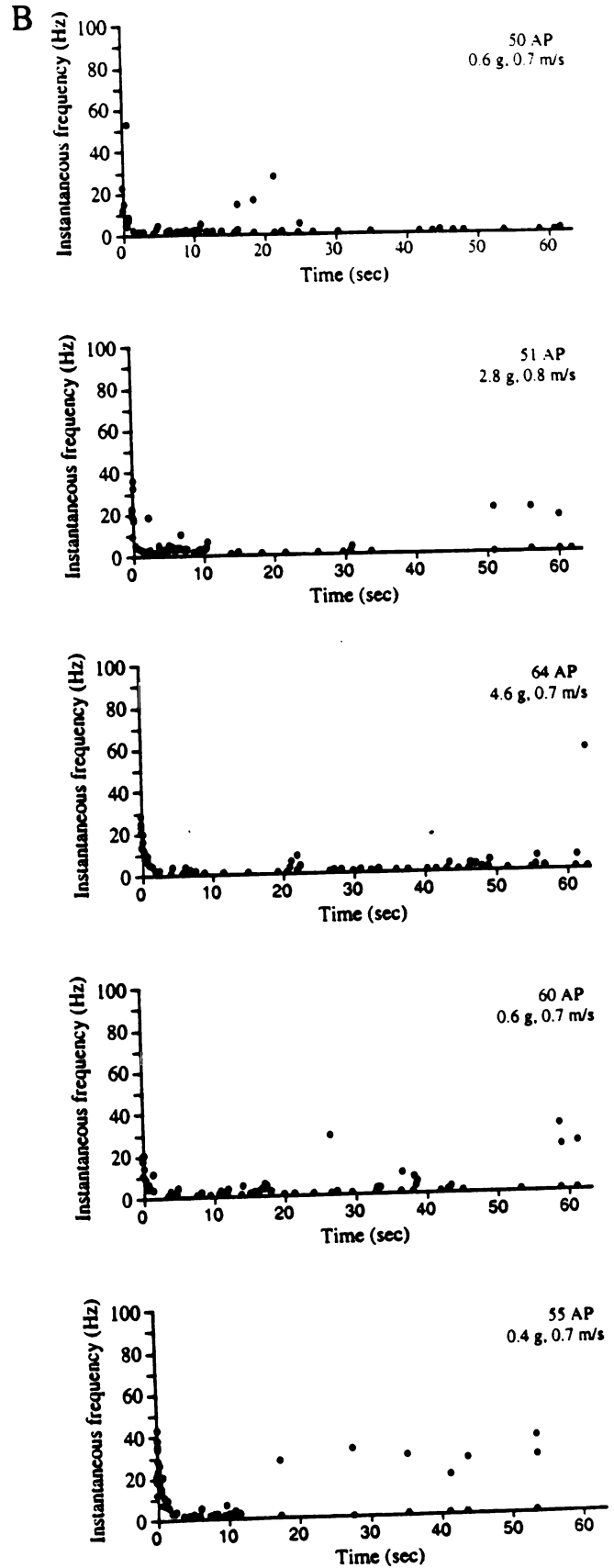
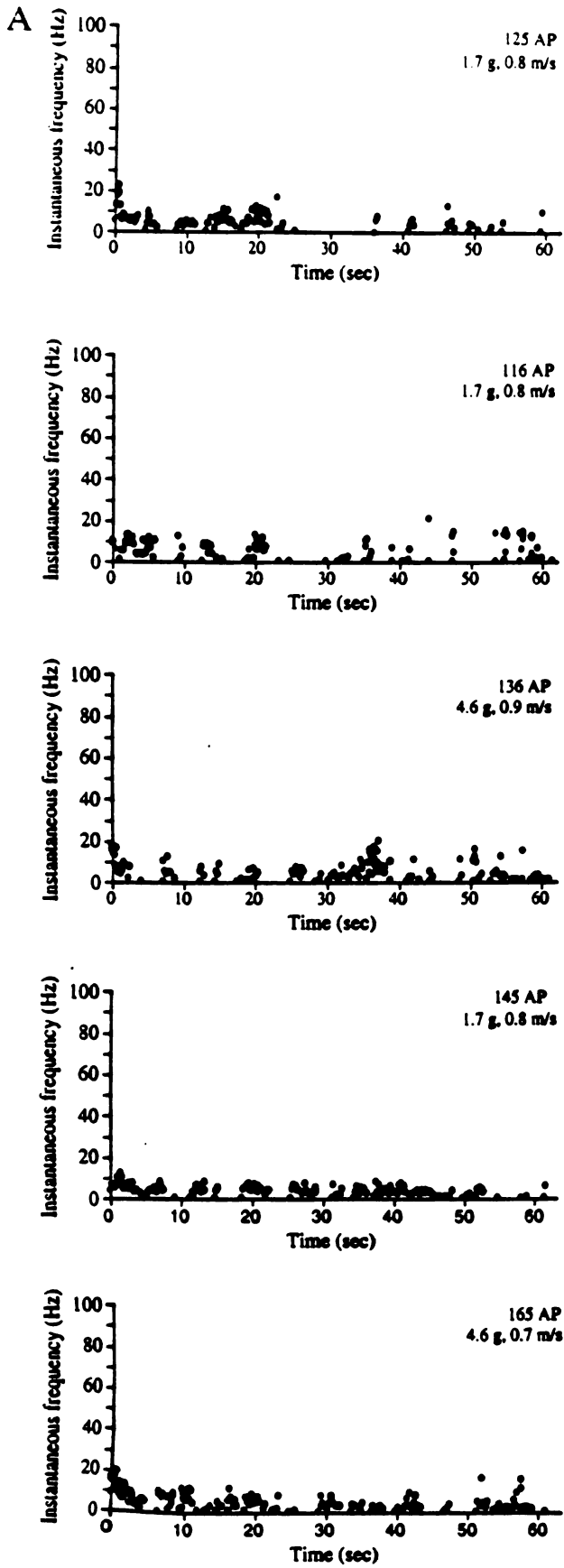




**Figure 3: Hyperresponsive vincristine-treated nociceptors respond to mechanical stimulation in a constant frequency firing mode or a variable frequency firing mode.** The temporal characteristics of the response to mechanical stimulation is shown for five different constant frequency mode high-firing vincristine-treated nociceptors in **A** and for five different variable frequency mode high-firing vincristine-treated nociceptors in **B**.

Constant frequency high-firing vincristine C-fibers



Variable frequency high-firing vincristine C-fibers

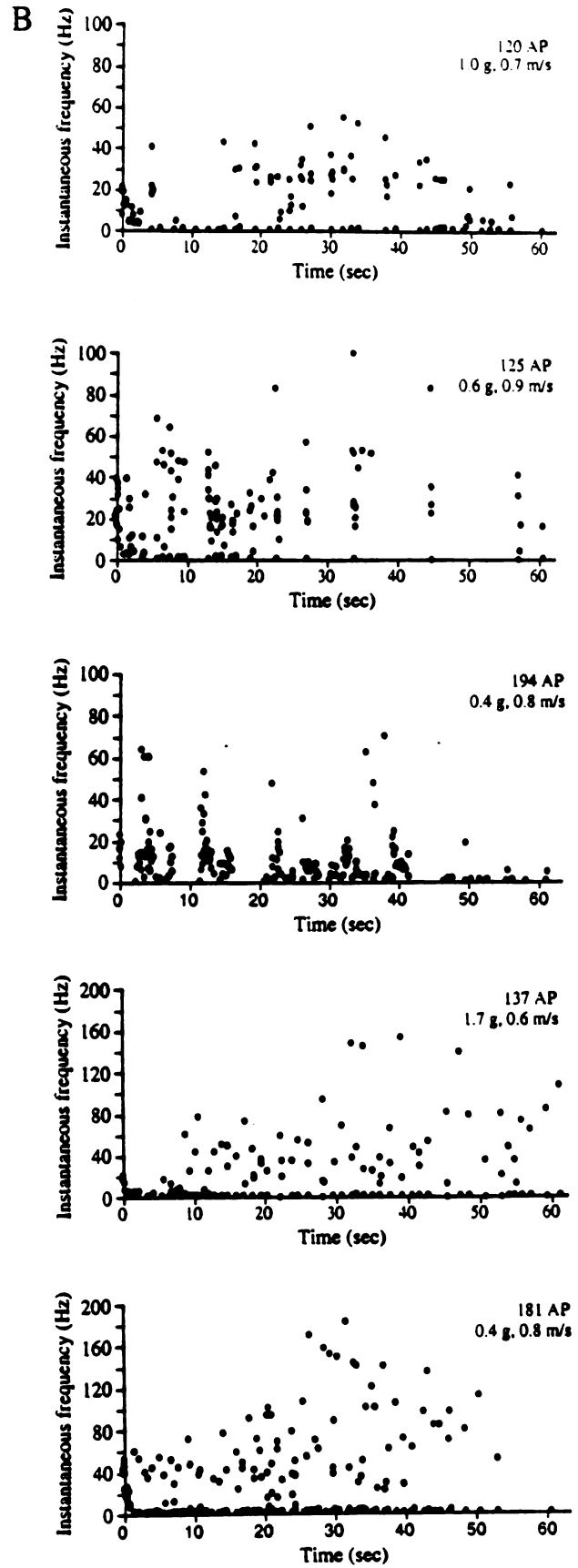


**Figure 4: Distribution of interspike intervals for entire nociceptor response to mechanical stimulation.** The average distribution of interspike intervals for the whole response (60 sec) to sustained mechanical stimulation (10 g, 1 min) for **A:** control C-fibers (n=21), **B:** low-firing vincristine-treated C-fibers (n=11), **C:** constant frequency high-firing vincristine-treated C-fibers (n=10), and **D:** variable frequency high-firing vincristine-treated C-fibers (n=8). Binwidth is 0.1 s.

# ISI Analysis for Whole Trial (60 sec)

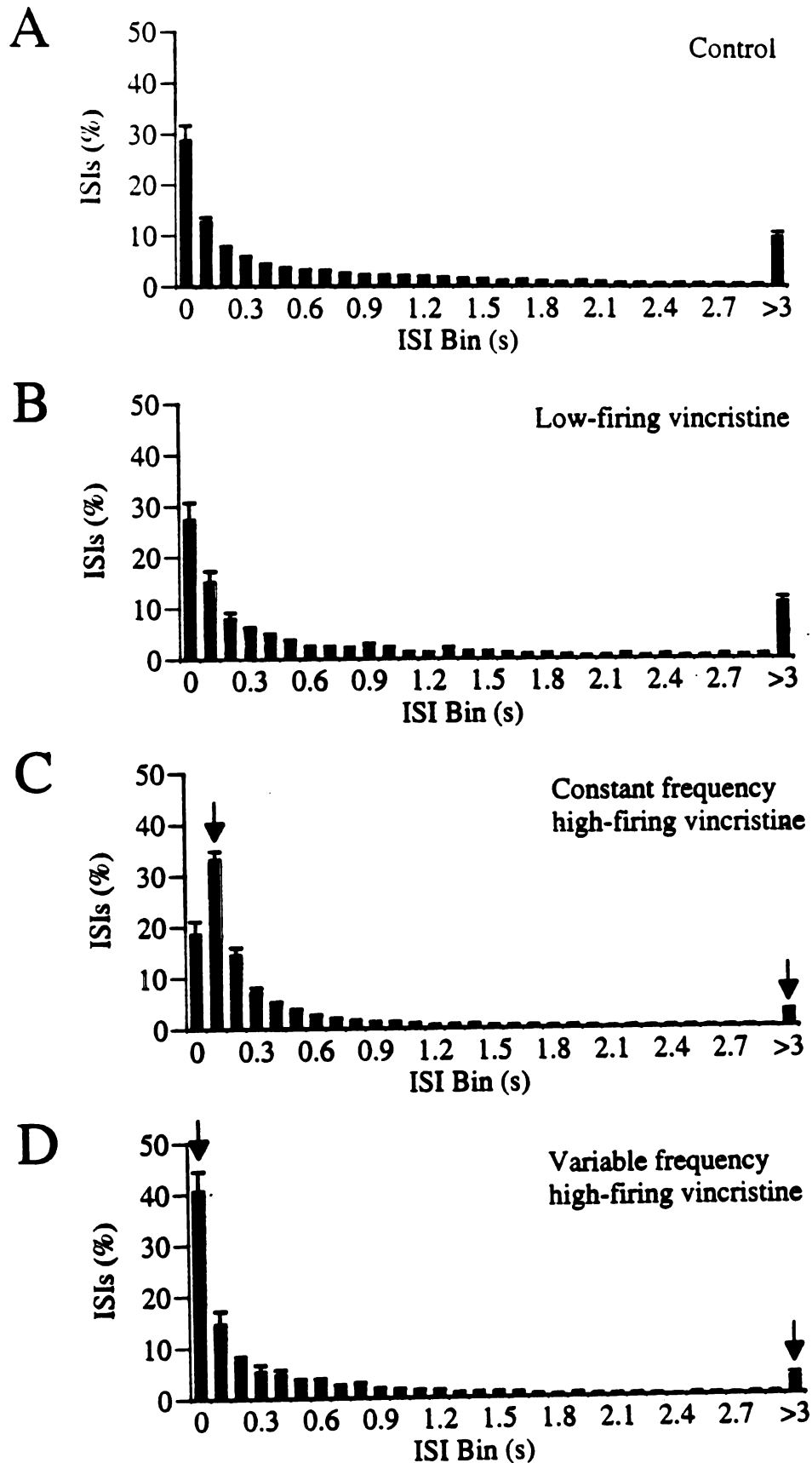


**Figure 5: Distribution of interspike intervals for the burst period of the nociceptor response to mechanical stimulation.** The average distribution of interspike intervals for the burst period of the response (first 10 sec) to sustained mechanical stimulation (10 g, 1 min) is shown for **A:** control C-fibers (n=21), **B:** low-firing vincristine-treated C-fibers (n=11), **C:** constant frequency high-firing vincristine-treated C-fibers (n=10) and **D:** variable frequency high-firing vincristine-treated C-fibers (n=8). Binwidth is 0.1 s.

# ISI Analysis for Burst Period (initial 10 sec)

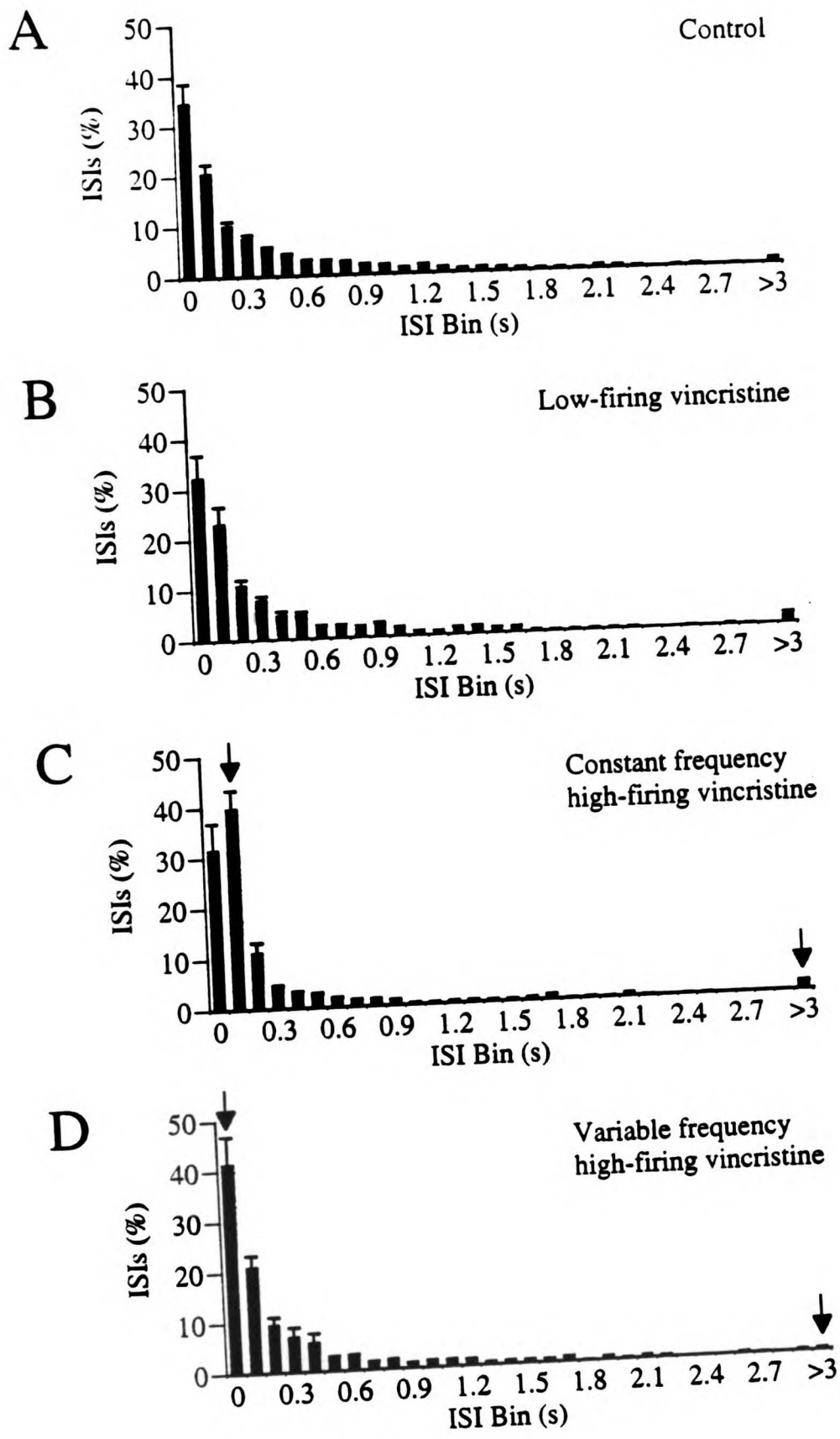


**Figure 6: Distribution of interspike intervals for the plateau period of the nociceptor response to mechanical stimulation.** The average distribution of interspike intervals for the plateau period of the response (last 50 sec) to sustained mechanical stimulation (10 g, 1 min) is shown for **A:** control C-fibers (n=21), **B:** low-firing vincristine-treated C-fibers (n=11), **C:** constant frequency high-firing vincristine-treated C-fibers (n=10) and **D:** variable frequency high-firing vincristine-treated C-fibers (n=8). Binwidth is 0.1 s.

# ISI Analysis for Plateau Period (final 50 sec)

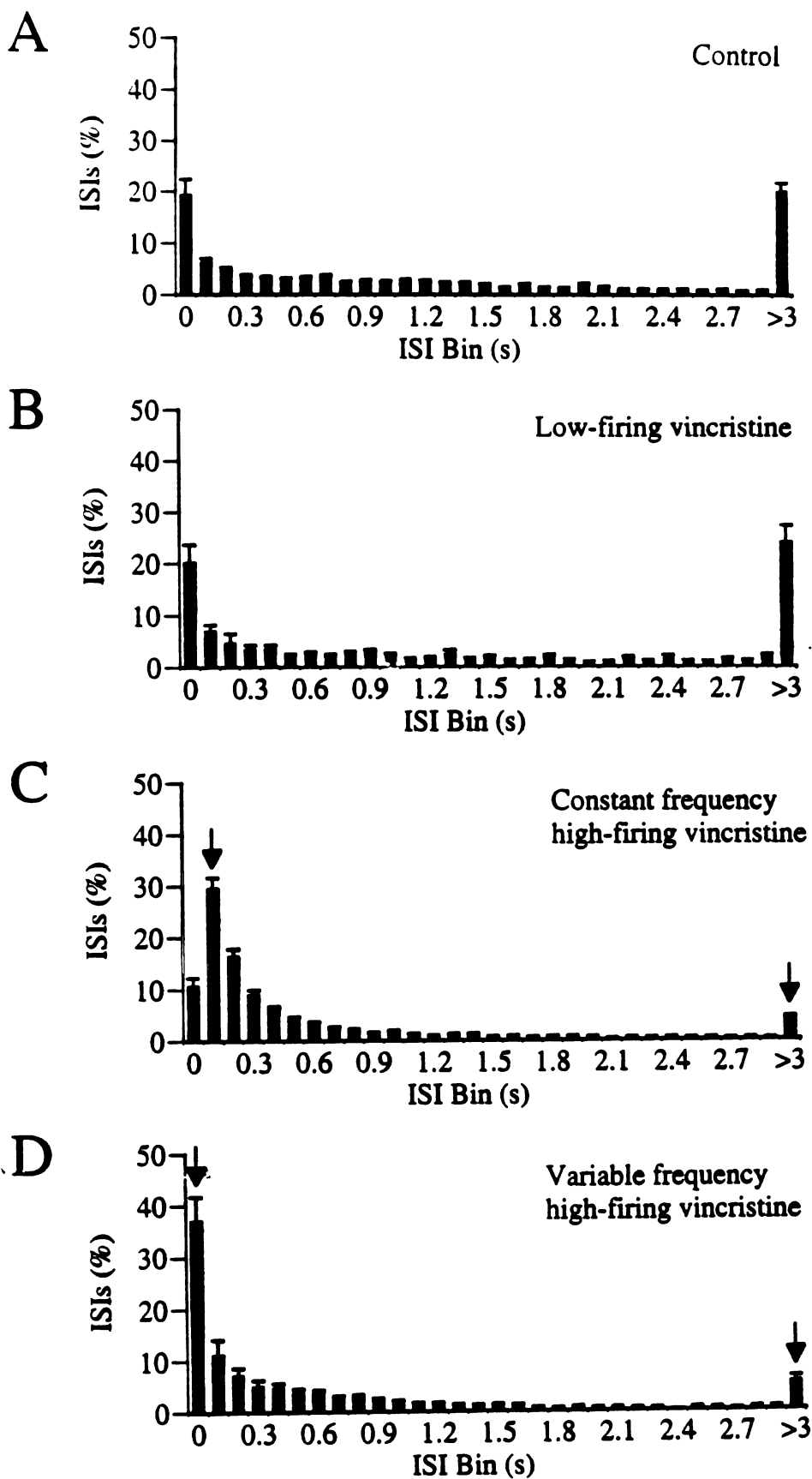
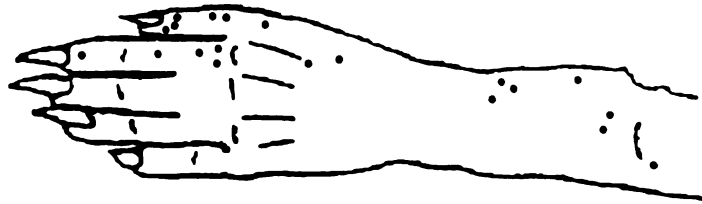


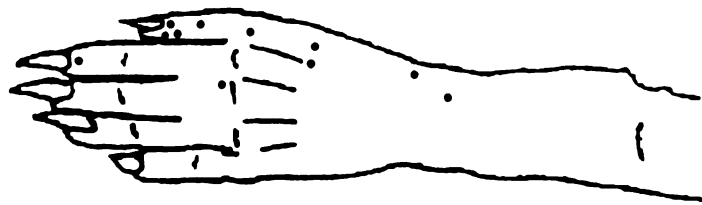


**Figure 7: Temporal firing mode in hyperresponsive nociceptors is not correlated with receptive field location.** The receptive field locations for all C-fibers studied is shown for **A:** control C-fibers, **B:** low-firing vincristine-treated nociceptors, and **C:** constant frequency (⊙) and variable frequency (★) high-firing vincristine-treated nociceptors. In these drawings of the left hindpaw, top is medial and bottom is lateral.

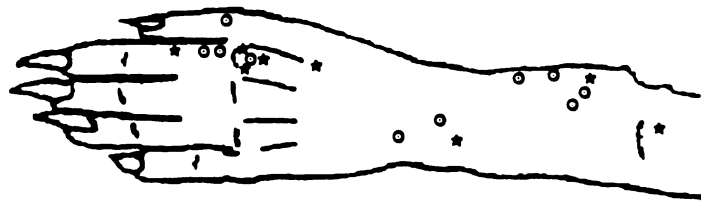
A Control



B Low-firing vincristine



C High-firing vincristine



o Constant frequency mode

\* Variable frequency mode

**Table 1: Characteristics of control, low-firing vincristine, and high-firing vincristine-treated nociceptors**

	n	Conduction Velocity (m/s)	Mechanical Threshold (g)	Total Response (AP) (Average Firing Frequency)	Burst Response (AP) (Average Firing Frequency)	Plateau Response (AP) (Average Firing Frequency)
Control: All	21	0.80 ± 0.02	1.5 ± 0.3	58.5 ± 4.2 (1.0 AP/s)	28.0 ± 1.6 (2.8 AP/s)	30.3 ± 3.6 (0.6 AP/s)
Vincristine: low-firing	11	0.74 ± 0.03	2.0 ± 0.6	50.3 ± 3.5 (0.8 AP/s)	26.7 ± 1.9 (2.7 AP/s)	23.9 ± 3.1 (0.5 AP/s)
Vincristine: high-firing	18	0.76 ± 0.02	2.3 ± 0.4	126.5 ± 4.9* (2.1 AP/s)	40.8 ± 2.7* (4.1 AP/s)	85.6 ± 3.8* (1.7 AP/s)

See Results section for definition of groups. \* represents  $p < 0.05$  as compared to the mean value for control C-fibers.

Table 2: Characteristics of variable frequency mode and constant frequency mode high-firing vincristine-treated nociceptors

	n	Conduction Velocity (m/s)	Mechanical Threshold (g)	Total Response (AP) (Average Firing Frequency)	Burst Response (AP) (Average Firing Frequency)	Plateau Response (AP) (Average Firing Frequency)
Vincristine: Variable frequency high-firing	8	0.73 ± 0.03	1.3 ± 0.5	119 ± 5.4 (2.0 AP/s)	38.0 ± 2.7 (3.8 AP/s)	81.2 ± 7.0 (1.6 AP/s)
Vincristine: Constant frequency high-firing	10	0.77 ± 0.03	3.1 ± 0.5†	132 ± 7.4 (2.2 AP/s)	42.9 ± 4.5 (4.3 AP/s)	89.1 ± 3.8 (1.8 AP/s)

See Results section for definition of groups. † represents  $p < 0.05$  Mann Whitney U.

**Chapter V:**

**Microtubule disorientation and axonal swelling  
in unmyelinated sensory axons  
during vincristine-induced painful neuropathy in rat**

## **Abstract**

Neuropathic pain accompanies peripheral nerve injury following a variety of insults including metabolic disorders, traumatic injury, and exposure to neurotoxins such as vincristine and taxol. Vincristine, a microtubule depolymerizing drug, produces a peripheral neuropathy in humans that is accompanied by painful paresthesias and dysesthesias (Sandler et al., 1969; Holland et al., 1973). The recent development of an animal model of vincristine-induced neuropathy provides an opportunity to investigate mechanisms underlying this form of neuropathic pain. Systemic vincristine (100  $\mu\text{g}/\text{kg}$ ) produces hyperalgesia to mechanical stimuli during the second week of administration that persists for more than a week (Aley et al., 1996). To test the hypothesis that changes in microtubule structure in nociceptive sensory neurons accompany vincristine-induced hyperalgesia, we analyzed unmyelinated axons in saphenous nerves of vincristine-treated rats. This study constitutes the first quantitative ultrastructural analysis of the cytoskeleton of unmyelinated axons in peripheral nerve during neuropathic hyperalgesia. Although there was no evidence of unmyelinated fiber loss, there was a significant decrease in microtubule density in unmyelinated axons from vincristine-treated rats. This decrease in microtubule density was not due to a decrease in the mean number of microtubules per axon. Rather, there was a significant increase in the cross-sectional area of unmyelinated axons, suggesting swelling of axons. In addition, vincristine-treated axons had significantly fewer microtubules cut in cross-section and significantly more tangentially-oriented microtubules per axon compared to controls. These results suggest that vincristine causes disorganization of the axonal microtubule cytoskeleton, as well as an increase in the caliber of unmyelinated sensory axons.

## Introduction

Chemotherapy-induced pain is a form of neuropathic pain associated with neurotoxic drugs such as vincristine and taxol and is characterized by painful paresthesias and dysesthesias. The clinical antineoplastic efficacy of vincristine is limited by the development of a mixed sensorimotor neuropathy (Sandler et al., 1969; Holland et al., 1973) that appears to occur in two major stages (Weiss et al., 1974; Kaplan and Wiernik, 1982; McCarthy and Skillings, 1992). In the early stage, peripheral axons are damaged by vincristine and the principal symptoms are paresthesias and dysesthesias. In the later stage, which occurs more frequently when higher doses are given for longer periods of time, axons are lost and the principal clinical finding is loss of motor function.

Several lines of evidence suggest that alterations in peripheral nerve function underlie the sensory abnormalities in vincristine-induced painful peripheral neuropathy. Vincristine is thought to exert its antineoplastic effects by inhibiting microtubule dynamics in mitotic spindles, and thus preventing cell division (Olmsted and Borisy, 1973; Himes et al., 1976; Owellen et al., 1976; Jordan et al., 1992a; Lobert et al., 1996). However, the neuropathy observed in patients treated with vincristine has been hypothesized to result from effects of vincristine on neuronal microtubules resulting in impaired axonal transport in peripheral nerves (Shelanski and Wisniewski, 1969; Bradley et al., 1970; Casey et al., 1973; Weiss et al., 1974). It is thought that peripheral neurons are highly sensitive to vincristine because nerve terminal function is dependent on intact axonal transport and maintenance of the peripheral terminal (Shelanski and Wisniewski, 1969). Interestingly, the paresthesias and dysesthesias reported in humans are most pronounced in the distal extremities (Sandler et al., 1969; Holland et al., 1973), namely those areas innervated by the longest sensory neurons which are presumably those most sensitive to disruption of axonal transport. Although there are clear alterations in axonal microtubules following direct application of vincristine to peripheral nerve *in vitro* (Green et al., 1977; Sahenk et al., 1987) or *in vivo* (Schlaepfer, 1971), there have been no quantitative ultrastructural

studies of microtubules in peripheral axons during the neuropathic hyperalgesia and nociceptor hyperresponsiveness induced by systemic administration of vincristine.

The recent development of an animal model of vincristine-induced painful neuropathy (Aley et al., 1996) provides the opportunity to investigate the mechanisms underlying this form of nerve injury. Rats treated systemically with vincristine (100  $\mu\text{g}/\text{kg}$ ) develop mechanical hyperalgesia during the second week of vincristine administration that persists for more than a week. Electrophysiological recordings during the peak of mechanical hyperalgesia revealed that approximately half of the C-fiber nociceptors in the peripheral nerves of vincristine-treated rats are markedly hyperresponsive to suprathreshold mechanical stimulation (Tanner et al., 1997). In addition, the mean conduction velocities of A-fibers and C-fibers are significantly slowed. To test the hypothesis that ultrastructural changes in microtubules in nociceptive sensory neurons accompany vincristine-induced hyperalgesia and nociceptor hyperresponsiveness, we employed light and electron microscopy to measure changes in microtubules and axonal structure in unmyelinated sensory neurons in rats treated with vincristine.



## **Methods**

### *Animals*

Experiments were performed on 200-300 g male Sprague-Dawley rats (Bantin and Kingman, Fremont, CA). Rats were housed in a temperature- and humidity-controlled environment and were maintained on a 12-hour light/dark cycle. Food and water were available *ad libitum*. Experiments were approved by the Committee on Animal Research at the University of California at San Francisco and adhered to the Society for Neuroscience Guidelines for the Use of Animals in Research.

### *Vincristine Treatment*

Vincristine sulfate (Sigma, St. Louis, MO) was dissolved in saline to a stock concentration of 1 mg/ml, with pH between 4.5 and 5.2, and stored at 4°C. The drug was then diluted daily in saline to a concentration of 100 µg/ml that was administered intravenously into the tail vein at a dose of 100 µg/kg followed by 0.5 ml of saline. Treatments occurred daily (Monday through Friday) for 2 weeks with the dosage calculated based on daily body weight. Control rats were weight-matched and untreated. Previous behavioral experiments have demonstrated that repeated intravenous saline injections have no effect on behavioral nociceptive threshold (Aley et al., 1996).

### *Light and Electron Microscopy*

Rats were perfused through the heart with physiological saline followed by 2% paraformaldehyde, 2% glutaraldehyde, 0.1% picric acid in 0.1 M sodium cacodylate buffer, pH 7.4, 24 hours following the final injection of vincristine (see Figure 1). Maximal mechanical hyperalgesia occurs at this time point (Aley et al., 1996); the withdrawal threshold to mechanical stimuli was decreased >15% in > 90% of vincristine-treated rats at this time (K.O. Aley and J.D. Levine, unpublished observations). In

addition, since the terminal half-life of vincristine in rats after intravenous injection is 7.5 hours (Zhou et al., 1990), there should be little drug present in the rat at this time point.

The saphenous nerve was chosen for analysis because it innervates the hindlimb where the behavioral hyperalgesia was documented. The saphenous nerve contains predominantly sensory axons with a small population of postganglionic sympathetic axons; there are no motor axons in the saphenous nerve. Saphenous nerves were carefully dissected from the proximal aspect of the thigh to the branch point distal to the knee joint. Two millimeter segments of the distal portion of the nerve were post-fixed in buffered 1% osmium tetroxide, dehydrated in graded ethanols, and embedded in Epon-Araldite. Embedded nerves were cut in cross-section at 100 nm or 1  $\mu$ m thickness, and sections were stained with toluidine blue for light microscopy. Seventy nanometer ultra-thin sections were prepared using a diamond knife, collected onto parlodian-coated slot grids, and stained with lead citrate and uranyl acetate. Sections were viewed and photographed in a Zeiss EM10C electron microscope operated at 60 kV.

### *Stereological Analysis*

Cross-sections of saphenous nerves were photographed in their entirety at 2,000X magnification and photomontages were prepared from electron micrographs at 5,000X final magnification. All unmyelinated axons were counted in photo montages derived from each of two randomly chosen vincristine-treated rats and two weight-matched controls. The cross-sectional area of each nerve was then measured using NeuroLucida software (MicroBrightField Inc., Colchester, VT). The number of unmyelinated axons in each nerve was divided by its cross-sectional area to obtain the density of unmyelinated axons in each nerve. All analyses were performed blind to the treatment of the rat.

Microtubule profiles were counted in cross-sections of saphenous nerves from five vincristine-treated and five control rats. All unmyelinated axons that were enveloped by Schwann cells that had their nuclei in the plane of section were photographed at 25,000X.

Microtubules were quantitated in photo montages of axons prepared at 62,500X final magnification.

Microtubules oriented longitudinally in axons were cut in cross-section; these were identified as circular profiles 25 nm in diameter with electron-lucent centers and were quantitated as *cross-sectioned microtubules*. In contrast, *tangential microtubules* could be distinguished by their rod-like shape, electron-lucent oval end, 25 nm width and variable length. Axons surrounded by collagen clearly not cut in cross-section were excluded from analysis because this indicated undulation of the axons. Microtubules were counted by a single investigator and counts were performed blind to the treatment of the rat.

#### *Axonal Cross-sectional Area*

In cross-sections of all nerves, Schwann cells with nuclei in the plane of section and all associated unmyelinated axons were photographed at 25,000X magnification. Photo montages of these Schwann cells and associated cross-sectioned axons were prepared from electron micrographs at 62,500X final magnification. The cross-sectional area, minor axis length, and major axis length of each axon was measured using Neurolucida software. Cross-sectional area was determined from the number of pixels within the axon perimeter. The mean axonal diameter was calculated as the average of the minor and major axes. In addition, the form factor, a measure of the extent of elongation of the axonal profile, was calculated as the ratio of the minor axis to the major axis. Each unmyelinated axon was numbered to allow for correlative analysis of axonal area and microtubule count. Axons surrounded by collagen that was clearly not cut in cross-section were excluded from analysis.

#### *Statistical Analysis*

Data are expressed as mean  $\pm$  standard error of the mean (SEM). Analysis of variance (ANOVA) was used to test for significant differences in cross-sectional area

measurements and microtubule counts. Student's t-test was used to evaluate differences in axon densities and form factors.

## Results

Data were collected from 5 vincristine-treated rats ( $274 \pm 17$  g) and 5 weight-matched control rats ( $274 \pm 20$  g). Vincristine-treated rats did not gain weight normally during the course of the treatment, as has been described previously (Aley et al., 1996); there was an average decrease in body weight during vincristine treatment of  $6.9 \pm 5.9\%$ .

### *Peripheral nerve appears normal during vincristine-induced neuropathy*

As shown in Figure 2, light micrographs of 1  $\mu\text{m}$ -thick sections of saphenous nerves from vincristine-treated rats did not appear appreciably different from those of control rats. In both cases, nerves were composed of 1 to 4 fascicles, each surrounded with a layer of perineurial tissue 2 to 3 cells thick. Groups of unmyelinated axons were evident interspersed between large and small myelinated axons in both control and vincristine-treated tissue. The density, shape, and general integrity of myelinated sensory axons were similar in the control and vincristine-treated tissue. There was no apparent loss of either myelinated or unmyelinated axons. In addition, the shape and size of the endoneurial vessels, and the thickness of the vessel walls appeared unaffected in vincristine-treated tissue. There did not appear to be a difference in the amount of endoneurial connective tissue or the number of perivascular cells, endoneurial fibroblasts, or mast cells (Figure 2).

As shown in Figure 3, ultra-thin cross-sections of nerves viewed by low magnification electron microscopy did not reveal any gross abnormalities in the vincristine-treated tissue samples. In both experimental groups, collagen fibers filled the endoneurial space and were usually cut in cross-section. Unmyelinated axons were surrounded by thin extensions of Schwann cell cytoplasm, and myelinated axons were wrapped by tightly compacted myelin sheaths. Most axons in both control and vincristine-treated nerves contained mitochondria, microtubules and organelles of the lysosomal system. However, approximately 15% of unmyelinated axons in control sections and 10% of unmyelinated

axons in vincristine-treated sections contained no microtubules and only a few organelles (also see Figure 6).

*Vincristine treatment does not cause a loss of unmyelinated sensory axons*

To determine if there was a loss of unmyelinated axons with vincristine treatment, we counted the number of axons and determined the cross-sectional area of saphenous nerve in two vincristine-treated and two control rats. There was no decrease in the absolute number of unmyelinated axons in vincristine-treated nerves (Table 1). Since there is variability in branching of the saphenous nerve that may cause apparent differences in the absolute number of axons, we also found no significant difference in the density of unmyelinated axons in nerves from vincristine-treated rats and weight-matched controls (Table 1). However, many vincristine-treated unmyelinated axons were larger and more irregularly shaped compared to controls (see Figure 4).

*Vincristine treatment alters the cytoskeleton in unmyelinated sensory axons*

High magnification electron micrographs revealed several differences between the cytoskeletal structure in control and in vincristine-treated axons (Figure 4). Microtubules were present in both control and vincristine-treated axons. Most microtubules were oriented longitudinally along the axis of the axon and were cut in cross-section; these *cross-sectioned microtubules* were identified as circular profiles 25 nm in diameter with electron-lucent centers. In contrast, some microtubules were oriented tangential to the plane of section; these *tangential microtubules* could be distinguished by their rod-like shape, electron-lucent oval end, 25 nm width and variable length and appeared to be more prevalent in vincristine-treated axons.

Neurofilaments were apparent as black profiles 10 nm in diameter. Whereas neurofilaments were distributed homogeneously throughout the axoplasm in most control

axons (Figure 4A), there appeared to be more neurofilaments in many vincristine-treated axons (Figure 4B). Moreover, the neurofilaments in vincristine-treated axons appeared to be abnormally clustered in the central portion of the axoplasm.

*Vincristine treatment decreases the density of microtubules in unmyelinated sensory axons.*

The mean density of microtubules (MT) in vincristine-treated unmyelinated axons ( $51.3 \pm 1.7$  MT/ $\mu\text{m}^2$ ,  $n = 594$ ) was significantly lower ( $p < 0.0001$ ) than that seen in control unmyelinated axons ( $63.5 \pm 1.7$  MT/ $\mu\text{m}^2$ ,  $n = 931$ ) (Figure 5). We did not observe a correlation between the total number of microtubules and axonal area in either control or vincristine-treated nerves. Unmyelinated axons in vincristine-treated rats had a 19% decrease in the density of microtubules. This reduction was not restricted to axons of a particular caliber. There was however no increase in the percentage of vincristine-treated axons with a microtubule density of zero.

*Vincristine does not decrease the total number of microtubules in unmyelinated sensory axons.*

To determine whether vincristine induced depolymerization of axonal microtubules, microtubules were counted in cross-sections of axons from vincristine-treated and control nerves. The mean number of microtubules per axon in vincristine-treated axons ( $13.1 \pm 0.5$  MT,  $n = 594$ ) was not significantly different ( $p > 0.05$ ) from that seen in control axons ( $13.8 \pm 0.4$  MT,  $n = 931$ ) (Figure 6). There was no increase in the percentage of vincristine-treated axons that did not contain microtubules.

*Vincristine treatment increases the axonal cross-sectional area and diameter of unmyelinated sensory axons.*

As shown in Figure 7, the mean cross-sectional area of unmyelinated axons in nerves from vincristine-treated rats ( $0.29 \pm 0.01 \mu\text{m}^2$ ,  $n = 594$ ) was significantly larger ( $p < 0.0001$ ) than that of unmyelinated axons in nerves from control rats ( $0.24 \pm 0.004$ ,  $n = 931$ ). Our data demonstrate a rightward shift of the entire unmyelinated axonal population in vincristine-treated axons, rather than an effect on a subpopulation of axons. This change reflects a 21% increase in the axonal cross-sectional area of unmyelinated axons in the peripheral nerves of vincristine-treated rats.

To determine whether the increase in axonal cross-sectional area of unmyelinated axons in vincristine-treated rats was the result of these axons being cut obliquely, the major and minor axes of each axonal profile were measured. From these data, a form factor, the ratio of the minor axis to the major axis, was calculated which reflected the extent of elongation of the axonal profile. The average of the minor and major axes of the axonal profile approximated the mean axonal diameter. As shown in Table 2, unmyelinated axons from vincristine-treated rats had significantly larger ( $p < 0.001$ ) minor axes, major axes, and thus, mean axonal diameters compared to control unmyelinated axons. However, there was no difference ( $p > 0.05$ ) in the average form factor between vincristine-treated and control axons, indicating that the increase in axonal diameter was not due to oblique sectioning of vincristine-treated tissue.

*Vincristine treatment decreases the number and density of cross-sectioned microtubules but increases the number and density of tangential microtubules in unmyelinated axons.*

The density of *cross-sectioned microtubules* in vincristine-treated unmyelinated axons ( $39.3 \pm 1.5 \text{ MT}/\mu\text{m}^2$ ,  $n = 594$ ) was significantly lower ( $p < 0.0001$ ) than that seen in control unmyelinated axons ( $54.6 \pm 1.7 \text{ MT}/\mu\text{m}^2$ ,  $n = 931$ ). However, the density of *tangential microtubules* in vincristine-treated unmyelinated axons ( $12.0 \pm 0.7 \text{ MT}/\mu\text{m}^2$ ,  $n = 594$ ) was significantly greater ( $p < 0.0001$ ) than that seen in control unmyelinated axons



( $9.0 \pm 0.5$  MT/ $\mu\text{m}^2$ , n = 931). This change reflects a 28% decrease in the density of *cross-sectioned microtubules* and a 33% increase in the density of *tangential microtubules* in unmyelinated axons in the peripheral nerve of vincristine-treated rats.

There was a statistically significant decrease ( $p < 0.0009$ ) in the mean number of *cross-sectioned microtubules* per axon in vincristine-treated axons ( $9.9 \pm 0.4$  MT, n = 594) compared to control axons ( $11.8 \pm 0.4$  MT, n = 931) (Figure 8). In addition, there was a concomitant significant increase ( $p < 0.0001$ ) in the mean number of *tangential microtubules* per axon in vincristine-treated axons ( $3.1 \pm 0.2$  MT, n = 594) compared to control axons ( $2.0 \pm 0.1$  MT, n = 931) (Figure 8). This change reflects a 16% decrease in the density of *cross-sectioned microtubules* and a 55% increase in the density of *tangential microtubules* in unmyelinated axons in the peripheral nerve of vincristine-treated rats.

## Discussion

Our study provides evidence that vincristine-induced painful neuropathy is accompanied by ultrastructural changes in unmyelinated sensory neurons. Most striking was the significant increase in the number of microtubules that were tangentially-oriented in unmyelinated axons, suggesting cytoskeletal disorganization and microtubule disorientation. This was accompanied by a decrease in the density of microtubules in unmyelinated axons from vincristine-treated rats. This decrease in microtubule density was not due to loss of microtubules, but rather due to an unexpected increase in the axonal cross-sectional area of vincristine-treated axons. Moreover, this microtubule disorientation and axonal swelling occurred in the absence of other morphological abnormalities in peripheral nerve. There were no signs of axonal degeneration or loss, unlike what has been reported in other nerve injury models (Basbaum et al., 1991; Coggeshall et al., 1993).

### Vincristine causes disorientation, but no loss of axonal microtubules

Our data document a significant increase in the number of tangential microtubules in vincristine-treated axons. Since there was a concomitant decrease in the number of cross-sectioned microtubules and since microtubules are not thought to form *de novo* in the axon (Baas and Ahmad, 1992), these tangential microtubules are probably not a new population of microtubules. Rather we propose that tangential microtubules are pre-existing axonal microtubules that became disoriented in the axoplasm following vincristine administration. There is a 55% increase in the number of tangential microtubules per axon which implies that 7-8 % of microtubules at any point along the axon become newly disoriented during vincristine-induced neuropathy. The extent to which this degree of disorientation would affect cytoskeletal functions such as axonal transport is unknown.

The mechanisms by which axonal microtubules become disoriented following exposure to vincristine have not been investigated, but may involve partial depolymerization resulting in shorter microtubules without complete loss of microtubules.

In our *in vivo* model, we observed microtubule disorientation without concomitant reduction in the number of microtubules per axon. These data are in agreement with an earlier study of the effects of systemic vincristine on cat vagus nerve (Green et al., 1977). The authors reported no robust depolymerization or loss of axonal microtubules, but did report neurofilament aggregation, similar to that observed in this study. In an *in vitro* model, direct exposure of transected peripheral nerve to vincristine induces disorientation in normally longitudinally-aligned axonal microtubules (Sahenk et al., 1987). In that model, vincristine causes depolymerization of microtubules, with a resultant shift to shorter length microtubules, and a reduction in the number of microtubules per axon. Microtubule shortening might result in loss of tethering of microtubules to adjacent cytoskeletal or membranous elements by microtubule associated proteins (Robson and Burgoyne, 1988), and thus, cause microtubule disorientation.

#### Mechanisms of vincristine action on peripheral nerve

Although the effects of vinca alkaloids on microtubule dynamics have been studied extensively in differentiated axons in culture (Baas and Ahmad, 1993; Ahmad and Baas, 1995), little is known about the mechanism of vincristine action on peripheral nerve when administered systemically *in vivo*. Vincristine has been shown *in vitro* to depolymerize microtubules when administered at doses in the micromolar range, but only prevent microtubule assembly in the nanomolar range (Jordan et al., 1992a; Jordan et al., 1992b; Baas and Ahmad, 1993; Zheng et al., 1993; Wilson and Jordan, 1994; Tanaka et al., 1995). Higher concentrations of vinca alkaloids are effective in the promotion of axonal microtubule depolymerization and the formation of tubulin paracrystals (Green et al., 1977; Dustin, 1984), usually when applied locally to axons either *in vitro* (Green et al., 1977; Sahenk et al., 1987) or *in vivo* (Shelanski and Wisniewski, 1969). While the precise concentration of vincristine that reaches peripheral axons in the present study is unknown,

our data suggest that concentrations that reach peripheral axons are sufficient to cause microtubule disorientation, but not extensive depolymerization.

#### Vincristine causes axonal swelling

Unmyelinated axons in the peripheral nerve of vincristine-treated rats had significantly larger axonal cross-sectional areas than control axons. Since there was no difference in the form factor between vincristine-treated and control axons, vincristine appears to cause a true increase in axonal caliber. This increase in axonal diameter and cross-sectional area could be due to direct action of vincristine on axonal microtubules, secondary effects on axonal neurofilaments, or indirect changes in the osmotic environment surrounding the axons. Axonal diameter has been shown to be positively correlated with microtubule number in normal unmyelinated axons (Friede and Samorajski, 1970) and with neurofilament expression and content in axons following axotomy (Hoffman et al., 1987). In addition to its effects on the axonal cytoskeleton, vincristine could affect the function of cells that constitute the blood-nerve barrier and compromise the local ionic environment of peripheral axons. Vincristine could cause osmotic dysregulation and endoneurial edema as has been demonstrated in crush injuries (Munger et al., 1992; Sommer et al., 1993; Jacobs and Ro, 1994; Sommer et al., 1995; Sasaki et al., 1997) or diabetic neuropathy models (Jacobsen, 1976; Mizisin et al., 1986).

#### Role of vincristine-induced ultrastructural changes in nociceptor hyperresponsiveness and mechanical hyperalgesia

Qualitative studies of the anatomy of peripheral nerve during hyperalgesia associated with traumatic injury to the nerve have shown loss of myelinated and partial loss of unmyelinated axons distal to the injury (Basbaum et al., 1991; Coggeshall et al., 1993). It has been hypothesized that this loss of large myelinated sensory neurons and their inhibitory effects on nociceptive processing in the spinal cord could underlie neuropathic

sensory abnormalities following this form of nerve injury (Basbaum et al., 1991; Coggeshall et al., 1993). In the present neuropathic model system we found no evidence for axonal loss of either unmyelinated or myelinated axons (Topp, KS, Tanner, KD, and Levine, JD, manuscript in preparation). Therefore, we suggest that vincristine-induced hyperalgesia in rat is a model of early stage vincristine-induced neuropathy which is characterized by painful paresthesias and dysesthesias and is distinct from the late stage which is characterized by loss of function and loss of axons. Since the data support the interpretation that painful peripheral neuropathy can occur in the absence of gross morphological damage in peripheral nerve or loss of peripheral sensory axons, we hypothesize that vincristine-induced hyperalgesia involves abnormalities specifically in nociceptor function. Consistent with this hypothesis, approximately half of C-fiber nociceptors exhibit marked hyperresponsiveness to mechanical stimulation during vincristine-induced hyperalgesia (Tanner et al., 1997).

We propose that the disorientation of microtubules, increase in axonal diameter, and decrease in microtubule density observed in unmyelinated axons might contribute to nociceptor hyperresponsiveness by disrupting the axonal cytoskeleton and consequently impairing axonal transport and/or by modifying the function of the cytoskeleton in the nerve terminal and altering the transduction of noxious stimuli. The decrease in microtubule density and disorientation of microtubules in unmyelinated axons seen following vincristine treatment could result in impairment of axonal transport, as has been previously hypothesized (Shelanski and Wisniewski, 1969; Bradley et al., 1970; Casey et al., 1973; Weiss et al., 1974). Axonal microtubules support fast and slow axonal transport of cellular components both anterogradely and retrogradely (Sheetz et al., 1989; Allan et al., 1991; Cleveland and Hoffman, 1991; Sheetz and Martenson, 1991; Hirokawa, 1993). The extent to which the disorientation observed in axonal microtubules in vincristine-induced neuropathy would affect axonal transport is unknown. However, if axonal transport was impaired, cytoskeleton disorganization would produce alterations of the complement of

proteins present in the nerve terminal and secondarily cause changes in the excitability of nociceptors, as has been suggested for the axotomy model of neuropathy (Devor et al., 1993).

Although our analysis focused on the axons of unmyelinated sensory neurons, similar changes in cytoskeletal structure might occur at the peripheral nerve terminal and more directly affect stimulus transduction. Since vinca alkaloids are thought to act primarily on the labile population of microtubules within an axon (Binet et al., 1990) and microtubules in the nerve terminal are more labile than mid-shaft axonal microtubules (Ahmad et al., 1993), they may be most susceptible to the effects of vincristine. Vincristine-induced disorientation of nerve terminal microtubules could disrupt mechanical transduction and/or adaptation mechanisms that occur during a response to suprathreshold stimulation. Although the mechanisms of mechanical transduction are unknown, microtubules are required for touch sensitivity in *C. elegans* (Chalfie, 1993) and several proposed models of mechanotransduction include a role for cytoskeletal elements (Guharay and Sachs, 1984; Hudspeth, 1989; Wang et al., 1993). In addition, several lines of evidence suggest that the cytoskeleton is involved generally in the anchoring of ion channels and receptors, as well as in the desensitization of some of these receptors following activation (Srinivasan et al., 1988; Bigot and Hunt, 1990; Kirsch et al., 1991; Rosenmund and Westbrook, 1993).

In conclusion, we have provided the first quantitative ultrastructural evidence that systemic vincristine treatment causes disorientation of axonal microtubules, axonal swelling, and a subsequent decrease in axonal microtubule density in unmyelinated axons in the absence of axonal degeneration or axonal loss. Thus, these structural alterations in unmyelinated sensory axons could contribute to nociceptor hyperresponsiveness and behavioral mechanical hyperalgesia observed in rats treated with vincristine, as well as paresthesias and dysesthesias experienced by patients receiving vincristine as a chemotherapeutic agent.

## **References**

Ahmad FJ, Baas PW (1995). Microtubules released from the neuronal centrosome are transported into the axon. *J Cell Sci* *108*, 2761-2769.

Ahmad FJ, Pienkowski TP, Baas PW (1993). Regional differences in microtubules dynamics in the axon. *J Neurosci* *13*, 856-866.

Aley KO, Reichling DB, Levine JD (1996). Vincristine hyperalgesia in the rat: a model of painful vincristine neuropathy in humans. *Neuroscience* *73*, 259-265.

Allan V, Vale R, Navone F (1991). Microtubule-based organelle transport in neurons. In *The Neuronal Cytoskeleton*, R Burgoyne, ed. (New York: Wiley-Liss), pp. 257-282.

Baas PW, Ahmad FJ (1992). The plus ends of stable microtubules are the exclusive nucleating structures for microtubules in the axon. *J Cell Biol* *116*, 1231-1241.

Baas PW, Ahmad FJ (1993). The transport properties of axonal microtubules establish their polarity orientation. *J Cell Biol* *120*, 1427-1437.

Basbaum AI, Gautron M, Jazat F, Mayes M, Guilbaud G (1991). The spectrum of fiber loss in a model of neuropathic pain in the rat: an electron microscopic study. *Pain* *47*, 359-67.

Bigot D, Hunt SP (1990). Effect of excitatory amino acids on microtubule-associated proteins in cultured cortical and spinal neurones. *Neurosci Lett* *111*, 275-280.

Binet S, Chaineau E, Fellous A, Lataste H, Krikorian A, Couzinier J-P, Meininger V (1990). Immunofluorescence study of the action of navelbine, vincristine and vinblastine on mitotic and axonal microtubules. *Int J Cancer* 46, 262-266.

Bradley WG, Lassman LP, Pearce GW, Walton JN (1970). The neuromyopathy of vincristine in man. Clinical, electrophysiological and pathological studies. *J Neurol Sci* 10, 107-131.

Casey EB, Jellife AM, Le QP, Millett YL (1973). Vincristine neuropathy. Clinical and electrophysiological observations. *Brain* 96, 69-86.

Chalfie M (1993). The differentiation and function of the touch receptor neurons of *Caenorhabditis elegans*. *Brain Res Rev* 18, 227-246.

Cleveland D, Hoffman P (1991). Slow axonal transport models come full circle: Evidence that microtubule sliding mediates axon elongation and tubulin transport. *Cell* 67, 453-456.

Coggeshall RE, Dougherty PM, Pover CM, Carlton SM (1993). Is large myelinated fiber loss associated with hyperalgesia in a model of experimental peripheral neuropathy in the rat? *Pain* 52, 233-42.

Devor M, Govrin Lippmann R, Angelides K (1993). Na<sup>+</sup> channel immunolocalization in peripheral mammalian axons and changes following nerve injury and neuroma formation. *J Neurosci* 13, 1976-1992.



Dustin P (1984). Microtubule Poisons. In *Microtubules*, ed. (New York: Springer-Verlag), pp. 171-233.

Friede RL, Samorajski T (1970). Axon caliber related to neurofilaments and microtubules in sciatic nerve fibers of rats and mice. *Anat Rec* 167, 379-388.

Green LS, Donoso JA, Heller BI, Samson FE (1977). Axonal transport disturbances in vincristine-induced peripheral neuropathy. *Ann Neurol* 1, 255-262.

Guharay F, Sachs F (1984). Stretch-activated single ion channel currents in tissue-cultured embryonic chick skeletal muscle. *J Physiol (Lond)* 352, 685-701.

Himes RH, Kersey RN, Heller BI, Samson FE (1976). Action of the vinca alkaloids vincristine, vinblastine, and desacetyl vinblastine amide on microtubules in vitro. *Cancer Res* 36, 3798-3802.

Hirokawa N (1993). Axonal transport and the cytoskeleton. *Current Opinion Neurobiol.* 3, 724-731.

Hoffman P, Cleveland D, Griffin J, Landes P, Cowan N, DL P (1987). Neurofilament gene expression: a major determinant of axonal caliber. *Proc Natl Acad Sci (USA)* 84, 3472-3476.

Holland JF, Scharlau C, Gailani S, Krant MJ, Olson KB, Horton J, Shnider BI, Lynch JJ, Owens A, Carbone PP, Colsky J, Grob D, Miller SP, Hall TC (1973). Vincristine

treatment of advanced cancer: a cooperative study of 392 cases. *Cancer Res* 33, 1258-1264.

Hudspeth AJ (1989). How the ear's works work. *Nature* 341, 397-404.

Jacobs JM, Ro LS (1994). A morphological study of experimental mononeuropathy in the rat: early ischemic changes. *J Neurol Sci* 127, 143-52.

Jacobsen J (1976). Axonal dwindling in early experimental diabetes. I. A study of cross-sectioned fibers. *Diabetology* 12, 539-546.

Jordan M, Thrower D, Wilson L (1992a). Effects of vinblastine, podophyllotoxin and nocodazole on mitotic spindles. *J Cell Sci* 102, 401-416.

Jordan MA, Thrower D, Wilson L (1992b). Mechanism of inhibition of cell proliferation by vinca alkaloids. *Cancer Res* 51, 2212-2222.

Kaplan RS, Wiernik PH (1982). Neurotoxicity of antineoplastic drugs. *Semin Oncol* 9, 103-130.

Kirsch J, Langosch D, Prior P, Littauer UZ, Schmitt B, Betz H (1991). The 93-kDa glycine receptor-associated protein binds to tubulin. *J Biol Chem* 266, 22242-22245.

Lobert S, Vulevic B, Correia JJ (1996). Interaction of vinca alkaloids with tubulin: A comparison of vinblastine, vincristine, and vinorelbine. *Biochemistry* 35, 6806-6814.

McCarthy GM, Skillings JR (1992). Jaw and other orofacial pain in patients receiving vincristine for the treatment of cancer. *Oral Surg Oral Med Oral Pathol* 74, 299-304.

Mizisin AP, Powell HC, Myers RR (1986). Edema and increased endoneurial sodium in galactose neuropathy. Reversal with an aldose reductase inhibitor. *J Neurol Sci* 74, 35-43.

Munger BL, Bennett GJ, Kajander KC (1992). An experimental painful peripheral neuropathy due to nerve constriction. I. Axonal pathology in the sciatic nerve. *Exp Neurol* 118, 204-14.

Olmsted JB, Borisy GG (1973). Microtubules. *Annu Rev Biochem* 42, 507-540.

Owellen RJ, Hartke CA, Dickerson RM, Hains FO (1976). Inhibition of tubulin-microtubule polymerization by drugs of the Vinca alkaloid class. *Cancer Res* 36, 1499-1502.

Rosenmund C, Westbrook GL (1993). Calcium-induced actin depolymerization reduces NMDA channel activity. *Neuron* 10, 805-814.

Sahenk Z, Brady ST, Mendell JR (1987). Studies on the pathogenesis of vincristine-induced neuropathy. *Muscle Nerve* 10, 80-84.

Sandler SG, Tobin W, Henderson ES (1969). Vincristine-induced neuropathy. A clinical study of fifty leukemic patients. *Neurology* 19, 367-374.

Sasaki H, Kihara M, Zollman PJ, Nickander KK, Smithson IL, Schmelzer JD, Willner CL, Benarroch EE, Low PA (1997). Chronic constriction model of rat sciatic nerve: nerve blood flow, morphologic and biochemical alterations. *Acta Neuropathol (Berl)* 93, 62-70.

Schlaepfer WW (1971). Vincristine-induced axonal alterations in rat peripheral nerve. *J Neuropathol Exp Neurol* 30, 488-505.

Sheetz M, Martenson C (1991). Axonal transport: beyond kinesin and cytoplasmic dynein. *Current Opin. Neurobiol.* 1, 393-398.

Sheetz M, Steuer E, Schroer T (1989). The mechanism and regulation of fast axonal transport. *Trends Neurosci.* 12, 474-478.

Shelanski ML, Wisniewski H (1969). Neurofibrillary degeneration induced by vincristine therapy. *Arch Neurol* 20, 199-206.

Sommer C, Galbraith JA, Heckman HM, Myers RR (1993). Pathology of experimental compression neuropathy producing hyperesthesia. *J Neuropathol Exp Neurol* 52, 223-33.

Sommer C, Lalonde A, Heckman HM, Rodriguez M, Myers RR (1995). Quantitative neuropathology of a focal nerve injury causing hyperalgesia. *J Neuropathol Exp Neurol* 54, 635-43.

Srinivasan Y, Elmer L, Davis J, Bennett V, Angelides K (1988). Ankyrin and spectrin associate with voltage-dependent sodium channels in brain. *Nature* 333, 177-180.

Tanaka E, Ho T, Kirschner MW (1995). The role of microtubule dynamics in growth cone motility and axonal growth. *J Cell Biol* 128, 139-155.

Tanner KD, Reichling DB, Levine JD (1997). Mechanical hyperresponsiveness of nociceptors in vincristine-induced neuropathy in rat. *submitted*.

Wang N, Butler JP, Ingber DE (1993). Mechanotransduction across the cell surface and through the cytoskeleton. *Science* 260, 1124-1127.

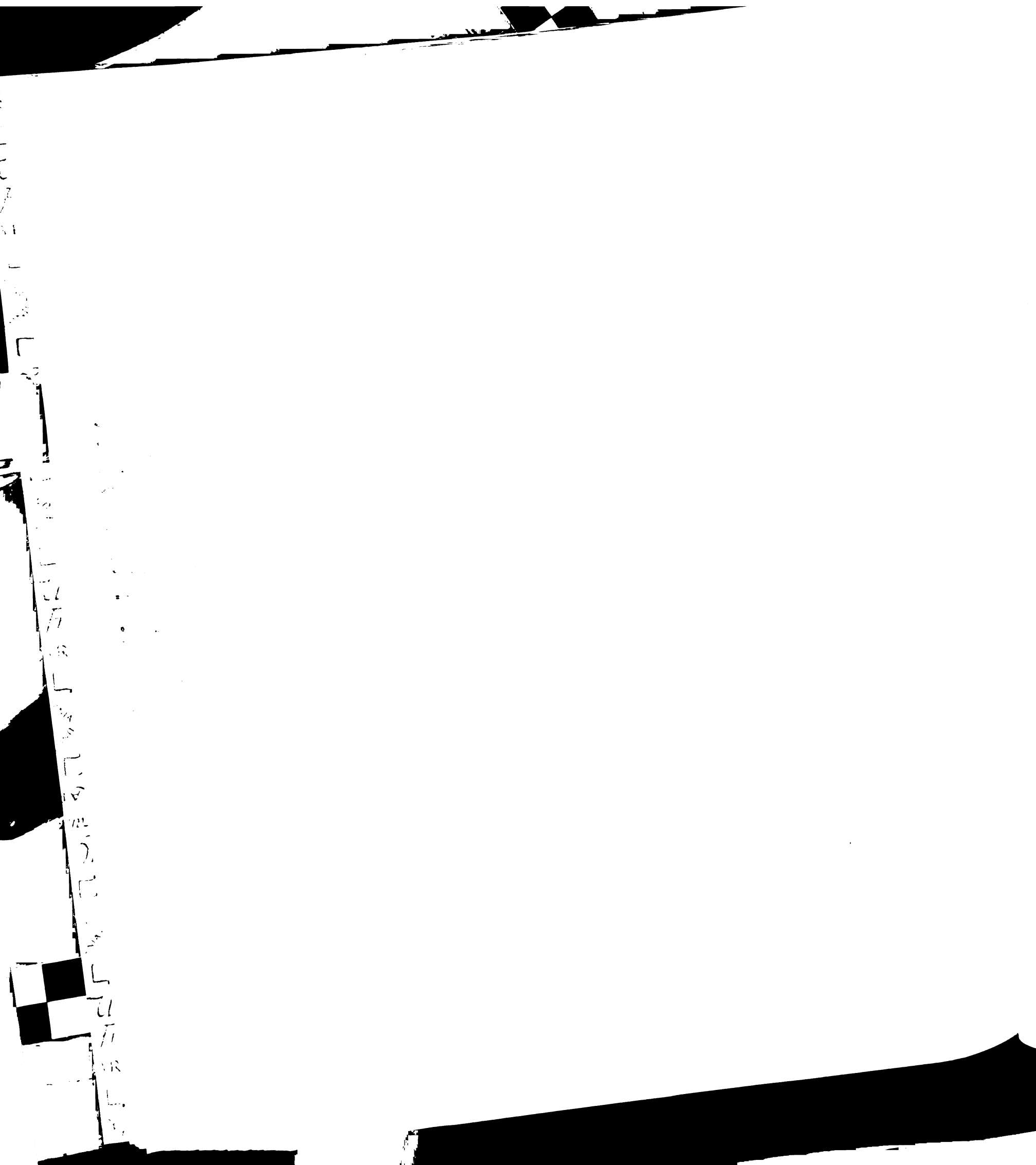
Weiss HD, Walker MD, Wiernik PH (1974). Neurotoxicity of commonly used antineoplastic agents. *N Engl J Med* 291, 127-133.

Wilson L, Jordan MA (1994). Pharmacological probes of microtubule function. In *Microtubules*, SS Hyams, CW Lloyd, eds. (New York: Wiley-Liss), pp. 59-83.

Zheng J, Buxbaum RE, Heidemann SR (1993). Investigation of microtubule assembly and organization accompanying tension-induced neurite initiation. *J Cell Sci* 104, 1239-1250.

Zhou XJ, Martin M, Placidi M, Cano JP, Rahmani R (1990). In vivo and in vitro pharmacokinetics and metabolism of vinca alkaloids in rat. II. Vinblastine and vincristine. *Eur J Drug Metab Pharmacokinet* 15, 323-332.

**Figure 1: Schematic of experimental timeline.** Rats were injected intravenously with 100  $\mu\text{g}/\text{kg}$  vincristine sulfate (V) on days 1-5 and days 8-12. The magnitude of mechanical hyperalgesia in vincristine-treated rats is shown schematically above the timeline (Aley et al., 1996). Electrophysiological recordings performed during the time period indicated by the arrow have demonstrated that unmyelinated sensory neurons are hyperresponsive to mechanical stimulation (Tanner et al., 1997). The mechanical withdrawal threshold of >90% of vincristine-treated rats was decreased >15% during the time period indicated by the arrow (K.O. Aley and J.D. Levine, unpublished observations). All ultrastructural analysis was performed on tissue harvested on days 13 (\*), 24 hours after the final dose of vincristine and during the peak of mechanical hyperalgesia.



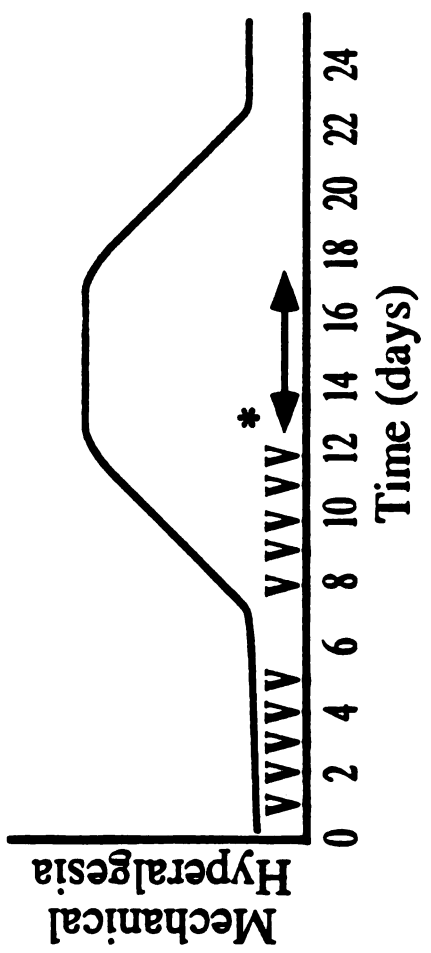




**Figure 2: Peripheral nerve appears normal at the light microscopic level during vincristine-induced neuropathy.** Light micrographs of 1  $\mu\text{m}$ -thick sections of saphenous nerves from control (A) and vincristine-treated rats (B) appeared similar. Note that the density, shape, and general integrity of myelinated sensory axons was similar in the control and vincristine-treated tissue. Groups of unmyelinated axons (**black arrows**) were evident interspersed between large and small myelinated axons in both control and vincristine-treated tissue. There was no clear loss of either myelinated or unmyelinated axons. In addition, there did not appear to be any morphological differences in the endoneurial vessels. Bar = 10  $\mu\text{m}$ .

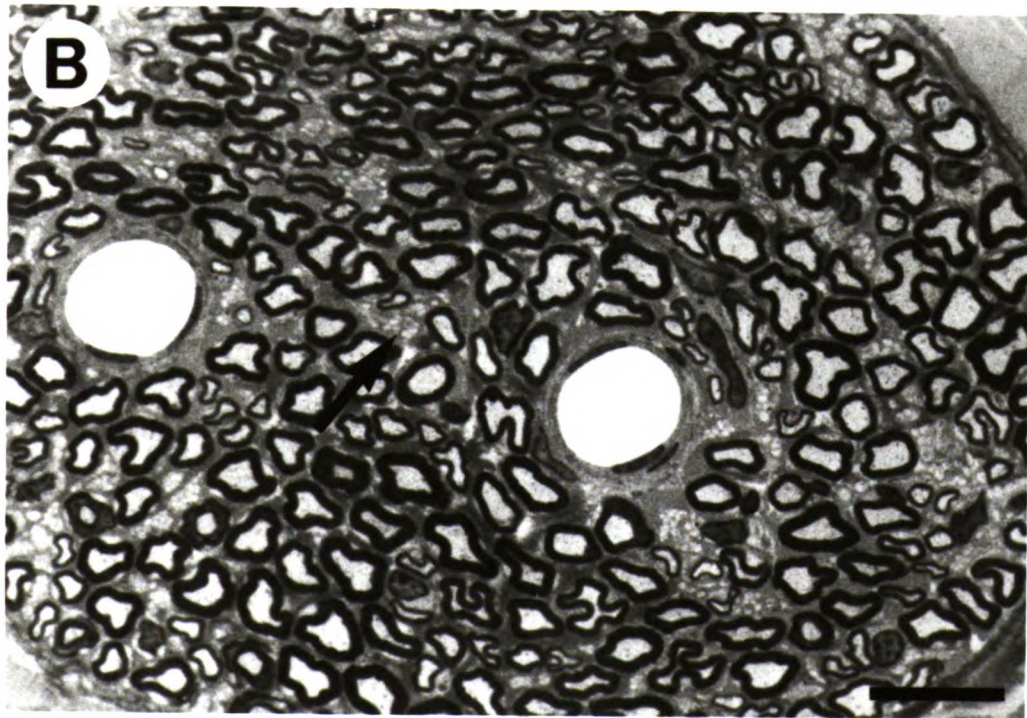
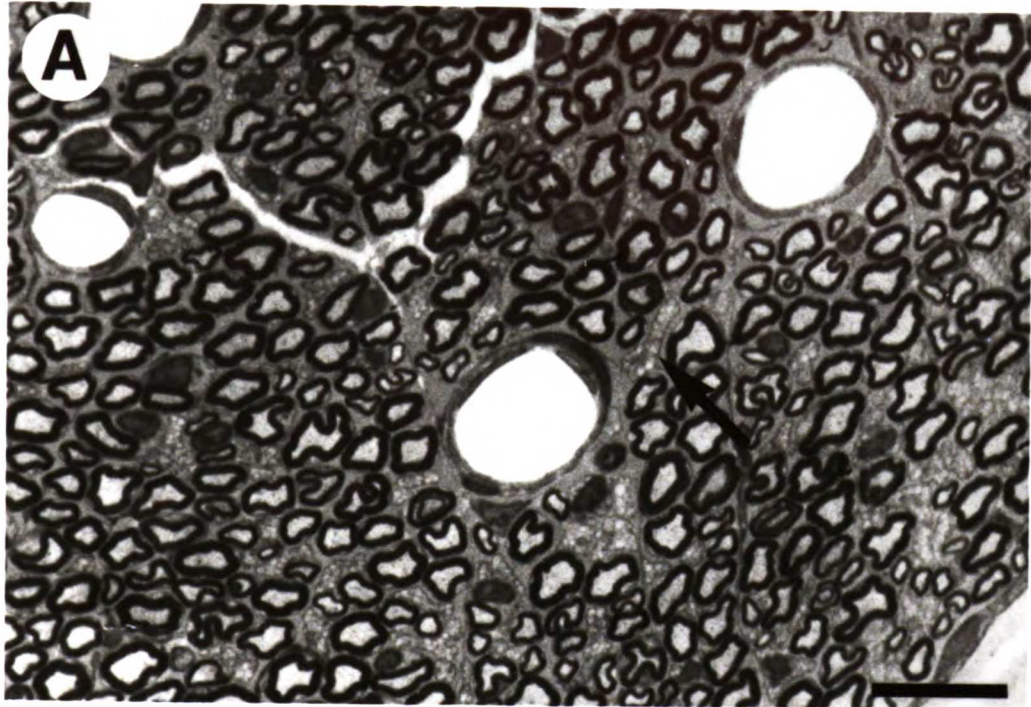
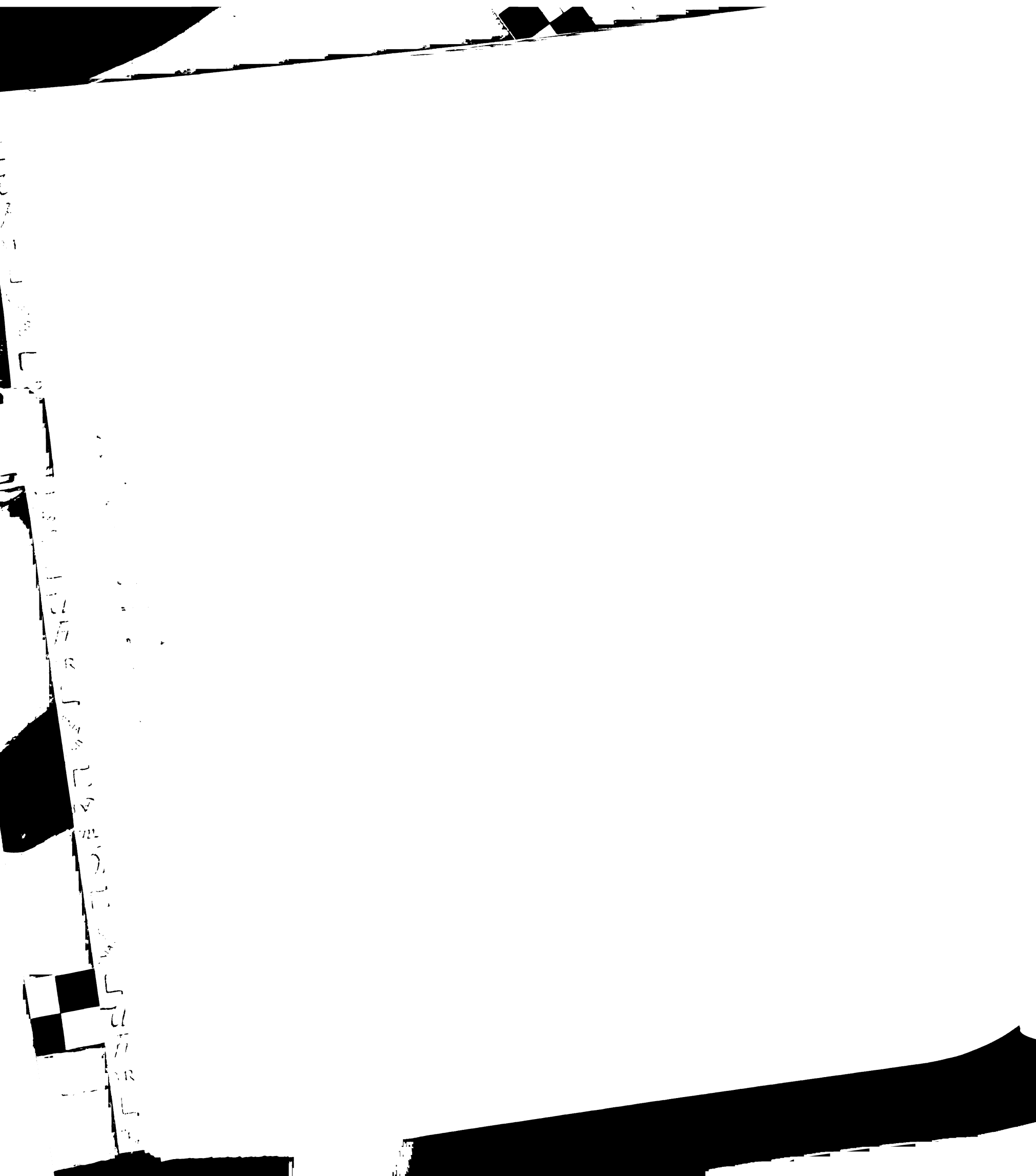
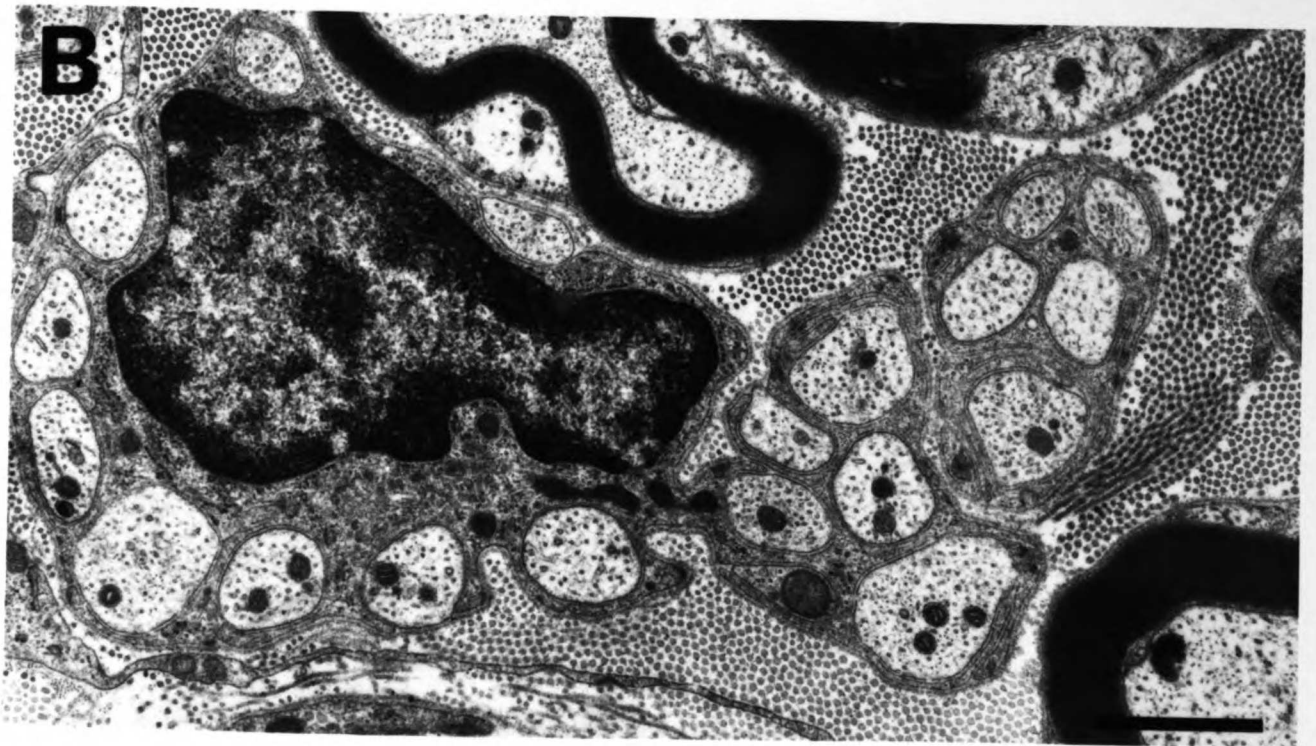
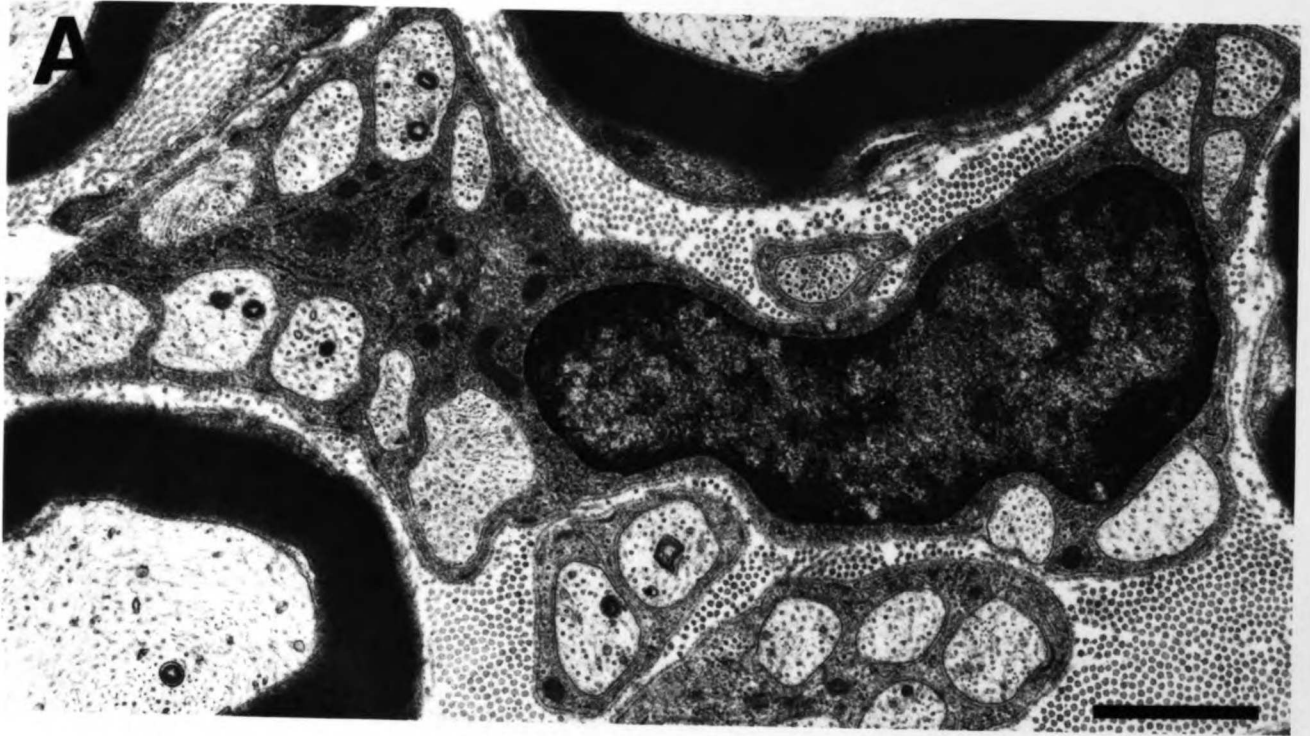




**Figure 3: Unmyelinated sensory axons appear normal in high magnification electron micrographs during vincristine-induced neuropathy.** Ultra-thin cross-sections of nerves viewed with high magnification electron microscopy revealed no apparent differences between control (A) and vincristine-treated (B) unmyelinated axons. Unmyelinated axons were surrounded by thin extensions of Schwann cell cytoplasm. Note that both control and vincristine-treated axons contain organelles, including mitochondria, microtubules, neurofilaments, and organelles of the lysosomal system. Collagen fibers were evident in the endoneurial space and were usually cut in cross-section. Further quantitative analysis was performed on all unmyelinated axons associated with Schwann cells with their nuclei in the plane of section, such as those examples shown. Bar = 1  $\mu$ m.



Vertical text on the left side of the page, possibly a ledger or form, with a checkered pattern at the bottom. The text is mostly illegible due to the high contrast and is oriented vertically.



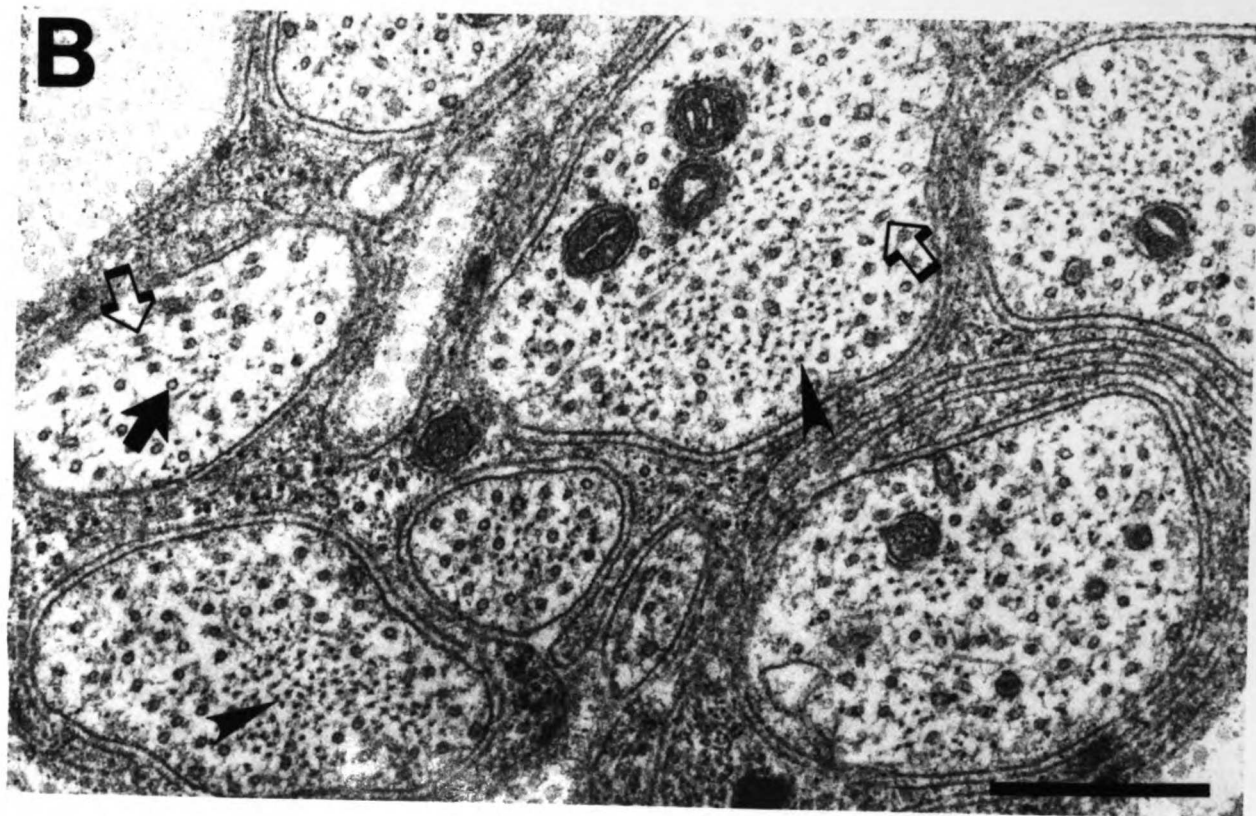
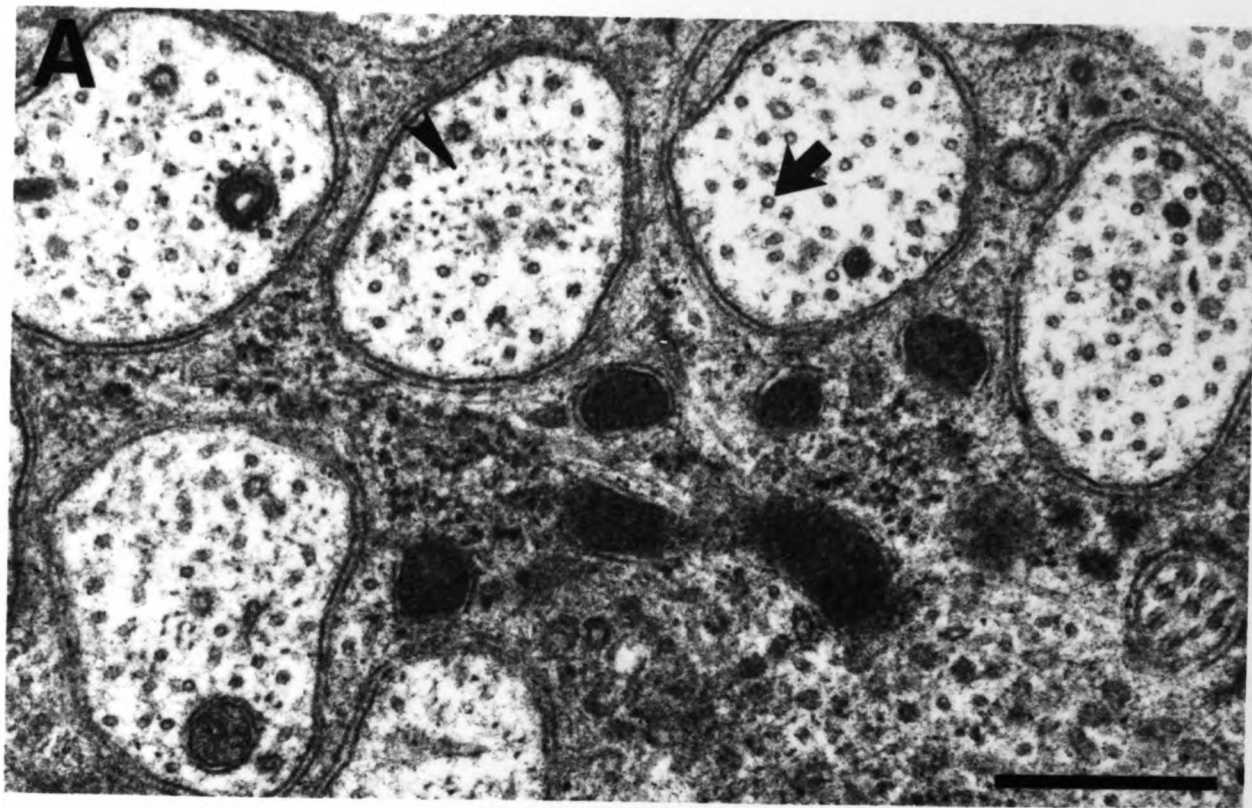


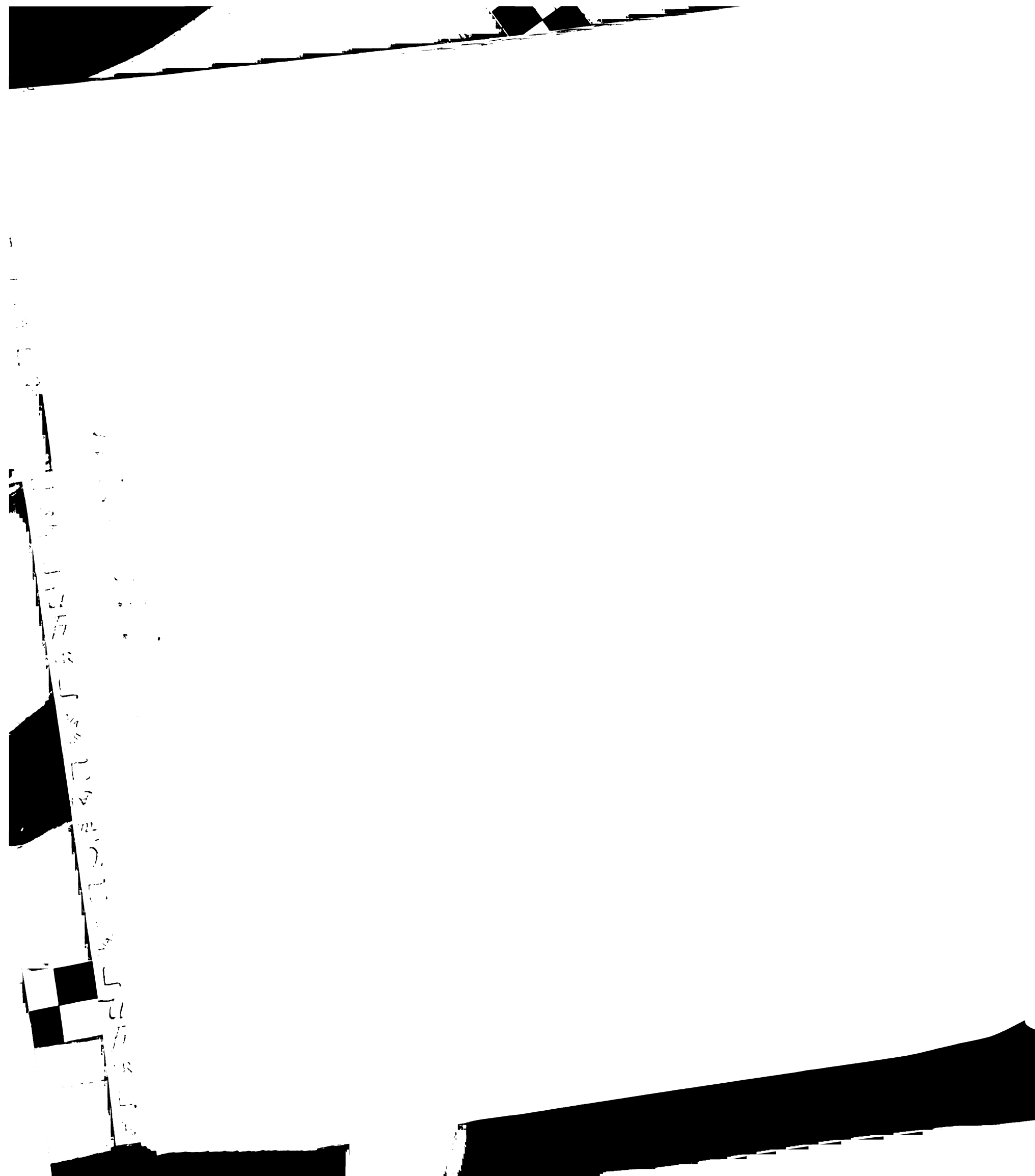
1  
2  
3  
4  
5  
6  
7  
8  
9  
10  
11  
12  
13  
14  
15  
16  
17  
18  
19  
20  
21  
22  
23  
24  
25  
26  
27  
28  
29  
30  
31  
32  
33  
34  
35  
36  
37  
38  
39  
40  
41  
42  
43  
44  
45  
46  
47  
48  
49  
50  
51  
52  
53  
54  
55  
56  
57  
58  
59  
60  
61  
62  
63  
64  
65  
66  
67  
68  
69  
70  
71  
72  
73  
74  
75  
76  
77  
78  
79  
80  
81  
82  
83  
84  
85  
86  
87  
88  
89  
90  
91  
92  
93  
94  
95  
96  
97  
98  
99  
100



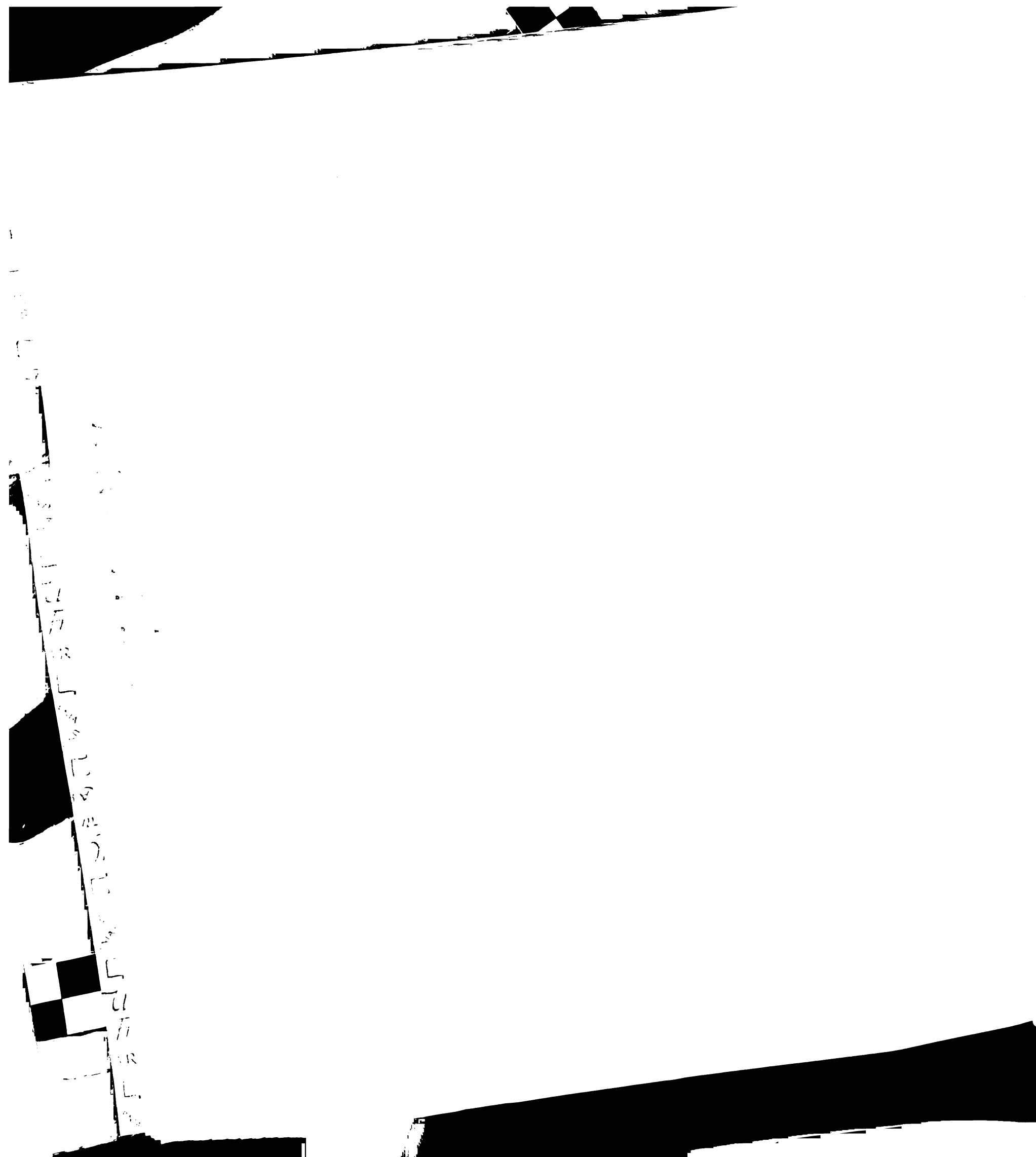
**Figure 4: Vincristine treatment alters the cytoskeleton in unmyelinated sensory axons.** Although there were no obvious abnormalities in vincristine-treated unmyelinated axons at the light or low magnification electron microscopic levels, examination of the axonal cytoskeletal structure with high magnification electron microscopy revealed several differences between control (**A**) and vincristine-treated (**B**) axons. Microtubules were present in both control and vincristine-treated axons. Most microtubules were oriented longitudinally along the axis of the axon and were cut in cross-section; these *cross-sectioned microtubules* were identified as circular profiles 25 nm in diameter with electron-lucent centers (**filled arrows**). In contrast, some microtubules were oriented tangential to the plane of section; these *tangential microtubules* were distinguished by their rod-like shape, electron-lucent oval end, 25 nm width and variable length (**open arrows**) and appeared to be more prevalent in vincristine-treated axons. Neurofilaments were apparent as black profiles 10 nm in diameter (**black arrowheads**). Whereas neurofilaments were distributed throughout the axoplasm in most control axons (see **A**), there appeared to be more neurofilaments in many vincristine-treated axons (see **B**). Neurofilaments in vincristine-treated axons also appeared to be abnormally clustered in the central portion of the axoplasm. In addition, many vincristine-treated unmyelinated axons were larger and more irregularly shaped (**B**) compared to those in the control (**A**). Note that the collagen in the endoneurial space was cut in cross-section. Bar = 1  $\mu$ m.







**Figure 5: Vincristine treatment decreases the density of microtubules in unmyelinated sensory axons.** To analyze quantitatively the microtubular cytoskeleton in unmyelinated axons, the density of microtubules was determined for each unmyelinated axon studied (see Methods and Figure 4 for details). The number of cross-sectioned and tangential microtubules were counted for each axon, and the total number of microtubules was their sum. The number of total microtubules in each axon was then divided by the area of that axon to obtain the density of microtubules in each axon. 594 vincristine-treated and 931 control unmyelinated sensory axons were analyzed. The average density of *total microtubules* per axon is shown on the left, and the distribution of the densities of *total microtubules* per axon is shown on the right for control (**open bars**) and vincristine-treated (**filled bars**) axons.



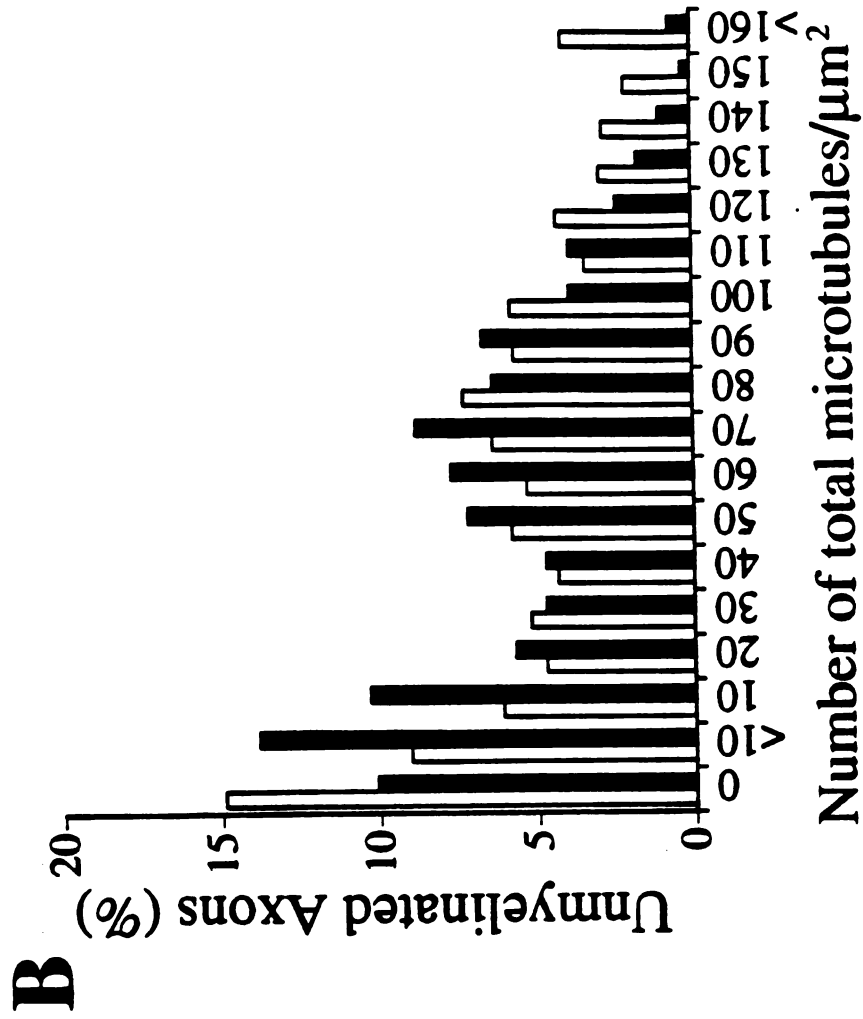
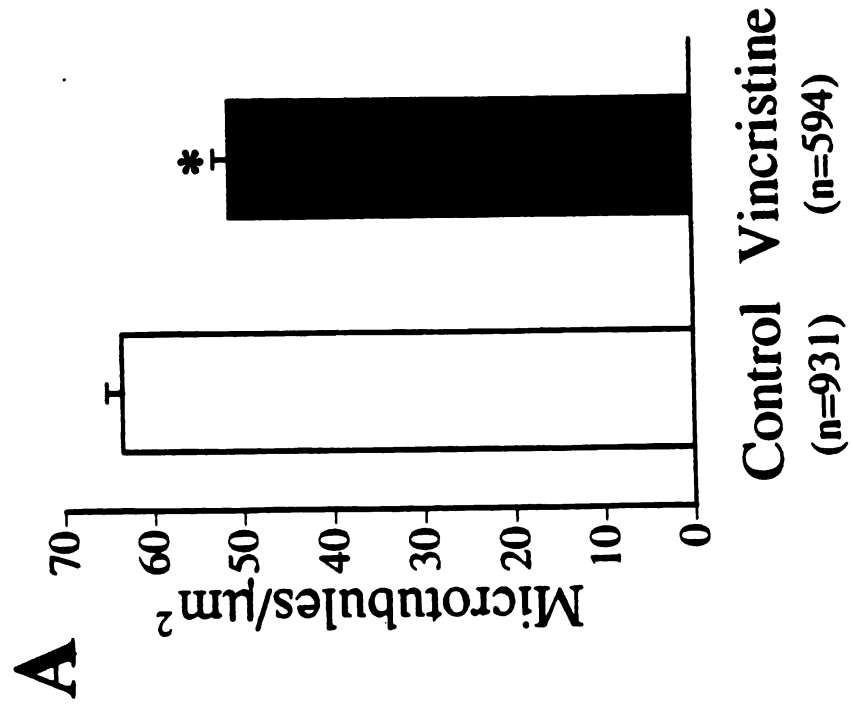


**Figure 6: Vincristine treatment does not decrease the total number of microtubules in unmyelinated sensory axons.** To determine whether the decrease in the density of microtubules per axon was due to a loss of microtubules, the absolute number of microtubules was determined for each unmyelinated axon studied (see Methods and Figure 4 for details). The number of cross-sectioned and tangential microtubules were counted for each axon, and the total number of microtubules was their sum. 594 vincristine-treated and 931 control unmyelinated sensory axons were analyzed. The average number of *total microtubules* per axon is shown on the left, and the distribution of the number of *total microtubules* per axon is shown on the right for control (**open bars**) and vincristine-treated (**filled bars**) axons.

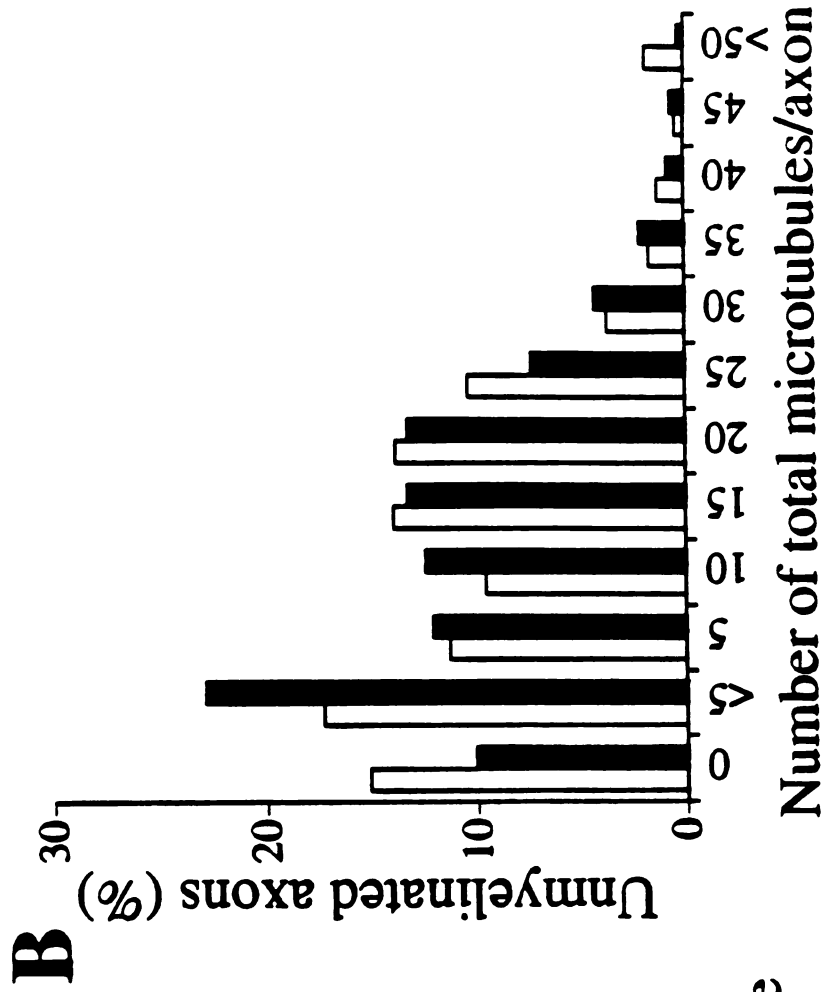
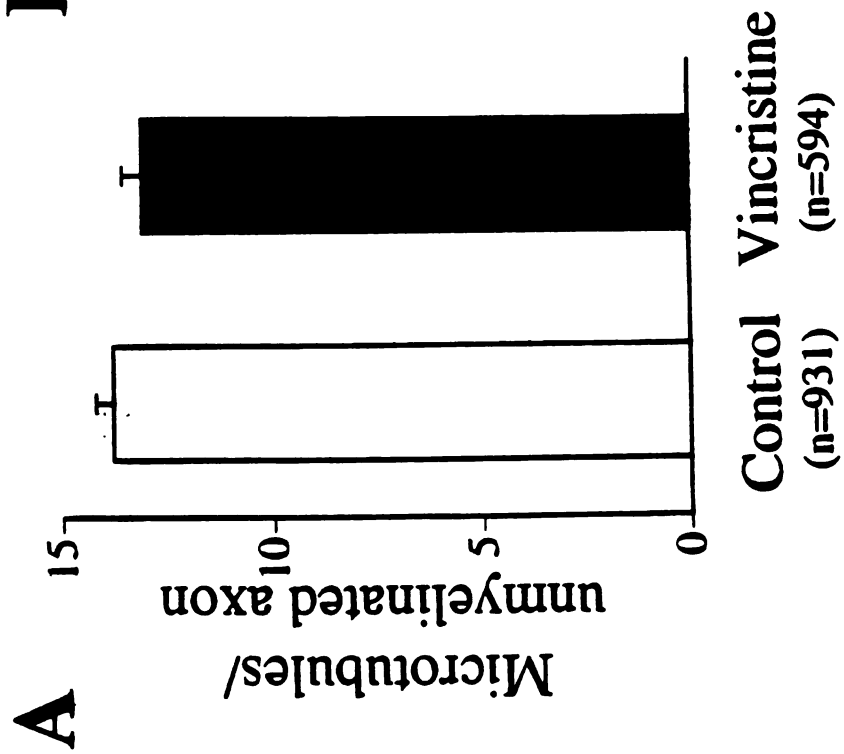


**Figure 7: Vincristine treatment increases the axonal cross-sectional area of unmyelinated sensory axons.** To determine whether the decrease in the density of microtubules in unmyelinated axons was due to an increase in the size of these axons, the cross-sectional area was determined for each axon studied (see Methods and Figure 4 for details). 594 vincristine-treated and 931 control unmyelinated sensory axons were analyzed. The average axonal cross-sectional area is shown on the left, and the distribution of the axonal cross-sectional areas for unmyelinated axons is shown on the right for control (**open bars**) and vincristine-treated (**filled bars**) axons.



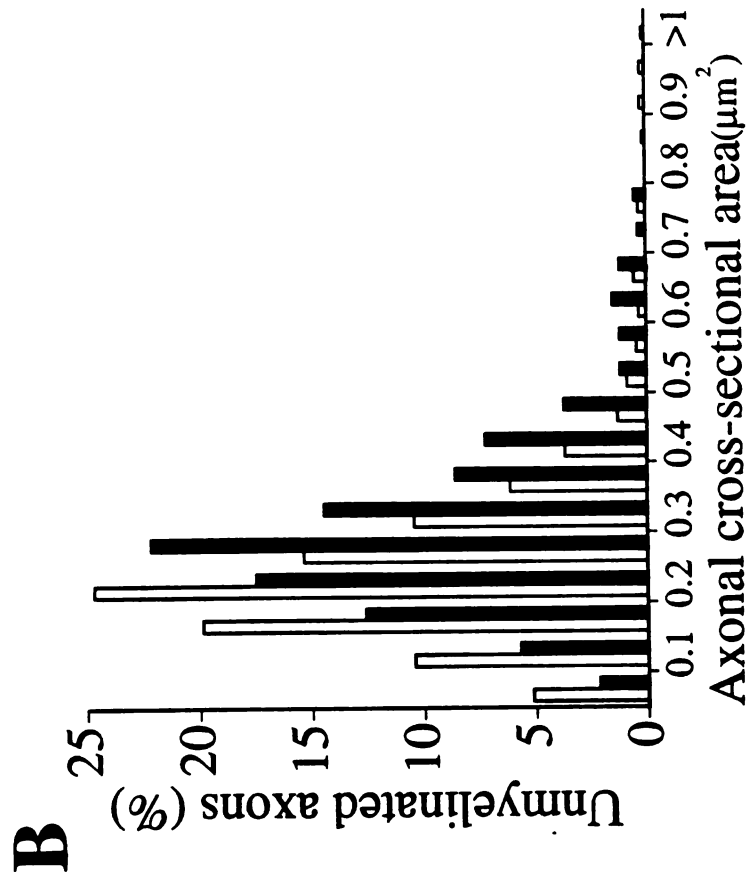
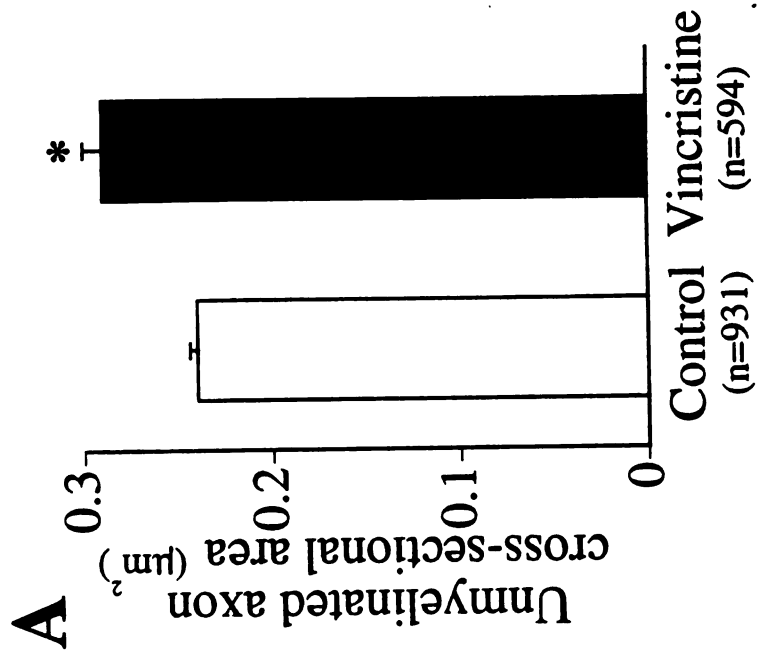


**Figure 8: Vincristine treatment decreases the number of cross-sectional microtubules and concomitantly increases the number of tangential microtubules per unmyelinated axon.** To determine whether the alterations in the density of *cross-sectional microtubules* and *tangential microtubules* in vincristine-treated nerves was due to a change in the number of *cross-sectioned microtubules* versus the number of *tangential microtubules* in addition to the increase in axonal cross-sectional area, the number of *cross-sectioned* versus *tangential microtubules* were counted for each axon studied (see Methods and Figure 4 for details). 594 vincristine-treated and 931 control unmyelinated sensory axons were analyzed. **A:** The average number of *cross-sectioned microtubules* per axon is shown on the left, and the distribution of the number of *cross-sectioned microtubules* per axon is shown on the right for control (**open bars**) and vincristine-treated (**closed bars**) axons. **B:** The average number of *tangential microtubules* per axon is shown on the left, and the distribution of the number of *tangential microtubules* per axon is shown on the right for control (**open bars**) and vincristine-treated (**filled bars**) axons. Note the different scale of the x- and y-axes in **B**.

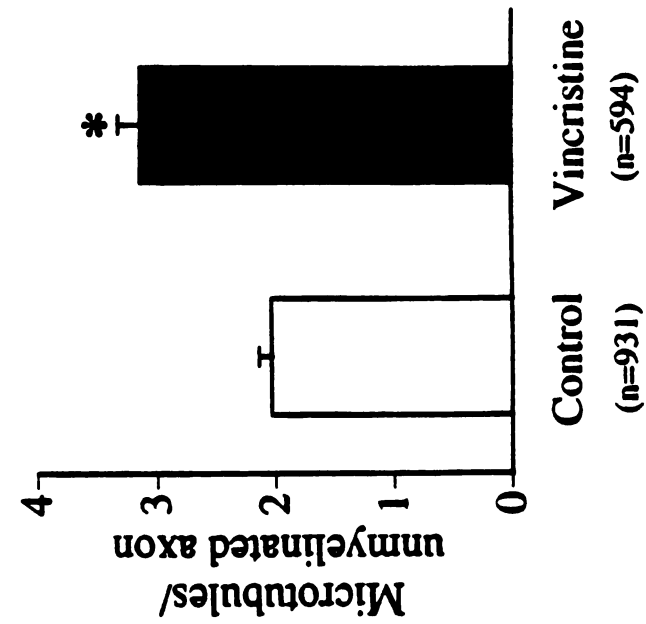
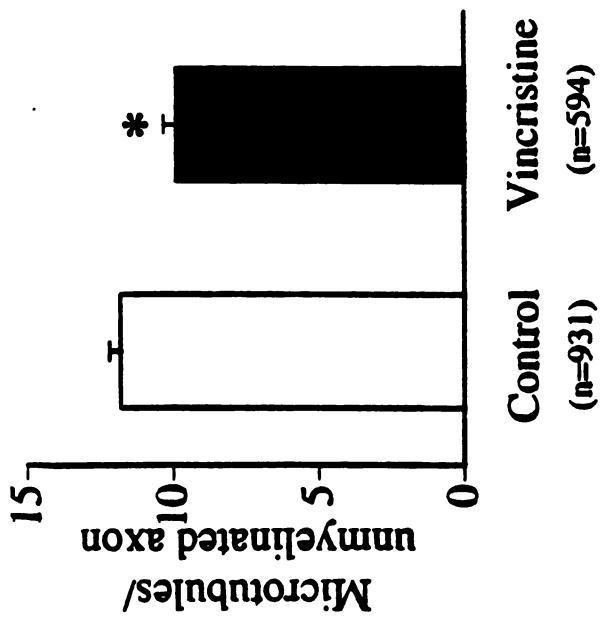
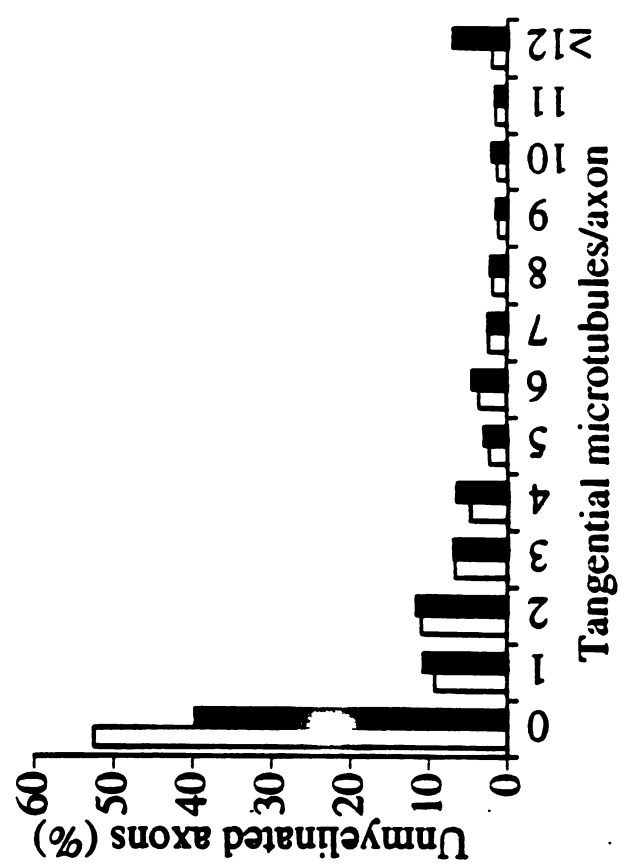
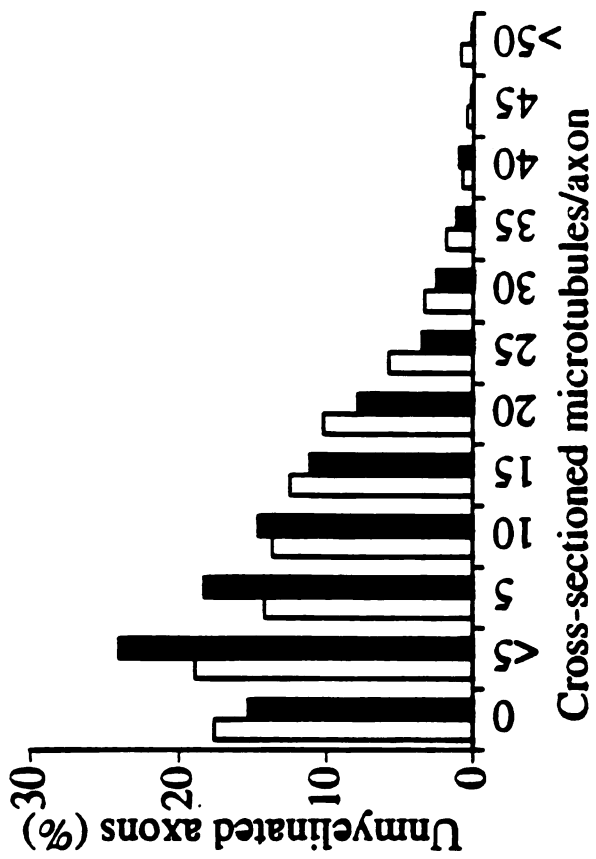


Table I: *Density of unmyelinated axons in the saphenous nerve of control and vincristine-treated rats*

	n	Total number unmyelinated axons	Cross-sectional area of saphenous nerve (mm <sup>2</sup> )	Density unmyelinated axons (per mm <sup>2</sup> )
Control	2	3192 ± 306	1.39 ± 0.03	2291 ± 174
Vincristine	2	4286 ± 2	1.87 ± 0.06	2292 ± 79

There was no significant difference in the density of unmyelinated axons in vincristine-treated rats as compared to controls. n values refer to the number of rats studied. See Methods for further details.

Table II: Axonal diameter and form factor for unmyelinated axons in control and vincristine-treated rats

	n	Minor Axonal Axis ( $\mu\text{m}$ )	Major Axonal Axis ( $\mu\text{m}$ )	Mean Axonal Diameter ( $\mu\text{m}$ )	Axonal Form Factor
Control	931	$0.56 \pm 0.01$	$0.69 \pm 0.01$	$0.62 \pm 0.01$	$0.877 \pm 0.003$
Vincristine	594	$0.59 \pm 0.01^*$	$0.76 \pm 0.01^*$	$0.67 \pm 0.01^*$	$0.872 \pm 0.003$

Axonal form factor is defined as the ratio of the minor axis to the major axis, reflecting the oblongness of the axonal profile. There was no significant difference in the form factor for unmyelinated axons in vincristine-treated rats as compared to controls. n values refer to the number of axons studied.

\*  $p < 0.001$ . See methods for further details.

## **Chapter VI:**

### **Summary and Future Directions**

## Summary

The mechanisms that contribute to chronic neuropathic pain states have been elusive. Investigation of C-fiber nociceptors during vincristine-induced painful neuropathy in rat has demonstrated a circumscribed change in nociceptors with characteristics that lend insight into mechanism. In the absence of changes in activation thresholds, spontaneous activity, C-fiber nociceptors become profoundly hyperresponsive to external stimulation. Approximately half of vincristine-treated C-fiber nociceptors are markedly hyperresponsiveness to mechanical stimulation, firing more than double the response of control nociceptors. Hyperresponsiveness can also occur to heat stimulation, implying that vincristine affects cellular components that are generally involved in responsiveness to all modalities of stimulus transduction. However, since heat hyperresponsiveness was pronounced in only a subset of mechanically hyperresponsive nociceptors and was never detected in the absence of mechanical hyperresponsiveness, vincristine may also specifically alter cellular mechanisms of mechanotransduction. Novel analysis of the temporal structure of nociceptor hyperresponsiveness suggests that multiple cellular mechanisms contribute to nociceptor hyperresponsiveness. Hyperresponsive vincristine-treated nociceptors fired in characteristic temporal patterns not seen in control or non-hyperresponsive vincristine-treated nociceptors. Constant frequency mode nociceptors fired in patterns such that a majority of ISIs were in the range of 100-300 msec, whereas variable frequency mode nociceptors fired in patterns such that a majority of ISIs were less than 100 msec. Hyperresponsive nociceptors that fire in constant frequency mode have significantly higher mechanical thresholds compared to both those that fire in variable frequency mode and control nociceptors. These data suggest that multiple mechanisms of different time-scales may contribute to vincristine-induced hyperresponsiveness in nociceptors. In addition, these characteristics of nociceptor hyperresponsiveness motivate testable hypotheses about changes in membrane biophysics that can be investigated with *in*

*vitro* studies of vincristine-treated nociceptors. Finally, anatomical studies have demonstrated disorganization of the axonal cytoskeleton without loss of axonal microtubules during the period of behavioral hyperalgesia and nociceptor hyperresponsiveness. Taken together, these studies of the physiological and anatomical changes in C-fiber nociceptors during vincristine-induced neuropathy provide the first evidence that changes in cytoskeleton may be linked with nociceptor responsiveness in the production of neuropathic pain.



## **Future Directions**

### **Are alterations in nociceptor function different following nerve injury and tissue injury?**

Following tissue injury and inflammation, nociceptive neurons characteristically have lower activation thresholds, as well as increased responsiveness to a suprathreshold stimulus. Both of these alterations in sensory transduction increase the sensitivity of nociceptors. In contrast, following nerve injury due to diabetes (Ahlgren et al., 1992), trauma (Koltzenburg et al., 1994), or neurotoxins (Tanner et al., 1997), the activation thresholds of nociceptive C-fibers are not lowered, but nociceptors are hyperresponsive to suprathreshold mechanical and/or heat stimulation. Thus, the alterations that occur following tissue injury appear to be distinct from those following nerve injury and suggest that the underlying mechanisms of these two forms of nociceptor plasticity are different. The dissociation between alterations in activation threshold and suprathreshold response properties suggests that these electrophysiological properties can be independently regulated and that there are distinct underlying mechanisms of these two aspects of mechanotransduction.

### **Are there a common subset of alterations in nociceptor function following neuropathies of diverse etiologies?**

The presence of nociceptor hyperresponsiveness in several neuropathy models of different etiologies suggests that there may be a subset of alterations in nociceptor function that occur following diverse insults to peripheral nerves. Future investigations of the mechanical responsiveness of C-fibers in the chronic constriction injury model and heat responsiveness in diabetic neuropathy would clarify whether nociceptive neurons are hyperresponsive to multiple modalities of stimulation. If common alterations in nociceptive nerve terminal transduction exist for multiple classes of peripheral neuropathies (toxic,

traumatic, and metabolic), then the underlying mechanisms of peripheral nerve injury might be mechanistically dissected, leading to new treatment strategies.

### **Is there a role for protein kinase C in vincristine-induced and trauma-induced neuropathy?**

Interestingly, the C-fiber hyperresponsiveness to mechanical stimulation seen in vincristine-treated rats is similar to C-fiber dysfunction observed in a rat model of diabetic painful peripheral neuropathy (Ahlgren et al., 1992; Ahlgren and Levine, 1994). In diabetic neuropathy, protein kinase C (PKC) is involved in the hyperresponsiveness of C-fibers during mechanical stimulation (Ahlgren and Levine, 1994). If a similar mechanism underlies hyperresponsiveness in the vincristine-treated C-fibers, then PKC inhibitors should similarly reverse vincristine-induced nociceptor hyperresponsiveness and behavioral hyperalgesia. The relationship between an action of vincristine on microtubules and a potential role for PKC in vincristine-induced neuropathy remains to be elucidated. One possibility is that  $\text{Ca}^{2+}$  entry via mechanotransducers (Lumpkin and Hudspeth, 1995) could couple changes in cytoskeletal function and cellular recruitment of PKC. Studies of the involvement of PKC in vincristine-induced and trauma-induced neuropathy could determine whether common or divergent mechanisms underlie nociceptor hyperresponsiveness in neuropathies of diverse etiology.

### **What are the ionic mechanisms of vincristine-induced hyperresponsiveness?**

This thesis provides a detailed description of nociceptor dysfunction during vincristine-induced neuropathy *in vivo* and suggests hypotheses about potential mechanisms that can only be investigated at the level of membrane biophysics *in vitro*. Previous studies have documented that putative nociceptors can be identified in dissociated primary cultures of dorsal root ganglion neurons and that the threshold and response properties of these putative nociceptors, as well as the types and densities of ion channels

present on their membranes can be studied(Leal et al., 1993; Weinreich, 1995; Gold et al., 1996a; Gold et al., 1996b). Whole cell voltage clamp and current clamp investigations of putative nociceptors from vincristine-treated rats can determine ionic mechanisms which contribute to nociceptor hyperresponsiveness.

## References

Ahlgren SC, Levine JD (1994). Protein kinase C inhibitors decrease hyperalgesia and C-fiber hyperexcitability in the streptozotocin-diabetic rat. *J Neurophysiol* 72, 684-692.

Ahlgren SC, White DM, Levine JD (1992). Increased responsiveness of sensory neurons in the saphenous nerve of the streptozotocin-diabetic rat. *J Neurophysiol* 68, 2077-2085.

Gold MS, Dastmalchi S, Levine JD (1996a). Co-expression of nociceptor properties in dorsal root ganglion neurons from the adult rat in vitro. *Neuroscience* 71, 265-75.

Gold MS, Shuster MJ, Levine JD (1996b). Role of a Ca(2+)-dependent slow afterhyperpolarization in prostaglandin E2-induced sensitization of cultured rat sensory neurons. *Neurosci Lett* 205, 161-4.

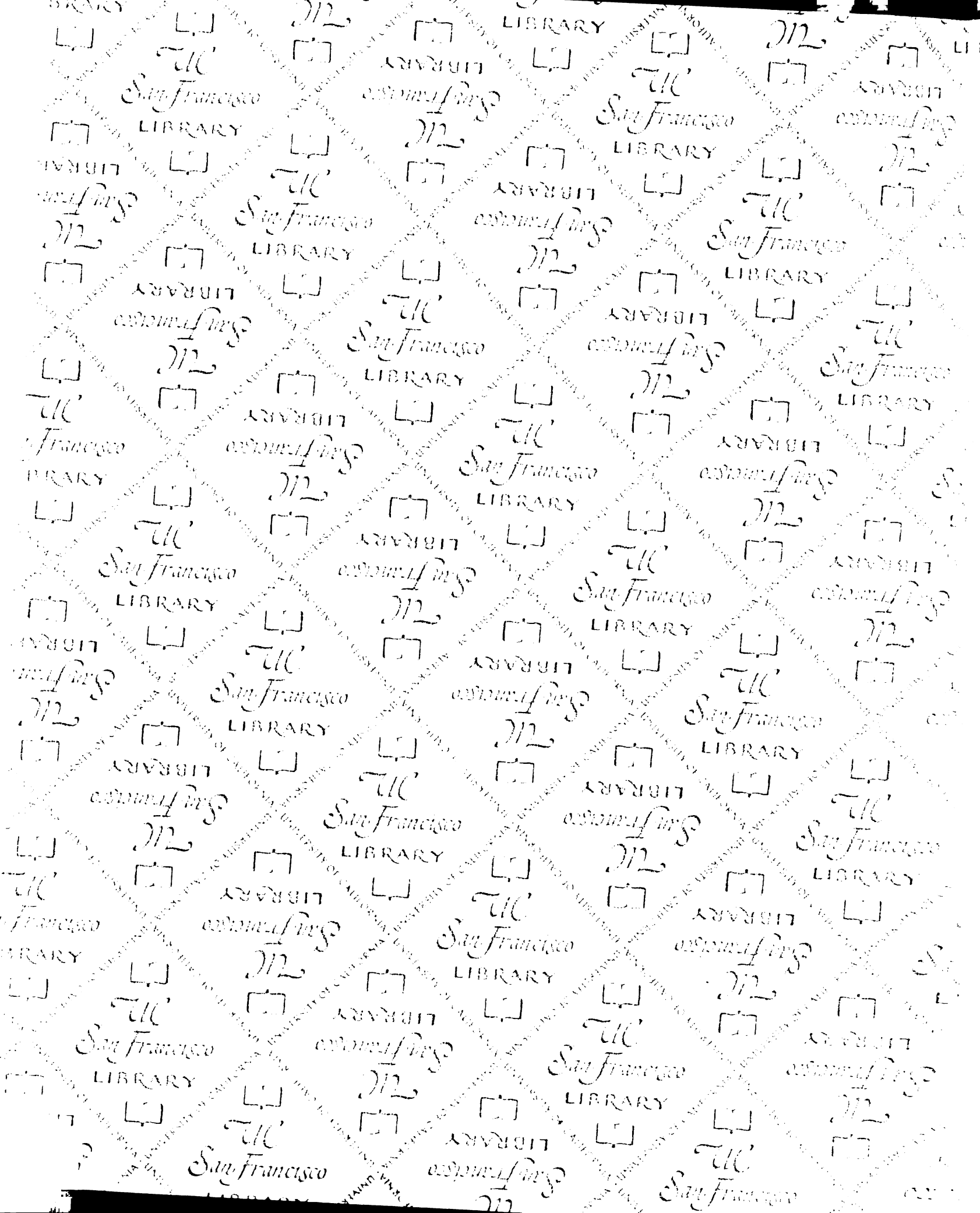
Koltzenburg M, Kees S, Budweiser S, Ochs G, Toyka K (1994). The properties of unmyelinated nociceptive afferents change in a painful chronic constriction neuropathy. In *Proc 7th World Cong Pain*, G Gebhart, D Hammond, T Jensen, ed. (Seattle: IASP Press), pp. 511-522.

Leal CH, Koschorke GM, Taylor G, Weinreich D (1993). Electrophysiological properties and chemosensitivity of acutely isolated nodose ganglion neurons of the rabbit. *J Auton Nerv Syst* 45, 29-39.

Lumpkin EA, Hudspeth AJ (1995). Detection of Ca<sup>2+</sup> entry through mechanosensitive channels localizes the site of mechano-electrical transduction in hair cells. *Proc Natl Acad Sci U S A* 92, 10297-10301.

Tanner KD, Reichling DB, Levine JD (1997). Mechanical hyperresponsiveness of nociceptors in vincristine-induced neuropathy in rat. *submitted*.

Weinreich D (1995). Cellular mechanisms of inflammatory mediators acting on vagal sensory nerve excitability. *Pulm Pharmacol* 8, 173-9.



# For reference

Not to be taken from the room.

